UNIVERSITÉ DE MONTRÉAL

FLUOROSCOPIC AND BIOKINEMATIC STUDY OF THE KNEE JOINT USING A 3-D ANALYZER

SHAFAGH GANJIKIA

DÉPARTEMENT DE GÉNIE BIOMÉDICAL

ÉCOLE POLYTECHNIQUE DE MONTRÉAL

MÉMOIRE PRÉSENTÉ EN VUE DE L'OBTENTION
DU DIPLÔME DE MAÎTRISE EN SCIENCES APPLIQUÉES

(GÉNIE BIOMÉDICAL)

Février 2000

© Shafagh Ganjikia, 2000

National Library of Canada
Bibliothèque nationale du Canada

Acquisitions and Bibliographic Services
Acquisitions et services bibliographiques

395 Wellington Street
Ottawa ON K1A 0N4
Canada

395, rue Wellington
Ottawa ON K1A 0N4
Canada

Your file Votre référence

Our file Notre référence

The author has granted a non-exclusive licence allowing the National Library of Canada to reproduce, loan, distribute or sell copies of this thesis in microform, paper or electronic formats.

L'auteur a accordé une licence non exclusive permettant à la Bibliothèque nationale du Canada de reproduire, prêter, distribuer ou vendre des copies de cette thèse sous la forme de microfiche/film, de reproduction sur papier ou sur format électronique.

The author retains ownership of the copyright in this thesis. Neither the thesis nor substantial extracts from it may be printed or otherwise reproduced without the author's permission.

L'auteur conserve la propriété du droit d'auteur qui protège cette thèse. Ni la thèse ni des extraits substantiels de celle-ci ne doivent être imprimés ou autrement reproduits sans son autorisation.

0-612-53575-4

Canada

UNIVERSITÉ DE MONTRÉAL

ÉCOLE POLYTECHNIQUE DE MONTRÉAL

Ce mémoire intitulé :

FLUOROSCOPIC AND BIOKINEMATIC STUDY OF THE KNEE JOINT USING A 3-D ANALYZER

présenté par : Ganjikia Shafagh

en vue de l'obtention du diplôme de : Maîtrise ès sciences appliquées

a été dûment accepté par le jury d'examen constitué de :

M. Savard Pierre, Ph.D., président

M. Yahia L'Hocine, Ph.D., membre et directeur de recherche

M. Duval Nicolas, MD., membre et codirecteur de recherche

M. de Guise Jacques Ph.D., membre et codirecteur de recherche

M. Fernandes Julio MD.

« À ma mère pour son amour et ses prières »

REMERCIEMENTS

Je voudrais tout d'abord remercier mon directeur principal L'Hocine Yahia pour ses conseils et sa présence lorsque j'en avais besoin, ainsi que sa confiance en moi. Je remercie également Nicolas Duval pour ses conseils cliniques et sa gentillesse. Il faut le considérer comme un ange sur la terre! Je remercie Jacques de Guise pour ses conseils et son appui.

Je remercie beaucoup A. Naddaf pour son support moral, son amitié illimitée et son aide au niveau mathématique.

Au département de génie biomédical, je remercie Mmes Louise Clément et Diane Giroux, toujours souriantes, gentilles et serviables.

Un grand merci à Maryam Tabrizian et Imed Gargouri pour me remonter le moral lorsque j'en avais besoin.

Je voudrais exprimer ma gratitude à Mmes. Louise Tremblay et Michelle Charbonneux à la radiologie pour leur disponibilité.

J'aimerais remercier l'ensemble des étudiants et du personnel du laboratoire LIO plus particulièrement, Gérald Parent pour son grand sourire et son aide technique, Yan Chevalier pour son aide artistique, et mes sujets d'expérience pour leur disponibilité en tout le temps.

En terminant, je remercie ma famille : ma mère Srowr, mon frère Farhad, ma sœur Fariba, mon conjoint Simon et ses parents (Kazimiera et Leszek) qui m'ont traitée comme leur propre fille.

RÉSUMÉ

BUT

La complexité de l'articulation du genou rend très difficile son évaluation clinique. Les examens instrumentés se font habituellement en 1-D ou en 2-D et l'examen physique donne des résultats subjectifs et inconstants. Le but de cette étude est de valider scientifiquement un analyseur fonctionnel du genou avant de débuter son utilisation en clinique. L'analyseur 3D est composé de senseurs de mouvements, d'un système d'attache permettant de fixer les senseurs sur le genou du sujet et d'un ordinateur permettant l'enregistrement numérique du mouvement, sa représentation graphique et son analyse. Un premier objectif est de déterminer, à l'aide d'une étude fluoroscopique, si le système d'attache minimise le mouvement de la peau par rapport de l'os. Un deuxième objectif spécifique est de déterminer un mouvement du genou assurant une bonne reproductibilité intra sujet. Le troisième objectif est de déterminer si l'ajout d'une charge de 3-kg à la cheville influencera la reproductibilité des indices cinématiques. Le quatrième objectif consiste à déterminer un mouvement du genou assurant une bonne reproductibilité intra sujet avec la charge. Et finalement, le dernier objectif consiste en déterminer si la méthode de calibrage à 8-points amène des résultats plus reproductibles que le calibrage à 3-points.

MATÉRIEL ET MÉTHODE

Le système d'attache permet la fixation externe de capteurs de mouvement et minimisant le mouvement de la peau par rapport aux os sous-jacents.

Étude fluoroscopique

Dans un premier temps j'ai réalisé une étude fluoroscopique chez 5 sujets avec des genoux normaux et dont la moyenne d'âge est de 28 ans. J'ai installé des marqueurs métalliques sur la peau du sujet et sur le système d'attache. Les sujets ont alors effectué 3 mouvements de flexion-extension active en position debout de 0 à 100 degrés. Les images fluoroscopiques furent numérisées à chaque 20 degrés. Un programme dans l'environnement de Matlab a été utilisé lequel sert à faire une estimation de 2D à 3D. Ceci est validé expérimentalement et mathématiquement. Les erreurs associées au mouvement des marqueurs dans le plan *XZ* sont calculées, ainsi que les erreurs associées aux rotations autour de l'axe *X* d'abduction (R_X) et de l'axe *Z* de rotation tibiale (R_Z) avec et sans le système d'attache.

Étude cinématique

Dans un deuxième temps le système d'attache fut installé dix fois sur le genou droit des mêmes 5 sujets et les mouvements des senseurs furent associés aux mouvements anatomiques par un calibrage 3-points. Lors de chaque séance, le sujet a effectué 10 mouvements de flexion-extension active dans 3 positions différentes : debout, assis et squat (accroupi). Les indices cinématiques d'abduction/adduction et de rotation tibiale en fonction de la flexion furent ensuite analysés et le coefficient de corrélation multiple calculé.

Étude cinématique avec la charge

Dans un troisième étape, un mouvement de flexion-extension active a été évalué chez 5 sujets normaux dans la position debout avec et sans charge (3-kg). Sans enlever le système d 'attache pendant 10 cycles du mouvement, on a enregistré 5 essais avec la charge et 5 essais sans la charge. Les indices cinématiques ont été analysés et le coefficient de corrélation multiple de Kadaba et al. (1989) calculé.

Finalement, le système d'attache fut retiré et replacé, et suite à l'ajout d'une charge de 3-kg à la cheville droite, un mouvement de flexion-extension active a été évalué chez ces mêmes 5 sujets normaux dans deux positions différentes, debout et assise. On a alors enregistré 10 cycles sur 10 essais en associant le mouvement des senseurs aux mouvements anatomiques par deux calibrages (3-points et 8-points) en parallèle. Les indices cinématiques ont été analysés et le coefficient de corrélation multiple de Kadaba et al. (1989) a été calculé.

RÉSULTATS ET DISCUSSION

L'étude fluoroscopique de validation démontre que les mouvements des marqueurs sont diminués en moyenne par un facteur de 6, 4.3, et 6.2 pour le déplacement dans le plan *XZ*, pour l'abduction (*Rx*) et pour la rotation tibiale (*Rz*) respectivement.

En ce qui concerne l'étude clinique, la moyenne du coefficient de corrélation dans toutes les positions est supérieure à 0.7 pour les cinq sujets. Un test ANOVA (1-way) ne démontre pas de différence significative pour les mouvements en flexion/extension obtenus pour les 3 positions (debout, squat, assis). Toutefois, la position assise a eu un coefficient de corrélation légèrement plus élevée dans la majorité de cas.

Quant aux résultats de l'étude cinématique du genou en position debout avec et sans la charge de 3 kg, ils montrent que l 'ajout de cette charge supplémentaire à la cheville n 'a pas influencé la reproductibilité des indices cinématiques dans la majorité de cas.

Les résultats de l'étude cinématique du genou en position debout et assise avec une charge de 3-kg montrent qu'il n'y a pas de différence significative pour les mouvements en flexion/extension obtenus (debout et assise). Par ailleurs, en ce qui concerne la comparaison des méthodes de calibrage, le calibrage 8-points n'a pas démontré de différence significative par rapport au calibrage 3-points a l'aide d'un test ANOVA. Toutefois, à l'aide d'une étude inter sujets, on peut observer des différences quant à la silhouette des courbes cinématiques, lesquelles sont plus uniformes pour des analyses

effectuées avec un calibrage à 8-points, et ce pour la plupart des sujets, que pour les analyses qui résultent du calibrage à 3-points.

CONCLUSION

Le fait de fixer les capteurs magnétiques sur le système d'attache permet de suivre le mouvement du fémur par rapport au tibia en trois dimensions, tout en minimisant l'erreur associée au mouvement de la peau. En effet, l'étude fluoroscopique démontre que les mouvements des marqueurs furent diminués considérablement par l'utilisation du système d'attache. De plus, les résultats d'étude cinématique montrent que l'analyseur du genou a le potentiel pour acquérir les propriétés cinématiques avec une bonne reproductibilité. Les résultats de l'étude inter sujets montrent que les courbes cinématiques issues du calibrage à 8-points sont plus uniformes dans la plupart des cas que celles issues du calibrage à 3-points. Ces résultats préliminaires représentent une importante indication de l'importance du calibrage de l'appareil, car ils montrent qu'une étude plus poussée pourrait permettre un calibrage adéquat pour effectuer des études cinématiques précises. Nous croyons donc que le système d'attache permet de proposer une méthode d'évaluation de la cinématique du genou de façon non effractive et en 3D. D'autres études seront nécessaires pour identifier des mouvements reproductibles au cours de situations spécifiques, telles que la marche, le saut, et la montée des escaliers.

ABSTRACT

INTRODUCTION

The complexity of knee joint makes its clinical evaluation extremely difficult. Most clinical tests are done in 1 or 2 dimensions in a static manner and the results are often subjective and not reproducible. To address this issue, our research group (GRBB, LIO and ETS) has developed a knee analyser which includes an exoskeleton attachment system, a kinematic tracking system (or sensors), a computer system, a display screen, and a program with a user interface in C environment for calculating the kinematic indices which, in turn, allows us to follow the 3D movement (both position and orientation) of femur and tibia of *in vivo* subject. One of the specific objectives of this study is to perform a fluoroscopic analysis to determine whether the exoskeleton attachment system reduces the relative skin movement with respect to the underlying bone. The second objective is to determine an appropriate reproducible movement among standing, squatting and sitting positions. The third objective is to investigate if a 3-kg charge has an effect on the reproducibility of kinematic measurements, and forth is to determine an appropriate reproducible movement between flexion-extension in the standing and sitting positions. Finally demonstrate whether a 3-point or 8-point method of establishing functional axes would result in uniform and reproducible data on different day.

MATERIAL AND METHOD

Fluoroscopic study

A fluoroscopic study was performed on 5 healthy subjects with an average age of 28 to validate the exoskeleton attachment system. Each subject performed 3 to 4 movements of active flexion-extension over the range of 0 to 100 degrees in standing position that

were then recorded on a video tape. The strip of images was digitized for each 20 degrees of flexion and they were then analyzed by a Matlab program. The Matlab program was validated by 2 different methods: experimental and mathematical methods. The 2 dimensional coordinates of markers were corrected to reflect the 3D nature of the movements. The RMS (root mean square) of the following parameters were calculated twice, first by placing the markers directly on the skin and then by placing them on the attachment system: rotation about the *X* axis, rotation about the *Z* axis and the displacement in the *XZ* plane corresponding respectively to the anatomic axes of abduction, tibial rotation and displacement of the markers with respect to the anatomical axes (XZ) .

Kinematic measurements

Secondly the exoskeleton attachment system was placed on the knee of the subjects. A suitable calibration correlates the movement of the sensors with the anatomical movements. Active flexion-extension movements were evaluated in 3 different positions: standing, squatting and sitting in different days and ten cycles were recorded for each movement. The kinematic indices (flexion-extension, abduction-adduction, internal-external rotation) were analyzed and the multiple correlations along with the statistical average of correlation coefficients for each position were calculated.

Kinematic study using a charge

In the last part of our study we have considered two different settings. In the first set of experiments, the exoskeleton attachment system was not replaced throughout the day. We recorded 10 cycles of active flexion-extension movement in the standing position by alternatively placing and removing a 3-kg charge 10 times over the ankle (5 times with and 5 times without the charge).

The second set of experiments was performed on different days by placing and removing the attachment system on the knee with the 3-Kg charge over the ankle at all times. We

recorded 10 cycles of active flexion-extension, 10 times in the standing and sitting positions with the 3-point and 8-point systems in parallel.

In each set of experiments, kinematic indices for flexion-extension, abduction-adduction, and tibial rotations were obtained. In this study, we used the adjusted coefficients of multiple determinations, to evaluate the similarity between various data recorded within a test day.

RESULTS AND DISCUSSION

Fluoroscopic results suggest that the attachment system reduces the movement of markers with respect to the underlying bone on the average by factors of 6, 4.3 and 6.2 for displacement in XZ plane, abduction (Rx) and rotation (Rz) respectively.

The statistical average of the correlation coefficients for different days and in different positions was larger than 0.7 for all 5 subject. A 1-way ANOVA test showed no significant statistical difference for flexion-extension in 3 different positions (standing, squatting and sitting). Sitting position, however, yields slimly a higher correlation coefficient in most cases.

The results showed that having a 3-kg charge has no significant effect on the reproducibility of flexion-extension. These results have also demonstrated that the statistical difference in flexion-extension between sitting and standing positions while having a charge over an ankle is negligible. Using the 8-point method to find the axes system, however, has resulted in a more uniform data over different days even though there was no statistical difference between the two methods (3-point, 8-point).

CONCLUSION

Fluoroscopic analysis has shown a considerable reduction of skin movement with respect to the underlying bone when the exoskeleton attachment system was placed on the subject's knee. The system allows us to develop a non-invasive method for

evaluating the kinematics indices (flexion-extension, abduction-adduction, internal-external rotation) of the knee in 3D with reproducible results. By fixing the magnetic sensors on the attachment system, we are able to follow the movement of the femur relative to tibia in 3D. I have demonstrated that there is no significant difference in reproducibility of kinematic indices while having a charge. The 8-point calibration method showed no difference statically but resulted in a more uniform pattern. This preliminary results (3-point versus 8-point) are quite exciting since it could result in an interesting improvement in kinematics measurements. Nevertheless, more research has to be performed to identify the most reproducible movements while a subject is walking, jumping and climbing.

CONDENSÉ

INTRODUCTION

Essentiel à la locomotion humaine, le genou est une articulation jouissant d'un mécanisme tridimensionnel complexe et fragile dont le dérèglement peut engendrer un handicap fonctionnel majeur. A long terme, un état pathologique mal diagnostiqué ou non décelé peut dégénérer et induire une condition irréversible. Pour mieux comprendre les mouvements du genou, l'analyse d'indices tridimensionnels est nécessaire. Elle est la première étape d'un processus qui permet de poser un diagnostic précis d'une atteinte fonctionnelle du genou et d'en prévoir un traitement adéquat.

L'articulation du genou est formée de l'articulation tibio-fémorale et de l'articulation fémoro-patellaire. Nous allons nous intéresser à l'articulation tibio-fémorale. Ces deux os sont reliés à l'aide de deux ménisques, des ligaments croisés antérieur et postérieur et de plusieurs autres ligaments et muscles. La forme asymétrique des condyles fémoraux, la capsule, les structures ligamentaires et le plateau tibial sont responsables des mouvements de glissement et de roulement des condyles du fémur sur les plateaux du tibia pendant la flexion-extension du genou qui en conséquence créé la rotation d'abduction-adduction et la rotation interne-externe.

Les plus récents travaux dans le domaine de l'analyse du mouvement du genou, effectués à l'aide de différentes méthodes par A. Cappello et al. (1997), J. Fuller et al. (1997), L. Chèze et al. (1998), K.J. Deuzio et al. (1997), ont pu avec succès évaluer le mouvement du genou. Malgré leurs méthodes et paramètres diversifiés, ces auteurs semblent d'accord pour dire que le mouvement de la peau par rapport à l'os sous-jacent est une cause majeure d'erreur expérimentale lors de l'évaluation de la cinématique du genou. Afin de minimiser le mouvement de la peau et des muscles, notre groupe de

recherche a mis au point un analyseur 3D qui est composé de senseurs de mouvements, d'un système d'attache permettant de fixer les senseurs de façon quasi rigide sur le genou du sujet et d'un ordinateur permettant l'enregistrement numérique du mouvement, sa représentation graphique et son analyse.

Le but de cette étude est de valider scientifiquement, à l'aide d'une étude fluoroscopique, un système d'attache du genou avant de débuter son utilisation en clinique. Un deuxième objectif spécifique est de déterminer un mouvement du genou assurant une bonne reproductibilité intra sujet. Le troisième objectif vise à établir l'influence de l'ajout d'une charge à la cheville peut influencer la reproductibilité des indices cinématiques. Le quatrième objectif est de déterminer un mouvement du genou assurant une bonne reproductibilité intra sujet avec la charge. Le dernier objectif est de déterminer si une méthode de calibrage à 8-points peut amener des résultats plus reproductibles que la méthode de calibrage à 3-points.

MATÉRIEL ET MÉTHODE

L'appareil de mesure

Le système d'attache permet de fixer des capteurs magnétiques de façon quasi rigide aux os du fémur et du tibia et d'enregistrer leur mouvement de façon non effractive. La première version de système d'attache fut développée et mise à l'étude en 1996. La présente étude utilise une troisième version du système d'attache, améliorée afin d'optimiser le confort et la facilité d'installation. La partie fémorale du système d'attache comprend 3 orthoplasts, une barre de suspension, un boîtier pour placer le capteur magnétique associé au fémur, un pont rigide qui relie les orthoplasts, de même que des vis d'ajustement. La partie tibiale est constituée d'une barre rigide avec bandes velcro pour un positionnement rigide sur le tibia, de même que deux trous et deux vis pour le support du capteur magnétique.

Étude fluoroscopique

Une fois l'outil d'analyse développé, il importe de le valider avant son utilisation clinique. Une partie de cette validation peut être effectuée par étude fluoroscopique. Pour cette étude, l'échantillon fut constitué de 5 sujets, tous présentant des genoux non pathologiques tel que déterminé par un examen clinique effectué par un chirurgien orthopédiste. Des marqueurs métalliques furent installés sur la peau des sujets de même que sur le système d'attache. Les sujets ont effectué 3 mouvements de flexion-extension active de 0 à 100 degrés en position debout, pendant lesquels des images fluoroscopiques du genou en mouvement furent acquises. Ces images fluoroscopiques furent numérisées à chaque 20 degrés et analysées à l'aide d'un programme Matlab qui fut créé dans notre laboratoire en 1996, et modifié en 1999 pour la présente étude. Les modifications apportées au programme furent entre autres une automatisation de certaines de ses fonctions, ce qui permit la création d'un programme modulaire plus convivial avec interface graphique.

Les images numérisées furent utilisées pour déterminer les axes anatomiques de même que la distance des marqueurs par rapport aux règles de référence. Celles-ci furent fixées sur la face antero-posterieure (AP) et medio-latérale (Ml), afin de permettre une correction de 2D à 3D.

Validation du programme d'analyse

L'hypothèse de départ fut que si les marqueurs sont attachés aux os, les coordonnées des marqueurs par rapport aux os doivent être invariables. Suivant cette hypothèse, un fantôme du genou gauche fut employé, avec des marqueurs sur le côté médial. 3 positions de flexion différentes (0 degré, 40 degrés, et 60 degrés) furent évaluées en fluoroscopie. L'erreur associée au mouvement des marqueurs sur l'os fut alors observée et mesurée. Cependant, puisque cette erreur peut être dépendante de la précision de l'utilisateur, une deuxième méthode de validation fut envisagée, et qui enlève le biais de l'évaluateur. À l'aide d'un programme Matlab, deux sphères virtuelles connectées en un

seul point furent créées, lesquelles représentent les deux condyles du genou. Des marqueurs furent placés sur le coté latéral et le programme Matlab fut employé pour évaluer l 'erreur associée à la position des marqueurs dans le plan *XZ* ainsi que l'erreur associée par rapport aux axes *X* et *Z* (la rotation autour l'axe *X* consiste en l'abduction-adduction, alors que la rotation autour l'axe *Z* représente le mouvement de rotation interne-externe).

Étude cinématique du genou en trois positions (debout, squat et assis)

Le système d'attache a été installé dix fois sur le genou droit de 5 sujets et les mouvements des senseurs furent associés aux mouvements anatomiques par un calibrage à 3-points qui assure la correspondance entre l'image 3D du genou générique et les os réels du sujet. Ce processus permet la visualisation simultanée du mouvement du genou virtuel sur un écran d'ordinateur en correspondance instantanée avec celui effectué par le sujet. Lors de chaque séance, le sujet a effectué 10 mouvements d'extension-flexion active dans 3 positions différentes : debout, assis et squat. Les indices cinématiques d'abduction/adduction et de rotation tibiale en fonction de la flexion ont été analysés et le coefficient de corrélation multiple a été calculé. Ce coefficient permet d'évaluer la reproductibilité inter et intra sujet des paramètres cinématiques.

Étude cinématique avec et sans charge (3kg)

Cette étude vise à vérifier si l 'ajout d'une charge à la cheville modifie le reproductibilité des indices cinématiques pour un même sujet. Un mouvement de flexion-extension active a été évalué chez 5 sujets normaux dans la position debout avec et sans charge (3-kg). Sans enlever le système d 'attache pendant les 10 cycles de mouvements, on a enregistré 5 essais avec la charge et 5 essais sans la charge. Les indices cinématiques ont ensuite été analysés et le coefficient de corrélation multiple de Kadaba calculé.

Étude cinématique du genou avec une charge (3kg)

Pour déterminer un mouvement du sujet permettant d'assurer une bonne reproductibilité des indices cinématiques pour un même sujet (positions debout et assis); et comparer le calibrage à 3-points avec le calibrage à 8-points, une charge de 3-kg fut placée à la cheville droite. Un mouvement de flexion-extension active a été évalué chez 5 sujets normaux dans deux positions différentes, soit debout et assise. Les mouvements des senseurs furent ensuite associés aux mouvements anatomiques par deux méthodes de calibrage (3-points et 8-points) établies en parallèle. 10 cycles de mouvements pour 10 essais (avec réinstallation du système d 'attache) furent enregistrés avec les deux méthodes de calibrage permettant des analyses parallèles et simultanées. Les indices cinématiques de ces mouvements furent alors analysés et le coefficient de corrélation multiple de Kadaba et al. (1989) calculé.

RÉSULTATS ET DISCUSSION

Les résultats de l'étude fluoroscopique de validation montrent, lorsqu'il n 'y a pas d'erreurs expérimentales, des erreurs minimes pour les positions des marqueurs dans le plan *XZ* et les mouvements de rotation autour des axes *X* et *Z*, ceci après correction de 2D à 3D. Les résultats démontrent une réduction considérable du mouvement de la peau par rapport aux os lors de l'utilisation du système. Cette réduction est d'un facteur de 3.3, 2.4 et 3.7 du côté latéral et d'un facteur de 8, 6.1 et 8.7 du côté médial. Aussi, l'erreur associée au déplacement dans le plan *XZ* a diminué de 13.7 mm à 4.6 mm du côté latéral, et 10.5 mm à 4.1 mm du côté médial, après la correction de 2D à 3D. L'erreur associée à la rotation autour de l'axe *X* (Rx) a diminué de 3.4 à 1.5 degrés du côté latéral, et de 2.3 à 1.7 dégrés du côté médial. L'erreur associée à la rotation autour de l'axe *Z* (Rz) a quant à elle diminué de 6.9 à 2 degrés du côté latéral, et 5.4 à 1.3 degrés du côté médial, et ce pour 4 sujets sur 5. En ce qui concerne le cinquième sujet, les résultats n'ont pas démontré de différence significative par rapport à l'utilisation ou non du système d'attache, et on suppose que celui-ci aurait pu être déplacé pendant

l'expérience, notamment par la présence de la veste assurant la protection contre les sources de radiation utilisées en fluoroscopie.

En ce qui concerne l'étude clinique, la moyenne du coefficient de corrélation dans toutes les positions est supérieure à 0.7 pour les cinq sujets. Un test ANOVA (1-way) n'a pas démontré de différence significative pour les mouvements en flexion/extension obtenus pour les 3 positions (debout, squat, assise). On observe toutefois que le coefficient de corrélation en position assise est le plus élevé (3/4).

Quant aux résultats de l'étude cinématique du genou en position debout avec et sans charge (3-kg), une test ANOVA (1-way) a démontré que l 'ajout d 'une charge à la cheville n 'a pas influencé la reproductibilité des indices d 'abduction et de rotation tibiale dans la majorité de cas (5/8). La fatigue du sujet peut avoir un effet important sur la reproductibilité des indices cinématiques. La réinstallation du système peut également avoir une influence directe sur la reproductibilité des indices analysés.

Pour l'étude cinématique du genou en position debout et assise avec une charge de 3-kg et utilisant deux méthodes des calibrage (3-points, 8-points), un test Anova (one-way) n'a pas démontré de différence significative pour les mouvements en flexion/extension obtenus en position debout et assise dans la majorité de cas (6/8). De plus, le calibrage à 8-points n'a pas démontré de différence statistiquement significative par rapport au calibrage à 3-points. Toutefois, grâce à une étude inter-sujets, on observe que les silhouettes des courbes cinématiques obtenues sont plus uniformes suite à l'utilisation d'une méthode de calibrage à 8-points, et ce pour la plupart des sujets, que pour les analyses effectuées suite à un calibrage à 3-points, lequel produit des courbes dont les silhouettes sont plus aléatoires.

CONCLUSION

L'étude fluoroscopique a démontré que les mouvements des marqueurs sont diminués en moyenne avec un facteur de 6, 4.3, et 6.2 pour le déplacement dans le plan *XZ*,

l'abduction (*Rx*) et la rotation tibiale (*Rz*), respectivement. Les résultats de notre étude cinématique montrent que l'analyseur de genou a le potentiel pour acquérir les propriétés cinématiques avec une bonne reproductibilité. En fixant les senseurs magnétiques sur le système d'attache, on est en mesure de suivre le mouvement du fémur par rapport au tibia en trois dimensions. Ce système nous permet de proposer une méthode pour évaluer la cinématique du genou d'une façon non effractive en trois dimensions. Par ailleurs, l'ajout d'une charge à la cheville n'influence pas la reproductibilité de l'abduction et de la rotation tibiale. Le calibrage à 8-points vs 3-points ne démontre pas de différence statiquement significative, sauf quant à l'uniformité des courbes cinématiques, lesquelles deviennent moins aléatoires lors d'un calibrage à 8-point.

D'autres études seront nécessaires pour identifier des mouvements reproductibles au cours de situations spécifiques, telles que la marche, le saut, et la montée des escaliers. Il importerait entre autres de procéder à une étude inter observateurs, une étude inter-sujets, et finalement d'améliorer la méthode de calibrage, ce qui est un aspect essentiel de l'utilisation clinique de l'appareil.

Finalement, pour approfondir la démarche de validation de l'étude fluoroscopique, il faut envisager prendre une mesure simultanée des images AP et ML afin reconstruire une géométrie 3D du genou. Ceci devrait augmenter la précision des analyses effectuées lors de certaines étapes de l'étude fluoroscopique.

TABLE OF CONTENTS

DÉDICACE IV

REMERCIEMENTS V

RÉSUMÉ VI

ABSTRACT X

CONDENSÉ XIV

TABLE OF CONTENTS XXI

LIST OF TABLES XXIV

LIST OF FIGURES XXVI

LIST OF ANNEXES XXIX

INTRODUCTION XXX

CHAPTER 1: LITERATURE REVIEW 1

1.1 INTRODUCTION 1
1.2 KNEE JOINT AND ITS ANATOMY 2
1.2.1 Articular surface 2
1.2.2 Articular capsule 3
1.2.3 Patellar ligament 3
1.2.4 Collateral ligaments 3
1.2.5 Cruciate ligaments 4
1.2.6 Menisci 4
1.2.7 Patella 4
1.2.8 Mechanics of the knee 5
1.3 NAVIGATION SYSTEMS 6
1.3.1 ELECTROMAGNETIC TRACKING DEVICES (FASTRACK) 6
1.3.2 ACOUSTIC TRANSDUCER SYSTEM 10
1.3.3 OPTOTRAK 13

1.4 REVIEW OF EXISTING 3D INSTRUMENT 16
1.4.1 Simple form of Goniometers 16
1.4.2 Triaxial Goniometer 17
1.4.3 Joint Laxity Measurement device 19
1.4.4 Dynamic sagittal knee test apparatus 22
1.4.5 Three-plane Goniometer 23
1.4.6 A Goniometric device using LEDS 26
1.5 DISCUSSION 27
1.6 CONCLUSION AND RECOMMENDATION 29
1.7 OBJECTIVES OF THESIS 31

CHAPTER 2: 3D KNEE ANALYZER VALIDATION BY SIMPLE FLUOROSCOPIC STUDY 33

2.1 SITUATION OF ARTICLE IN THESIS 33
2.2 ABSTRACT 35
2.3 INTRODUCTION 36
2.4 MATERIALS AND METHODS 38
2.4.1 Exoskeleton knee attachment 38
2.4.2 General theory 42
2.4.3 Experimental method 47
2.4.4 Analysing tools (fluoroscope) 49
2.4.5 Validation procedures 50
2.5 RESULTS AND DISCUSSION 51
2.5.1 Experimental validation 51
2.5.2 Mathematical validation 52
2.5.3 In vivo study 53
2.6 CONCLUSION 59
2.7 ACKNOWLEDGEMENTS 60

CHAPTER 3 : ÉTUDE BIOCINÉMATIQUE DU GENOU À L'AIDE D'UN ANALYSEUR 3D 61

3.1 SITUATION OF ARTICLE IN THESIS 61
3.2 RÉSUMÉ 63
3.3 SUMMARY 63
3.4 INTRODUCTION 65
3.5 MÉTHODE ET MATÉRIELS 67
3.5.1 Système de repérage magnétique (Fastrack) 67

3.5.2 Installation des senseurs de mouvement 68
3.5.3 Test d'environnement 69
3.5.4 Système d'axes 69
3.5.5 Acquisition des indices cinématiques et traitement des données 70
3.6 RÉSULTATS 71
3.7 DISCUSSION ET CONCLUSIONS 76
3.8 REMERCIEMENTS 77

CHAPTER 4: KINEMATIC STUDY OF THE KNEE WITH A 3D KNEE ANALYZER 78

4.1 SITUATION OF ARTICLE IN THESIS 78
4.2 ABSTRACT 80
4.3 INTRODUCTION 81
4.4 MATERIALS AND METHODS 83
4.4.1 3D knee analyzer 83
4.4.2 The coordinate system 84
4.4.3 Experimental acquisition 87
4.5 RESULTS AND DISCUSSION 89
4.6 CONCLUSION 97
4.7 ACKNOWLEDGEMENTS 98

CHAPTER 5: DISCUSSION 99

5.1 GENERAL DISCUSSION 99
5.1.1 3D kinematic measuring devices and 3D tracking system 100
5.1.2 Fluoroscopic validation 102
5.1.3 Kinematic Studies 103
5.1.4 Kinematic studies under a 3 kg charge 104

CHAPTER 6: CONCLUSIONS AND RECOMMENDATIONS 106

6.1 GENERAL CONCLUSION AND RECOMMENDATION 106
REFERENCES 108

LIST OF TABLES

Table 2.1: Design criteria of the exoskeleton attachment system (femoral part) 39
Table 2.2: Design criteria of the exoskeleton attachment system (tibial part) 40
Table 2.3: Accuracy measurements using a plastic knee model for 2 different markers . 52
Table 2.4: Position of a marker before and after 3-D estimation in 10 different images . 52
Table 2.5: Accuracy measurements using a mathematical model 53
Table 2.6: RMS errors for subject 1 54
Table 2.7: RMS errors for subject 2 54
Table 2.8: RMS errors for subject 3 55
Table 2.9: RMS errors for subject 4 55
Table 2.10: RMS errors for subject 5 56
Table 2.11: Mean accuracy measurements for 4 subjects 58
Tableau 3.1: La moyenne de coefficient de corrélation de 10 essais d'abduction et rotation tibiale en position debout 74
Tableau 3.2: La moyenne de coefficient de corrélation de 10 essais d'abduction et rotation tibiale en position squat 75
Tableau 3.3: La moyenne de coefficient de corrélation de 10 essais d'abduction et rotation tibiale en position assise 75
Tableau 3.4: Test d'ANOVA comparant les positions debout , squat et assise. 76
Table 4.1: Multiple correlation coefficient of abduction and tibial rotations in the standing position without a charge, using the 3-point method of calibration 91
Table 4.2: Multiple correlation coefficient of abduction and tibial rotations in the standing position with a charge 3-kg, using the 3-point method of calibration 91
Table 4.3: Multiple correlation coefficient of abduction and tibial rotation in the standing position without a charge, using the 8-point method of calibration 91

Table 4.4: Multiple correlation coefficient of abduction and tibial rotation in the standing position with a 3-kg charge using the 8-point method of calibration 92

Table 4.5: ANOVA 1-way testing the effect of charge on kinematic indices using the 2 different methods for determining the coordinate system of axes (3- and 8-point methods) 92

Table 4.6: Multiple correlation coefficient of abduction and tibial rotation in the standing position with a 3-kg charge, using 3-point calibration. 94

Table 4.7: Multiple correlation coefficient of abduction and tibial rotation in the sitting position with a 3-kg charge, using 3-point calibration. 94

Table 4.8: Multiple correlation coefficient of abduction and tibial rotation in standing position with a 3-kg charge, using 8-point calibration. 94

Table 4.9: Multiple correlation coefficient of abduction and tibial rotation in the sitting position with a 3-kg charge, using 8-point calibration. 95

Table 4.10: ANOVA 1-way comparing the standing position to the sitting position with a 3-kg charge, using 3-point of calibration. 95

Table 4.11: Intra-subject multiple correlation coefficients on different days with a charge over the ankle (using 8-point calibration) 96

Table 4.12: Intra-subject multiple correlation coefficients on different days with a charge over the ankle (using 3-point calibration) 96

Table 4.13: Anova 1-way testing intra subject correlation coefficients using 2 different methods of calibration (3-point and 8-point) 97

LIST OF FIGURES

Figure 1.1: Source; Netter, 1991. Sagittal section through knee joint.....5

Figure 1.2: Magnetic tracking system (FASTRAK).....9

Figure 1.3: Source; Morneburg et al. 1998. 3D real time gait analysis on treadmill or walking range. 12

Figure 1.4 : OPTOTRAK/3010 (position sensor, system control unit, PC interface card and cables, and strobes and marker kit).....15

Figure 1.5: The simplest form of Goniometer.....17

Figure 1.6: Source; Mills et al. 1991; The triaxial goniometer attached to a test subject 18

Figure 1.7: Source; Fraser et al., 1987. Joint laxity measuring device.....21

Figure 1.8: Source; Lamb et al., 1990. Dynamic Sagital knee test apparatus. 23

Figure 1.9: Source; Macleod et al. 1989. 3D measuring system (3-plane goniometer). ...25

Figure 1.10: Source ; Fine et al. 1987. Goniometric device 27

Figure 2.1: A) 3-D knee analyser. B) Exoskeleton attachment system with magnetic sensors. 37

Figure 2.2: The exoskeleton attachment system. On the lateral side, the femoral part is positioned on the superior part of the posterior condyle. The orthoplast (1) is placed between the ilio-tibial band and biceps femoris. On the medial side, a large circular pad or orthoplast (2) is positioned on the femoral epycondyle and the third orthoplast (3) is positioned on the adductor tubercule behind the adductor magnus. The tibial part is simply positioned on the tibial bone. 41

Figure 2.3: A) and B) Dx and Dz are the main parameters used for 3-D rotational estimation. Any rotation about the X or Z axis will change the value of these parameters, and hence allows us to calculate the rotation. This will make it possible to find the true 3-D coordinates from a 2-D image. Dx and Dz values are scaled to give $\delta z(f)$ and $\delta x(f)$ which are then used to find the rotation angles. C) The rotation angles can be determined by using the right triangle whose sides are $\delta z(f)$ (or $\delta x(f)$) and dc, as shown. 46

Figure 2.4: A and C represent markers on the skin. B & D are markers on the exoskeleton attachment. 48

Figure 2.5: Static images. A) Medio-lateral view. B) Antero-posterior view. 49

Figure 2.6: The GUI interface (fluoroscope). The larger window is the main window and the smaller one is the set-up window 50

Figure 2.7: Mathematical modelization of lateral and medial condyles using 2 spheres connected at 1 point. The dark points correspond to the markers. 51

Figure 2.8: Displacement of a marker before (*pmx*, *pmz*) and after (*px*, *pz*) 3-D estimation throughout different flexion angle (0 to 80) degrees. 59

Figure 3.1: Le système d'axes 66

Figure 3.2: Le système d'attache. Du côté latéral, le système d'attache s'appuie sur la partie supérieure du condyle postérieur. Cet appui se trouve entre la bandelette iliotibiale et le biceps femoris. Du côté médial, le dispositif s'appuie sur le tubercule des adducteur et derrière l'adducteur magnus. 66

Figure 3.3: Test d'environnement à l'aide d'une boîte de calibrage. L'axe de X représente le nombre de points qui sont numérises et l'axe Y représente l'erreur sur les capteurs (2,3) au niveau de fémur et tibia respectivement. 72

Figure 3.4: L 'abduction et rotation tibiale en fonction de la flexion-extension pour un sujet qui effectue un mouvement en flexion-extension en position assise. 73

Figure 3.5: a) Le coefficient de corrélation d'abduction en flexion-extension en position assise pour 10 essais consécutifs à différentes journées. b) La moyenne du coefficient de corrélation en abduction dans 3 positions différentes pour 5 différents sujets. 74

Figure 4.1: A) 3D knee analyzer. B) The attachment system on the lateral side is placed on the superior part of the posterior condyle. The orthoplast is positioned between the ilio-tibial band and the biceps femoris. On the medial side, large circular pads or othoplasts are placed on the femoral epicondyle, and the third orthoplast is positioned on the adductor tubercule behind the adductor magnus. . 84

Figure 4.2: Two different methods used to define coordinate systems for the femur and tibia. A) The coordinate system using 3 points on the femur and 3 points on the tibia. B) The coordinate system using 8 points on the femur. Points 1, 2 and 3 represent the plane on the floor with Z_{abs_femur} normal to this plane. The Y axis is the projection of the vector passing through points 4 and 5 on the plane formed by points 1, 2 and 3. The Z axis is tilted vector ⊥ to Y formed from the line which goes through point 6 on the patella and the mid point of points 7 and 8 (the pubic tubercle and the great trochanter). X is the cross product of Y and Z. C) The coordinate system using 8 points on the tibia. Points 1, 2 and 3 represent the plane on the floor with Z_{abs_tibiar} perpendicular to it. The Y axis is the projection on the floor of the vector joining points 4 and 5 and is ⊥ to Z_{abs_tibia} . The Z axis is the tilted vector ⊥ to Y formed by a line which goes through point 6 on the patella and is connected to the mid point of 7 and 8 (on the medial and lateral ankle). X is the cross product of Y and Z. 87

Figure 4.3: Multiple correlation coefficient of tibial rotation in the standing position for a typical subject. The X axes represents the trial number and the Y axis is the correlation coefficient. Note the gradual decrease in the correlation coefficient from the 1st to the 5th trial due to fatigue of the subject..... 90

Figure 4.4: A and B represent the intra-subject mean and error bar for 10 cycles during 10 different trials (on different days). The data in A seems to follow the pattern, and were obtained using the 8-point method for the coordinate system. B is the 3-point method with the data showing a random shape in this particular case..... 93

LIST OF ANNEXES

ANNEX I : ANNEXES FOR CHAPTER 1 ..... **116**

ANNEX II : ANNEXES FOR CHAPTER 2 ..... **117**

ANNEX III : ANNEXES FOR CHAPTER 3 ..... **129**

ANNEX IV : ANNEXES FOR CHAPTER 4 ..... **134**

INTRODUCTION

This thesis is composed of 6 chapters, three of which are articles that are submitted for publication to Annales de Chirurgie, the Knee and Clinical Biomechanics, respectively. The first chapter presents the background and pertinent literature to put into context the objectives of the work. To reduce skin movement, our research group has developed a 3D knee analyser which includes an exoskeleton attachment system, a kinematic tracking system (or sensors), a computer system, a display screen, and a program with a user interface in C environment for calculating the kinematic indices which, in turn, allows us to follow the 3D movement (both position and orientation) of femur and tibia of healthy subject. The first article appears in Chapter 2, in which I describe the skin movement with respect to the underlying bone on 5 *in vivo* subjects. I have conducted a flouroscopic study to demonstrate that the exoskeleton attachment system reduces the movement of skin with respect to the bone. This system allows us to study the kinemactis of knee in movement. The third chapter is focused on the study of kinematic indices and the correlation coefficients of abduction and tibial rotation of knee in 3 different positions: standing, squatting, sitting. Chapter 4 (article 3) is concerned with the study of the effect of a 3-kg weight over the ankle, along with the reproducibly of movement and kinematic indices. In this chapter I also examine the most reproducible movement while having a charge over the ankle in standing and sitting positions. The chapter ends with study of two different methods of calibration, namely the 3- and 8-point methods to determine which one of these methods produces a more reproducible result. In chapter 5, I summarise the results that I obtained throughout the thesis. Finally, in chapter 6, I draw some general conclusion some of the improvements and benefits that are gained if the 3D knee analyser is used to study the kinematics of knee joint.

CHAPTER 1

LITERATURE REVIEW

1.1 INTRODUCTION

Historically, research on the mechanics of human musculoskeletal system had primarily focused on experimental studies. More recently mathematical tools from the field of applied mechanics have been used to obtain a better understanding of the complicated mechanical behavior of the substructures which comprise the system.

The knee joint is one of the most complicated synovial joints in the musculoskeletal system. The knee is primarily a hinge joint that permits flexion and extension. In flexion, there is sufficient looseness to allow a small amount of voluntary rotation; in full extension, some terminal medial rotation of the femur achieves the close-packed position. The shape of the femoral condyles leads to rolling and sliding that includes components of abduction-adduction, in addition to internal-external rotation.

The biomehanical analysis of human joint has been under investigation for more than 100 years, using a variety of techniques. To have a better understand of this variety we will start with a brief review of knee anatomy and its mechanics.

It will follow with description of different navigation systems that are available for measuring kinematic indices. We study each navigation system in detail to be able to choose an appropriate system for our experimental purposes. Each device will be evaluated against a set of criteria (see Annex 1.A) in terms of its principles of operation and the advantages and limitations to its use in a clinical environment. The study will be restrict to those devices that record joint rotations in multi-degrees of freedom such as magnetic (Fastrack), acoustic (Transducer) and optical (Optotrak) sensors.

A brief review of a few Instrumented Space Linkage (ISL) instruments by different researchers (G.A. Fraser *et al.* (1987), S.Lamb *et al.* (1990), P.C. McLeod *et al.* 1989, and E.J. Fine *et al.* (1987))with multi-degrees of freedom are reported in this study.

I will then draw a conclusions on whether the existing measuring instruments are capable of answering the current clinicians' needs. Finally, we propose an alternative instrument to resolve the existing shortcomings of the current devices.

1.2 KNEE JOINT AND ITS ANATOMY

The human knee was once believed to be a simple hinge-like mechanism. This incorrect supposition is not surprising since the knee joint articulation is hidden beneath layers of skin and soft tissues involved in its function. There are three articulation in the knee the femoro-patellar articulation and two femoro-tibial joints. The latter two are separated by the intra-articular ligaments and the infrapatellar synovial fold. The three joint cavities are connected by restricted openings (Netter, 1991).

1.2.1 Articular surface

The articular surface of the femur consists of its medial and lateral condyles and the patellar surface. The condyles are shaped like thick rollers diverging inferiorly and posteriorly. Their surfaces gradually change from flatter curvature anteriorly to a tighter curvature posteriorly and are separated from the patellar surface by a slight groove. On the superior surface of the tibia, there are two separate, cartilage-covered areas. The surface of the medial condyle is larger, oval shaped, and slightly concavo-convex from before backward. The fossae of the articular surfaces are deepened by dislike menisci.

1.2.2 Articular capsule

The articular capsule of the knee joint is scarcely separable from the ligaments and aponeuroses opposed to it. Posteriorly, its vertical fibres arise from the condyles and intercondylar fossa of the femur; inferiorly, these fibres are overlain by the oblique popliteal ligament. The capsule attaches to the tibial condyles and, incompletely, to the menisci. The external ligaments reinforces the capsule are the fascia lata and the iliotibial tract;the medial patellar and lateral patellar retinacula; and the patellar, oblique popliteal, and arcuate popliteal ligaments. The tibial collateral ligament also closely reinforces the capsule on the medial side.

1.2.3 Patellar ligament

It is the continuation of the quadriceps femoris tendon to the tuberosity of the tibia. An extremely strong and relatively flat band, it attaches above the patella and continues over its front with fibres of the tendon, ending somewhat obliquely on the tibial tuberosity.

1.2.4 Collateral ligaments

These ligaments prevent hyperextension of the joint and any abduction-adduction angulation of the bones. The *tibial collateral ligament* is a strong, flat band that extends between the medial condyles of the femur and the tibia. It is well defined anteriorly, blending with the medial patellar retinaculum. The principal inferior attachment of the ligament is about 5 cm below the tibial articular surface immediately posterior to the insertion of the pes anserinus. The fibular collateral ligament is rounded, pencillike cord, which entirely separate from the capsule of the knee joint. It is attached to a tubercle on the lateral condyle of the femur above and behind the groove for the popliteus muscle. It ends below on the lateral surface of the head of the fibula, about 1cm anterior to its apex. The medial collateral ligament (MCL) structures appear to act as primary against valgus rotation of the knee. On the opposite side of the knee, the lateral collateral ligament

complexserves to limit joint openning to varus stress as well as resisting internal rotation forces (Gollehon et al. 1985)

1.2.5 Cruciate ligaments

The cruciate ligaments prevent forward or backward movement of the tibia under the femoral condyles. They are somewhat taut in all positions of flexion but become tightest in full extension and full flexion. They lie wholly within the capsule of the knee joint, in the vertical plane between the condyles, but are excluded from the synovial cavity by coverings of the synovial membrane. Both ligaments spread linearly their bony attachments, especially at the femoral condyles. The anterior cruciate ligament (ACL) arises from the rough, nonarticular area in front of the intercondylar eminence of the tibia and extends upward and backward to the posterior part of the medial aspect of the lateral femoral condyle. The posterior cruciate ligament (PCL) passes upward and forward on the medial side of the ACL. It extends from behind the tibial eminence to the lateral side of the medial condyle of the femur.

1.2.6 Menisci

These cresent-shaped wafers of fibro-cartilage surmount the peripheral parts of the articular surfaces of the tibia. The medial meniscus is larger than the lateral meniscus.

1.2.7 Patella

This large sesamoid is developed in the tendon of the quadriceps femoris muscle. It bears against the anterior articular surface of the inferior extremity of the femur and, by holding the tendon off the lower end of the femur, improves the angle of approach of the tendon to the tibial tuberosity. The convex anterior surface of the patella is striated vertically by the tendon fibers. The superior border is thick but the lateral and medial borders are thinner. The patella maintains a shifting contact with the femur in all positions of the knee. As the knee goes from fully flexed to fully extended position, first

the superior, then the middle, and lastly the inferior parts of the articular surface of the patella are brought into contact with the patella surfaces of the femur (see figure 1.1).

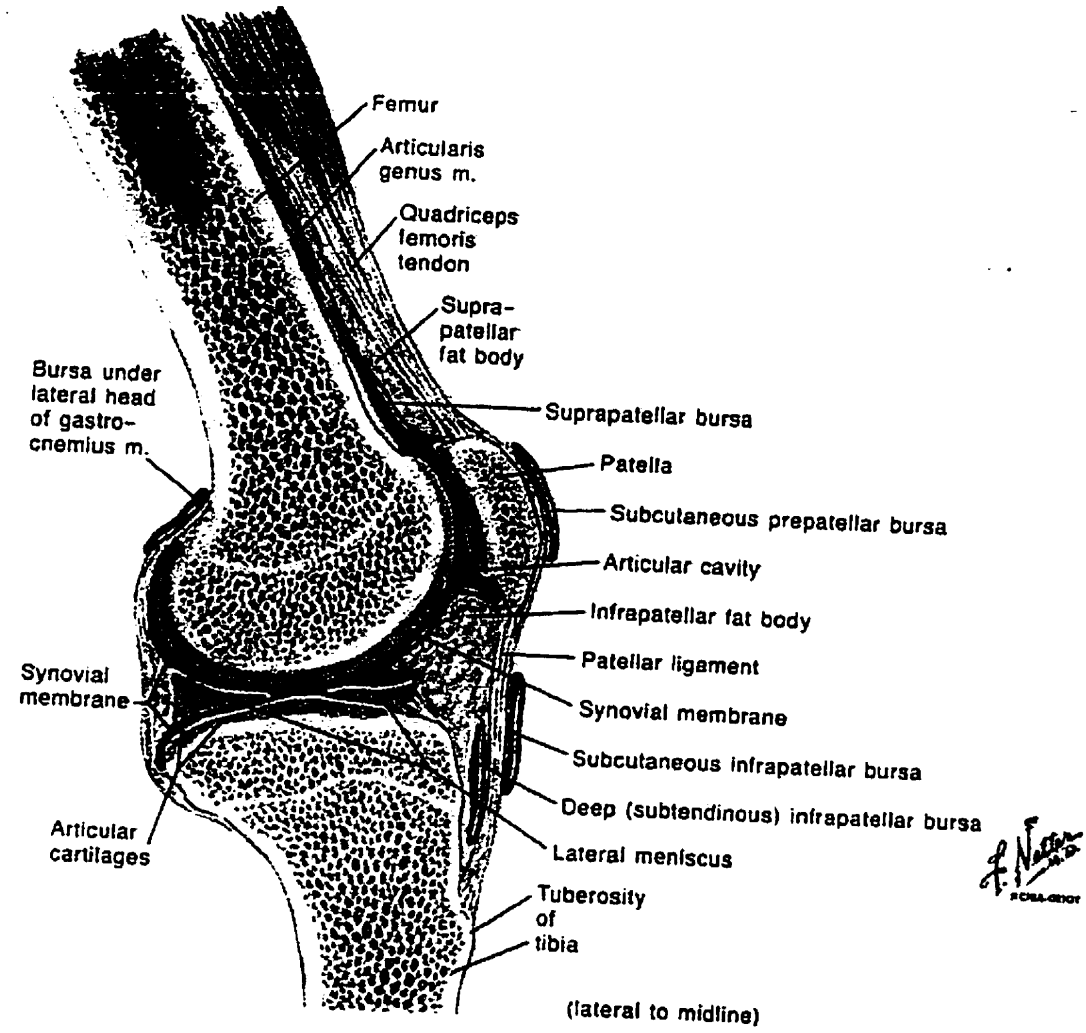

Figure 1.1: Source; Netter. 1991. Sagittal section through knee joint.

1.2.8 Mechanics of the knee

The primarily movement of the knee is flexion and extension. In flexion, there is sufficient looseness to allow a small amount of voluntary rotation of the femur (conjunction rotation) achieves the close packed position. The condyles of the femur

provide larger surfaces than those of the tibial condyles, and there is a component of rolling and gliding of the femoral surfaces that uses up this discrepancy. As the extended position is approached, the smaller lateral meniscus is displaced forward on the tibia and becomes firmly seated in a groove on the lateral femoral condyle, which tends to stop extension. However, the medial femoral condyle is still capable of gliding backward, thus bringing its flatter, more anterior surface into full contact with the tibia. These movements of conjunct rotation bring the curciate ligaments into a taut, or locked, position. The collateral ligaments become maximally tensed, and a full, closed packed, and stable position of extension results. The tension of the ligaments and the close approximation of the flatter parts of the condyles make the erect position relatively easy to maintain. The sequence of the actions in flexion is reversed in extension. Flexion can be carried through about 130 degrees and is finally limited by contact between calf and thigh. The muscles concerned in the movement at the knee are primarily thigh muscles (Netter, 1991).

1.3 NAVIGATION SYSTEMS

1.3.1 ELECTROMAGNETIC TRACKING DEVICES (FASTRACK)

The Fastrack tracking system uses electromagnetic field to determine the position and the orientation of a remote object. This system has been developed to determine the three-dimensional position and orientation of a sensor or any other reference frame relative to the source. The six degrees of freedom measurements are accomplished by generating near field, low frequency magnetic field vectors from a single assembly of three co-located stationary antennas called the transmitter (Xmtr), and detecting the field vectors with a single assembly of three co-located, remote sensing antennas called the receiver (Rcvr). The sensed signals are input to a mathematical algorithm that computes the receiver's position and orientation relative to the transmitter.

The magnetic field technology interprets the interaction of magnetic fields between three sets of orthogonal coils contained in both the source and the sensor. With appropriate alignment and attachment of the source and sensor to anatomical structures, the relative location and orientation of anatomical elements can be monitored (K.N. An et al. 1998).

The Fastrak consists of a System Electronics Unit (SEU), one to four receivers, and a signal capable of operating at any of four discrete carrier frequencies. Different carrier frequencies allow simultaneous operation of up to four Fastraks in close proximity to one another. The Fastrak has two possible interfaces to the host computer. Any single receiver may be operated at the fastest update rate (120 Hz); any two receivers at one half of this rate; any three at the fastest rate. Mixed rates are not permitted meaning that all active receivers should operate at the same update rate; therefore one can not be operated faster than the others. Active receivers are selected by a combination of software configuration commands and receiver selector switch settings. The device may also be used as a three-dimensional digitizer. A probe was fabricated by attaching the sensor to an acrylic rod with a sharp point at the opposite end. A spherical fit computer program has been developed which allows calibration of the relative location of the probe tip to the sensor's coordinate system (K. N. An et al., 1988).

The position of a point in space may be fully described by its relationship to any fixed and convenient three-axis (x, y, z) coordinate system (S.E. Logan et al., 1988). Orientation means direction in relationship to that position and may be fully described by three parameters or angles, such as azimuth (yaw), elevation (pitch), and roll. A typical electromagnetic tracking device system consists of a fixed magnetic- dipole transmitting antenna called a source; a freely movable magnetic dipole receiving antenna called a sensor; and the associated electronics. Both the source and sensor antennas consist of three mutually orthogonal loops (coils). The loops' diameters are kept very small compared to the distance separating the source and the sensor so that each loop may be regarded as a point or infinitesimal dipole. Exciting a loop antenna produces a field

consisting of a far-field component and a near or induction-field component. The far field intensity is a function of the loop size and the excitation frequency and decreases with the inverse cube of the distance ($1/r^3$). The induction-field or " quasi-static" field component intensity does not depend on frequency and decrease by the inverse cube of the distance ($1/r^3$). The quasi-static field is not detectable at long distance; in fact, its strength dominates at short distances where the far-field is negligible. Each loop of the source antenna is in turn excited with a driving signal identical in frequency and phase. Each excitation produces a single axis source dipole. The source excitation is a pattern of the three states. Exciting the source results in an output at the sensor of a set of three linearly independent vectors. The three output (sensor) vectors contain sufficient information to determine the position and the orientation of the sensor relative to the source.

Criteria

The static accuracy of Fastrack is 0.03"(0.08 cm) RMS for the *X*, *Y* or *Z* receiver position, and 0.15° RMS for receiver orientation. The instrument achieves the specified accuracy when the receiver is located within 30" (76 cm) of the transmitter. Operation with separations up to 120" (305 cm) is possible with a reduced accuracy. The receiver has angular coverage in all altitudes. The system is portable (see figure 1.2).

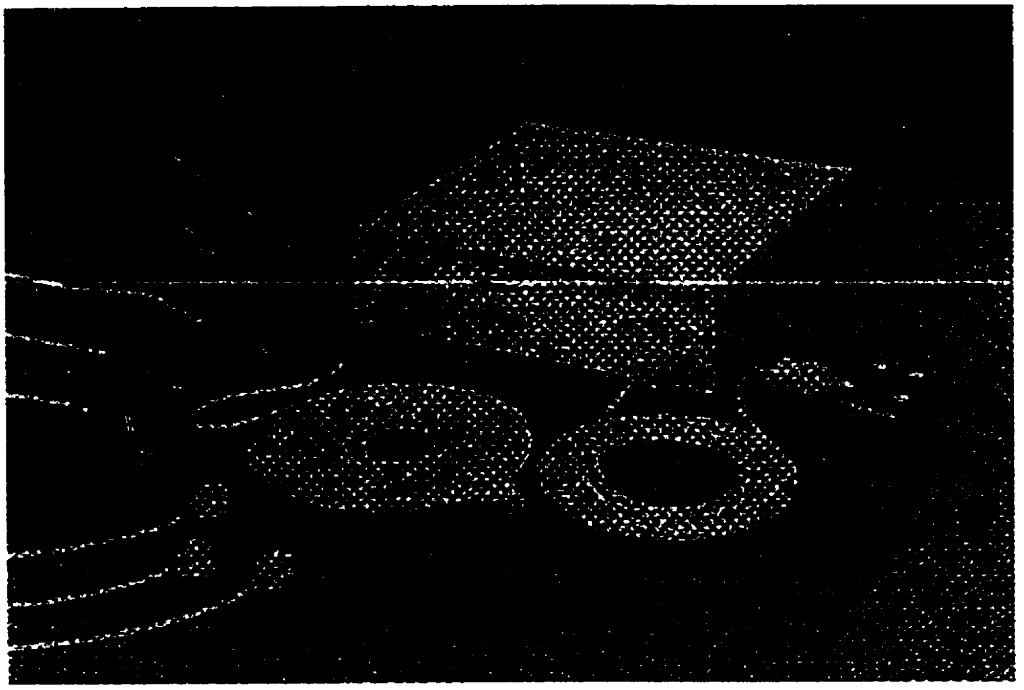

Figure 1.2: Magnetic tracking system (FASTRAK)

There is no risk involved in using this system. The cost is less than $12000.00. The system provides 6 degrees of freedom for kinematics measurements. The system can be easily purchased and does not require a long waiting period. The system does not suffer from shadowing problem. The intensity of the magnetic field is controlled by the SEU which automatically adjusts for the change in the distance between the source and the sensor, to keep the strength of the field reaching the sensor at a constant level. If movement of the sensor towards the source is too fast, the SEU cannot react fast enough and the signal reaching the sensor overdrives the system and an error signal is generated until compensation is achieved. Operation of the tracking system is affected by the presence of nearby metallic objects and conductors. Large nearby metallic objects particularly between the source and the sensor cause distortions in the magnetic fields and consequently affect the signals received by the sensor. The user can limit the operation range of the sensor in the X, Y and Z directions. Movements outside of this range will result in a software status error. The range of values is ± 65.48 inch or ±

166.32 cm (K.N. An et al. 1988). The system comes with a complete manual kit, which is very helpful for performing basic repairs.

1.3.2 ACOUSTIC TRANSDUCER SYSTEM

Acoustic sensors have been reported by some authors in three-dimensional kinematic studies of human joints such as wrist (Andrews and Youm, 1979), ankle (Siegler et al, 1988) and knee (Quinn and Mote, 1990). The system usually includes an array of acoustic sources (e.g. spark gaps) and an array of at least three non-collinear receivers (microphones), which define a Body Coordinate System (BCS). The acoustic waves generated and transmitted by the sources travel through the air, and are received by the microphone. Since the speed of sound is known, the system can calculate the location of the receiver relative to the sources. By fixing the sources (or the receiver) in the laboratory coordinate system, the complete three-dimensional location of the receiver (or the source) in the inertial reference system is determined. Once the spatial locations of all the markers in the array are determined, the position and orientation of the BCS can be calculated, thereby fully characterising the six degree of freedom (DOF) of the rigid body.

In a well-controlled experimental set-up, errors smaller than 0.5 mm in translation and 0.5° in rotation were reported (Quinn and Mote, 1990). However, the motion of soft tissue that is encountered in dynamic studies, the relative size and orientation of the source and sensor array segments-which are needed to create a good signal to noise ratio, the acoustic echoes, interference patterns and sparking introduced by multiple source/sensor pairs make this approach difficult to apply to dynamic motion studies of multiple body segments of human subjects.

This system works on the same principle of source and sensors as that of the electromagnetic transducer which is a triad of coils that create an electromagnetic field and a number of sensors which consist of small triads of electromagnetic coils which

detect magnetic fields emitted by the source. The source is the system's reference frame for sensor measurements. In some cases there is no physical attachment required between the source and the sensor.

CMS 70P Measuring System is among the newest ultrasound system. It measures the 3D real time motion analysis with optional analog channels (EMG). The measuring system consists of a convenient measuring sensor with stand, a basic unit and the appropriate markers and application aids. The measuring procedure is based on the determination of the spatial coordinates of miniature ultrasound transmitters. The sound pulse time between the transmitters and the three microphones integrated in the measuring sensor is measured. The measuring areas are of order 1.5 x 3 x 3 to 2 x 4 x 4. The system can optionally be equipped with 8 or 16 analog channels for simultaneous determination of EMG or force data, etc. The basic unit is connected to the parallel printer port of a personal computer. The kinematic data are transmitted synchronously with the analog data.The measuring sensor is connected to the stand by means of a ball-and-socket joint and can be brought into any desired position. The various application aids and a surface tracer can be plugged directly into the basic unit. A cable adapter with 10 channels can be supplied for operation of individual markers. Two measuring sensors can be combined for bilateral gait analysis. The standard sensor can replaced by special measuring sensors for extensions.

The system consists of a transducer and a basic unit as well as a table clamp or floor stand. The three dimensional measuring coordinates of the markers can be recorded at a total rate of 200 samples per second. The measuring process is based on the transmission time measurement of ultrasound pulses, which are sent by miniature sound transmitters (markers) to the three microphones fitted in the transducer.

A separate micro-computer is integrated for each microphone in the basic unit to digitalize the received ultrasound pulses. Real-time evaluations are available in the connected personal-computer. The system is thus suitable for feed-back tasks in the

medical treatment sector. In accordance with the scanning rate, areas of 1.2x2x2 to 2x4x4 m can be implemented. Time markings can be superimposed during data acquisition via 4 digital input channels. The transducer is freely movable by means of a ball joint, and can thus be easily moved to the relevant optimum measuring position. For this there is no need for any calibration. For medical analyses, the most diverse application aids are available as well as an ultrasound pointer. A cable adaptor with 10 channels is available for the connection of miniature individual markers.

The measuring station for gait analysis allows analysis of the kinematic parameters of the human gait. The measuring process is based on the technic ultrasound pulse time measurement. In this method small ultrasound markers are attached by means of adhesive patches to the hips, knees, ankles and balls of the feet, on the two lateral sides of the body. Thin foot contact switches are also stuck to the heels and the balls of the feet. Signals from the left and the right side of the body are measured in succession or simultaneously. In this report the time-dependence and the maximum values of the foot rotation and the lateral movements of the extremities are presented. The individual gait phases (see figure 1.3), the step length, the cadence and the average speed are evaluated. Information about instabilities is obtained from the averaged and normalized curves of all individual steps and from their standard deviation (Morneburg et al. 1998, Vogt et al. 1998 and Vogt et al.1999).

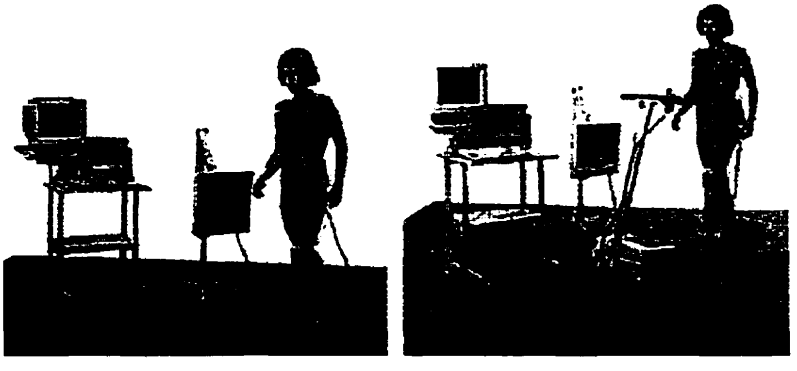

Figure 1.3: Source; Morneburg et al. 1998. 3D real time gait analysis on treadmill or walking range.

Criteria

This system offers the following accuracy: Rotations< 30 degree, with 0.3 degree of accuracy. Translations<1.5 cm, with 0.3 mm accuracy. In worst case is: 0.9 mm, 0.6 degree. This system has been used on cadavers (Quinn and Mote1990) however, it has also been used for pregnant women. No price is available since the system is custom made. Full 6 degrees of freedom are available for kinematic measurements. Since it is a custom made system, it may take some time to be prepared. No calibration is required and no problem with shadowing. Noise must be minimised to ensure the accuracy of measurements. The signal doesn't pass through tissue or dense object. The system is sensitive to humidity and air current.

Nevertheless, ultrasound system such CMS 70P Measuring System are somewhat new and there are not enough published informations available to evaluate them against the different sets of criteria (see Annex 1.A).

1.3.3 OPTOTRAK

Three-dimensional measurement of the human body was first performed by Braune and Fischer (1895) using four plates cameras to track 11 incandescent tube markers strapped onto segments of the subject dressed in black. Images of the tubes' movements resulted in stick figure animations of the subject's movement from which various kinematics and dynamic parameters were derived. Although moving about in dark with glowing markers is "ancient" in biomechanics, most human movement analyses are still performed using optical tracking of markers mounted on the surface of the skin. OptoTrak is among the systems which uses camera system (Logan et al., 1985). The OptoTrak system is a non-contact, high speed, high accuracy, three dimensional motion measurement and analysis system which provides 3D data in real time and sampling rates of up to 3500 points per second. Unlike systems that employ video based cameras and pattern recognition technology, the Optotrak uses three or more 1D sensors, each of which employs a 2048

element linear CCD array and a cylindrical lens. The system tracks target points defined by up to 256 miniature infrared emitting diodes.

To accommodate the diverse applications for which the Optotrak system can be used, two different configurations have been designed. The first, the Optotrak/3000 series, is designed for applications where the operating volume is fixed (1m x 1m at a distance of 2m, up to 2m x 3.5m at a distance of 6m). This configuration consists of three individual sensors mounted on a single, meter-long stabilised bar. The system is pre-calibrated, turnkey unit and therefore, requires no initial calibration sequence and minimal set-up time.

Optotrak/2000 series consist of a number of individual two sensor camera units. Altering the cameras' positions requires recalibration of the cameras' positions relative to the frame of reference. This process is quickly performed using the provided calibration frame and software.

The Optotrak system consists of four major hardware components: the target markers, the camera unit, the system unit and a user supplied host computer. The camera unit is responsible for sensing the positions of the target markers. Three functions are carried out by the system unit: the timing control of the Optotrak system, the processing of the camera sensor information and interfacing with the host computer.

The basic measurement instrument within the Optotrak system is the 1D sensor which consists of three components: an anamorphic (cylindrical) lens system, a 2048 element linear CCD array, and a signal processing circuitry. The sensor has a field-of-view (FOV) of 35 degrees and a useful depth-of-view (DOF) from 1 to 8m.

Criteria

Accuracy of Optotrak/3000 in the operating volume at 2m is 0.1mm in X and Y dimensions and 0.15 mm in depth, while the resolution is better than 0.01mm. Accuracy

of Optotrak/2000 is commensurate with the 3D bar at 2m and is 0.3 to 0.45 mm at 4 to 5m distances. Accuracy of the sensor is +/-1 part in 100,000 with the resolution of better than +/-1part in 250,000. The marker may be moved to any position in a 3D space with an accuracy of +/- 20 µm. The camera system in Optotrak has to be installed on the wall which takes a fair amount of place.

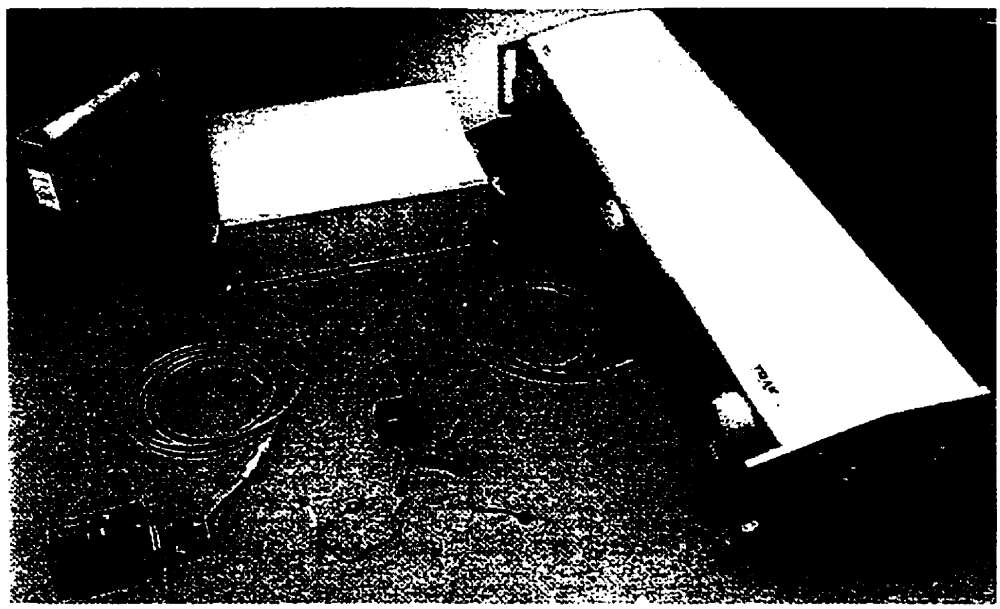

Figure 1.4 : OPTOTRAK/3010 (position sensor, system control unit, PC interface card and cables, and strobes and marker kit).

The system is very safe and causes no danger for the patient. A good quality OptoTrak costs about $100,000.00. Full 6 degrees of freedom is available by using this system. It could be ordered and within a short period of time can be purchased. There is the disadvantage of shadowing because of using cameras, as well as artefacts problem. However the system provides a good range and no mechanical attachment is necessary. The system connects to a standard PC/AT computer platform. Standard software is provided with Optotrak system for camera calibration, data collection, and real time or post hoc viewing of data. An optional Data Analysis Package (DAP) provides many

functions for manipulating the collected data. The package also provides the tools for producing hard copy of charts and graphs.

1.4 REVIEW OF EXISTING 3D INSTRUMENT

1.4.1 Simple form of Goniometers

ISL or Goniometers are devices designed for *in vivo* evaluation of rotational flexibility of the human knee. For example the triaxial goniometer non invasively mounts on the leg and directly measures the relative three degrees of freedom of rotations of the knee, sequentially and independently. The goniometer incorporates several unique design features which enhance the accuracy of the measurement. The load stand applies pure varus /valgus and internal/external axial moments either individually or in combination with the use of motors controlled by the subject (Mills et al., 1991).

Goniometers measure the relative rotation of a given joint. The simplest form of the goniometer is a single-axis potentiometer (see figure 1.5). As the shank flexes with respect to the thigh, the arm-C moves along the resistor AB, thereby changing the output resistance of the potentiometer. By providing a constant voltage-drop across the fixed ends of the resistor- Vi, the output voltage-V0 will change, tracking the change in the flexion angle of the knee. Clearly, the goniometer's centre of rotation needs to match the joint's centre of rotation in order to get a valid measurement.

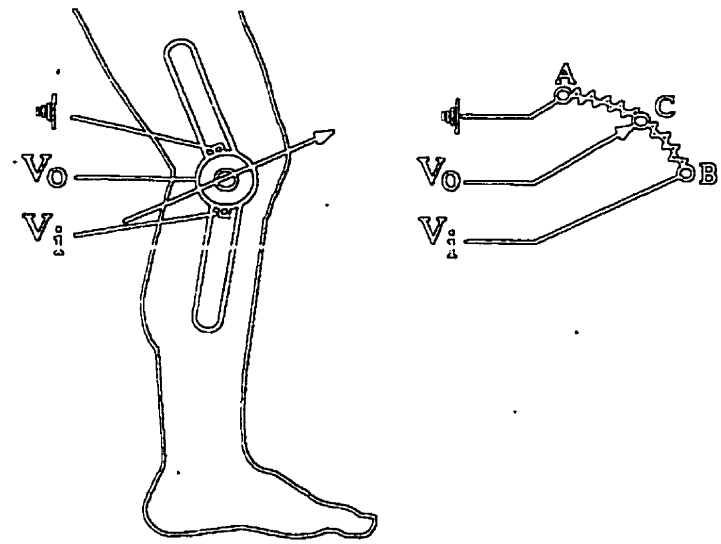

Figure 1.5: The simplest form of Goniometer

1.4.2 Triaxial Goniometer

A different design, based on a flexible cable instrumented by strain gauges, was introduced by Penny & Giles company (Blackwood, Gwent, UK). This design does not require the specification of the joint center and it can provide one or two rotational degrees of freedom per joint, however detailed studies of its accuracy, reliability and reproducibility are not yet available. Some studies have reported small errors produced in a goniometric system (less than 1 mm in translation and less than 1° in rotation (Suntay *et al*, 1983, Lewis *et al*, 1988).

The system has the accuracy of one degree of rotation, and one millimetre displacement. Lengths of order of 4 mm have an accuracy of 0.7 mm and longer lengths of order 3 cm have the accuracy of 1 to 2 mm. The sizes of Goniometers are variable because of its variety (Magnetic Goniometers, Optical Goniometers, mechanical Goniometers , etc.). See figure 1.6.

Figure 1.6 : Source; Mills et al. 1991; The triaxial goniometer attached to a test subject

Linkages are safe although somewhat awkward. Because the system needs to be custom made to fit the range requirements, this implies inherent manufacturing costs. It can provide 6 degrees of freedom. Many systems which are designed to uncover specific motions need software developments to permit full 6 degrees of freedom. The system requires regular verification of calibration and sometimes has problems of sticktion and alignment. For complicated motions, it is possible that linkages interfere with the patient's limbs. Using a single-axis goniometer to study the rotation of the knee joint presents two major difficulties:

1. *Cross Talk*: The contamination of the measured angle of rotation by an angle that is perpendicular to the measured angle which arises from an artifactual motion of the gonimeter due to an angular rotation unrelated to the rotation of the monitored degree of freedom.

2. *Mechanical constraining*: Modification of the joint's angular rotation due to the mechanical coupling of the adjacent links by the goniometer. The latter arises from the inability of the goniometer to follow the true rotation of the joint, thereby hindering the natural motion and introducing an artifactual measurement (Ladin et al., 1989). The relative joint rotations measured by such systems do not allow the incorporation of the measurements directly into the dynamic equations of the multi-link system. Therefore, additional information is needed in order to obtain the joint loads. The tight attachment of the goniometer across the joint presents a mechanical constraint limiting the motion of the soft tissues, thereby possibly modifying the natural motion of the joint. The cumbersome (sometimes heavy) nature of the goniometric system and the difficulty in accommodating different size limbs can be counted as disadvantage. The difficulties involved in monitoring either joints that are surrounded by large amounts of soft tissue (e.g. the hip) or that involve large structures with relatively small attachment areas (e.g. the ankle/subtalar complex) as well as non-linear effects that are inherent in a mechanical linkage system such as stick-slip and backlash problems are also among disadvantages (Ladin et al., 1991).

1.4.3 Joint Laxity Measurement device

Joint Laxity Measurement device by A. Fraser et al. was patented in 1987. The instrument is based on use of electrogoniometer with thigh restraints and a chair with dynamometer. A display screen with a computer is used for registration purposes. The subject is seated in the chair and femur is secured by restraining the thigh. The electrogoniometer is place on the tibial part for knee laxity evaluation. This system objective was to provide a method for measuring parameters related to the stability of

joints in human, to over come the poor accuracy and lack of completeness of the measurement throughout normal range of motion of the knee. In their method they secure a reference portion of the joint (that portion of the joint closest to the body) to a fix location and a three dimensional digitisation of the size, shape, position and coordinate system of the two portions is performed. By applying a force to the reference portion of the joint, a soft tissue compensation is performed. This will determine the amount of motion of the reference portion due to the applied force. Different forces are applied to the relative portion of a joint, which is moveable relative to the reference portion. This will result into the motion of relative portion with respect to the reference portion. Fraser *et al.* claim the present method is applicable to any joint in the human body where it is possible to restrain the reference portion of the joint. One of the biggest problems of this type of instrument is that it cannot be used for gait analysis and because of its limitation it will not be a good choice for kinematic measurements (Fraser et al. 1987).

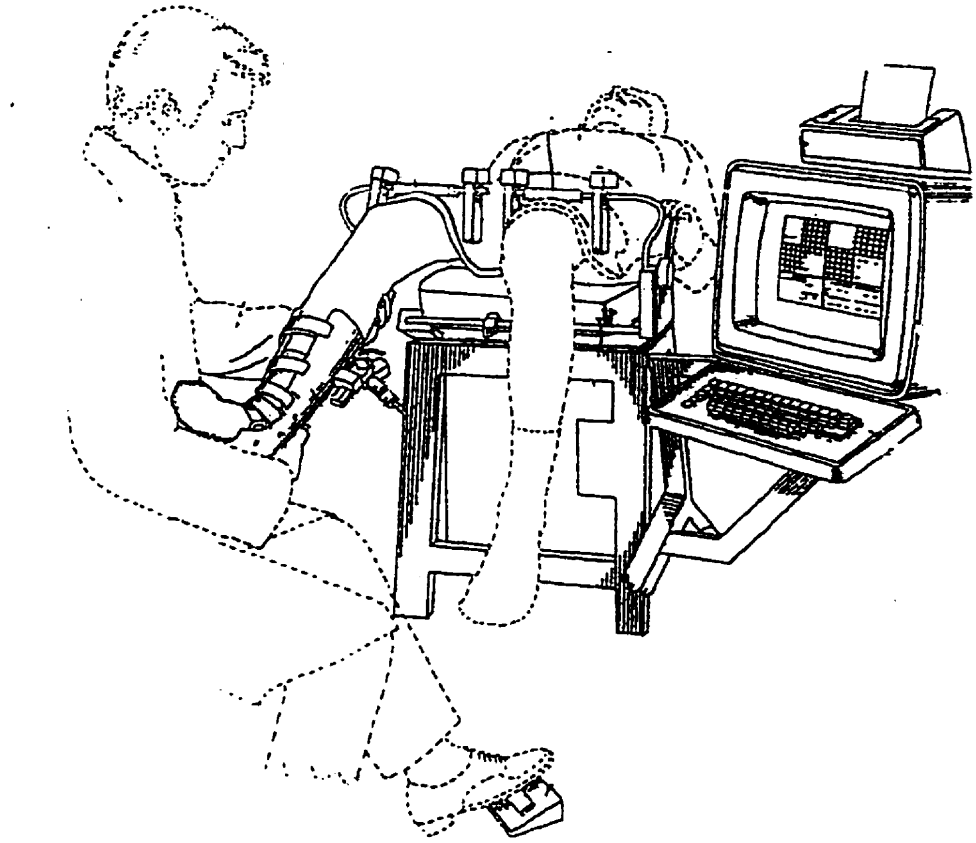

Figure 1.7 : Source: Fraser et al., 1987. Joint laxity measuring device

1.4.4 Dynamic sagittal knee test apparatus

Dynamic sagittal knee test apparatus is another example of a 3D analyzer which was patented by S. Lamb *et al.* in 1990. The dynamic knee test apparatus is essentially a skeletal structure that includes an upper thigh portion and a lower leg portion with an interconnecting spanning link portion which includes a linkage and a transducer assembly to allow both tibial rotation and varus-valgus moment angulation to be determined without reconfiguring the linkage assembly. The apparatus includes a patella assembly with an additional transducer for measuring anterior-posterior displacements of the tibia relative to the femur. This instrument is capable of measuring knee laxities wherein the patient walks or sits.

Since the knee does not operate like a hinge with a single axis of rotation, but rather the tibia moves in a complex motion with respect to the femur, the tibial frame cannot be directly connected to the femoral frame in measurement devices. The fact that this instrument connects femoral and tibia parts regardless of the number of links that is used is counted as one its major disadvantages. To our knowledge the most complex linkage cannot reproduce the natural movement of knee. The numerous linkages that has been used in this apparatus calls for quality control throughout each experiment (Lamb et al., 1990).

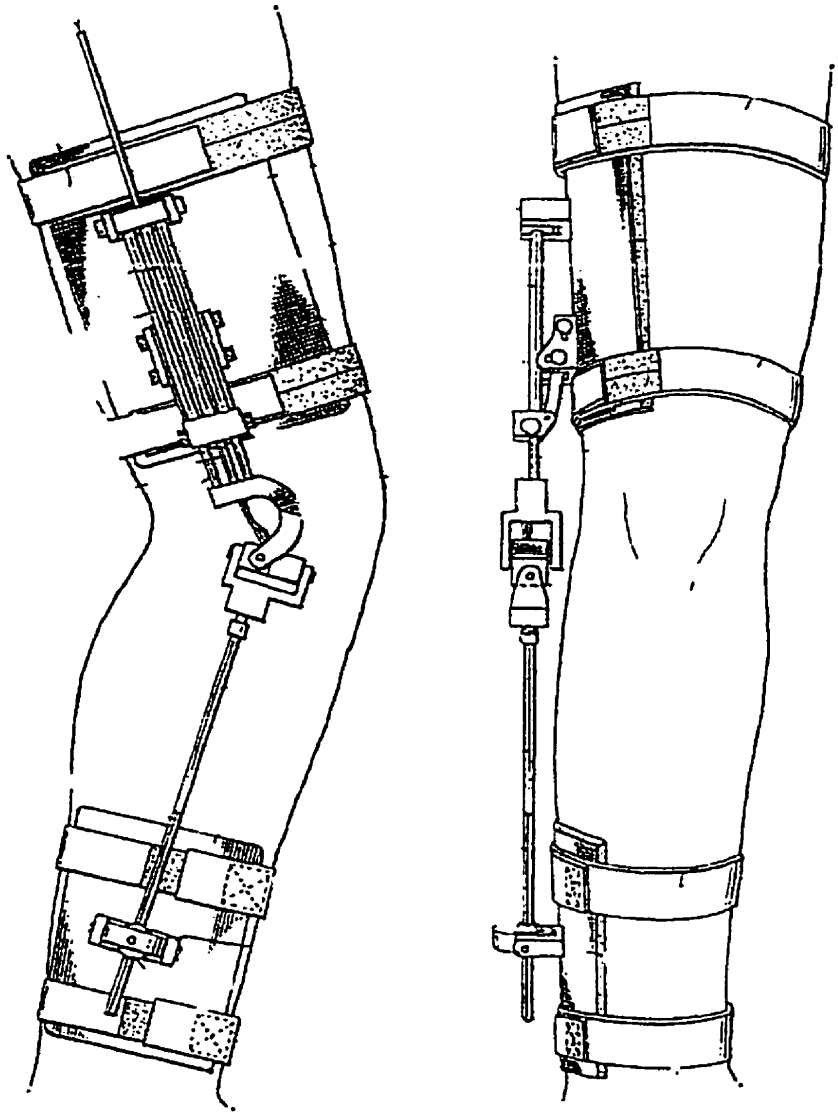

Figure 1.8: Source; Lamb et al., 1990. Dynamic Sagital knee test apparatus.

1.4.5 Three-plane Goniometer

Dynamic joint motion analysis technique by P.C. Macleod *et al.* in 1989 is also a 3D measuring system. This apparatus (three-plane goniometer) contains three small potentiometers which are closely spaced together to measure rotation of the knee about three different axes. The system is based on two principal parts (femoral and tibial)

which are connected by a yoke right on the knee joint. By a quick look at this instrument, one can conclude that the this system cannot follow the movement of knee joint.

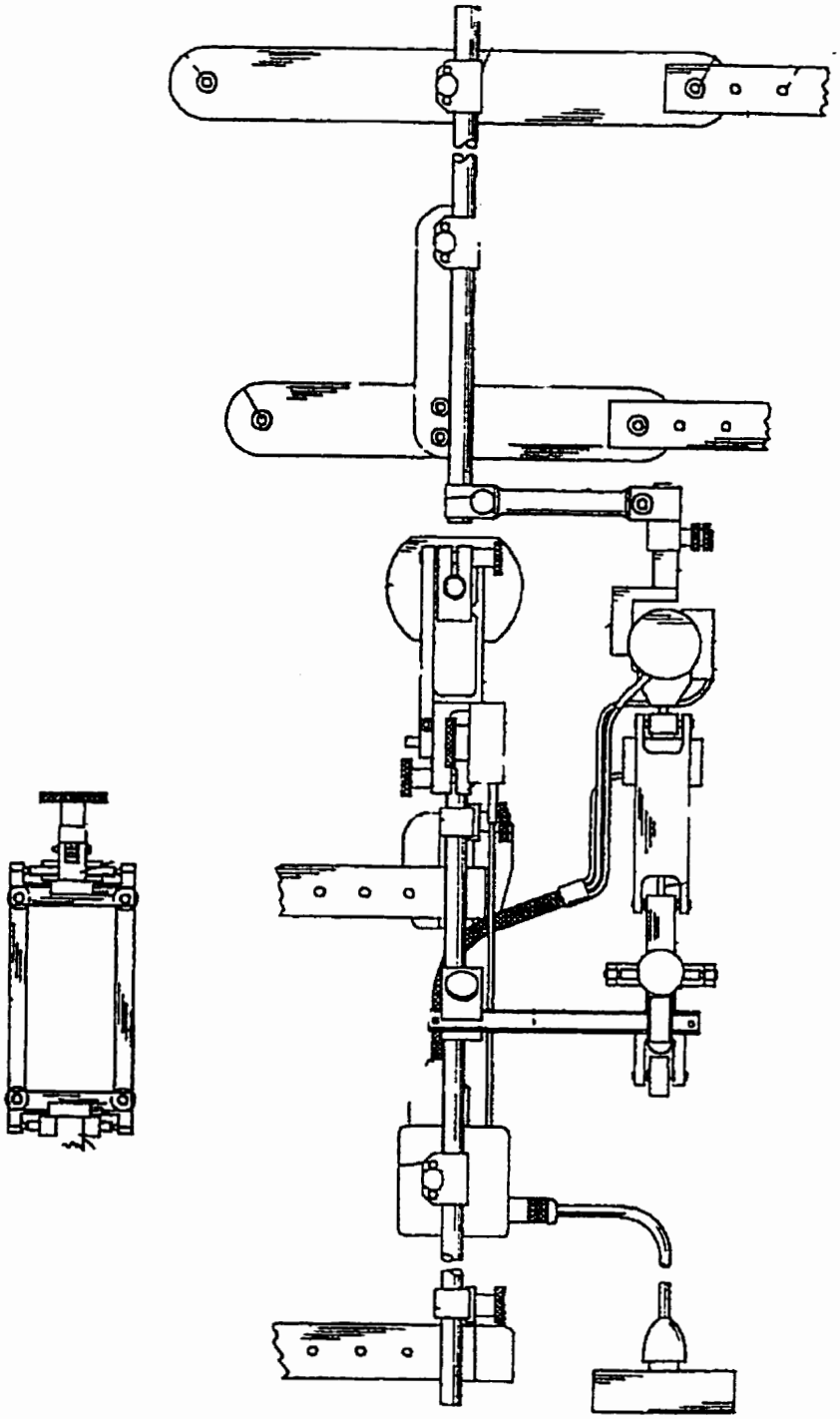

Figure 1.9: Source: Macleod et al. 1989. 3D measuring system (3-plane goniometer).

Since the whole system is connected together by a yoke and is attached by straps on the thigh and tibial part, a slight movement of one part, whether it is the femoral or the tibial part, causes the movement of the rest of the system. This type of apparatus suffers from cross talk such as the contamination of the measured angle of rotation by an angle that is perpendicular to the measured angle and mechanical constraint like modification of the joint's angular rotation due to the mechanical coupling of the adjacent links by the goniometer. The relative joint rotations measured by such systems do not allow the incorporation of the measurements directly into the dynamic equations of the muti-link system. Therefore, additional information is needed in order to obtain the joint loads. The tight attachment of apparatus across the joint presents a mechanical constraint that limits the motion of the soft tissues, thereby possibly modifying the natural motion of the joint. They are cumbersome and have difficulty accommodating different size limbs. There are inherent, nonlinear effects, such as stick-slip and backlash problems, in the mechanical linkage system.

1.4.6 A Goniometric device using LEDS

A goniometric device by E.J. Fine *et al.* was patented in 1987. They claim that this system is for monitoring the relative angular position of two human body portions hinged at a common joint and utilizes a brace mechanism, transducer circuits, an array of selection light-emitting diodes (LEDS), an array of movement response LEDS, indicia associating with each LED array with a series of angular values, preselection circuits and sensing circuits. These types of devices could be used primarily for obtaining rough (and inexpensive) approximations of some joint rotations or for detailed studies of a single joint in a controlled laboratory setting. This system also could not be considered a suitable choice for kinematic indices measurement since it uses a brace mechanism. As we have seen above, any type of mechanical joint compromises the natural movement of the joint and it is necessary to do quality control.

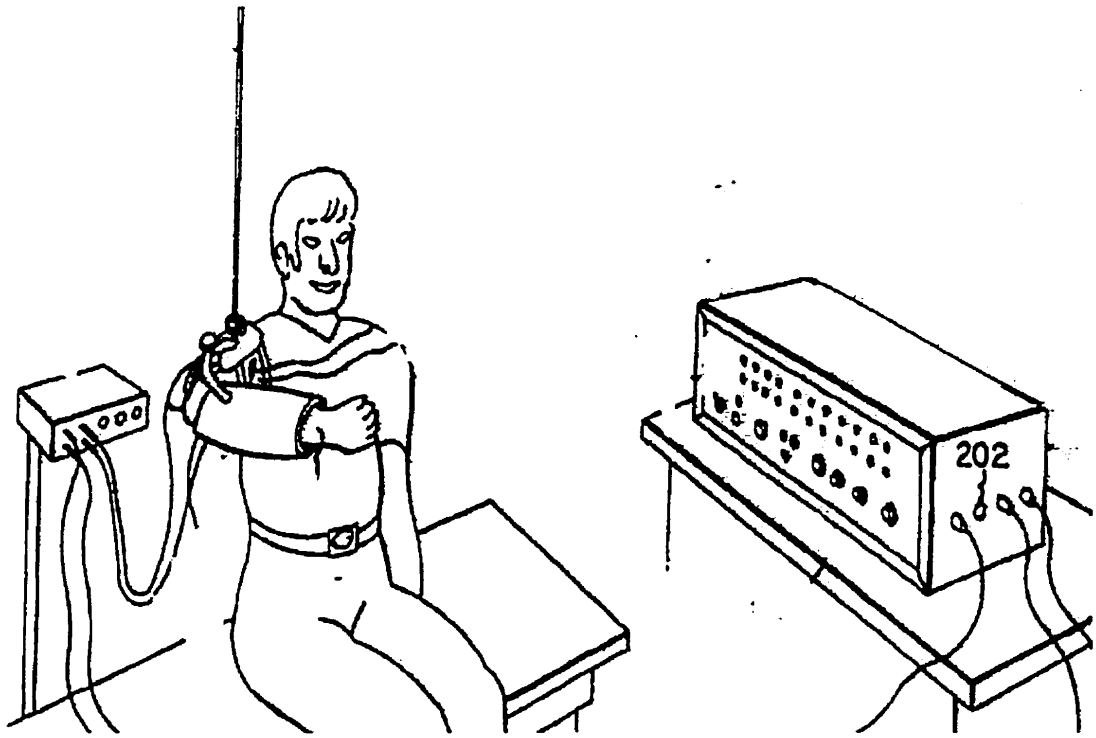

Figure 1.10: Source : Fine et al. 1987. Goniometric device

1.5 DISCUSSION

By looking at different tracking systems we can conclude that magnetic, acoustic and optical are among the major tracking system which one can currently use for kinematics analysis.

Magnetic systems emit either an AC or a DC magnetic field about three orthogonal base coils. The projection of these fields onto smaller orthogonal coils found in the receiver gives nine elements of information. Subtracting for the earth's ambient magnetic field, in the case of the DC systems, the position and the orientation of the sensor can be found with respect to the base emitter without a physical connection between the two. Accuracy of magnetic systems is of order of 2.5 mm rms in position and 0.5 degrees in rotation. However these systems can be calibrated to increase their position accuracy to 1 mm rms. One disadvantage of the system is its sensitivity to certain metals which can

perturb magnetic fields. Magnetic system are very flexible since they have no mechanical emitter-receiver linkage, other than a small cable connected to the sensor, and the magnetic field can pass through most solid objects. Several sensors can be used per emitter to track several limb segments simultaneously.

For 3D analysis, sonic systems require the placement of at least 3 ultrasound emitters on each limb segment and at least 3 receivers fixed in the laboratory frame. It is possible to calculate the position of the emitter and therefore compute the orientation of the limb with respect to the receivers based on the time of arrival of sonic signals. Acoustic systems have been used for human movement analysis for many years (Andrews et al., 1979 and Siegler et al., 1988).

Resolution of these systems has been found to be of order of 1 mm in position, and orientation error depends on the distance between emitters and receivers. One of their disadvantages is that the signal does not pass through the tissue or dense object. Therefore, neither the subject nor other objects must be placed between the transmitter and receiver. These systems are also sensitive to humidity and air currents. Ultrasound system such CMS 70P Measuring System are somewhat new and are worthwhile investigating for future.

Optical (or camera) systems are either passive or active marker based and can use several different light sources. Active optical systems have markers which emit light on the moving body which are tracked by cameras. Passive systems use markers placed on the moving body which reflect light from either ambient or source illumination. Optical systems offer the same freedom of movement as magnetic and ultrasound systems. The accuracy of cheaper optical system is comparable to their magnetic and acoustic counterparts. One of the disadvantages of this system is that they rely on a direct line of sight between the marker and the camera. These systems can suffer from artefacts due to reflections and their set-up can in some cases be time consuming, requiring on-site

calibration and proper camera placement. Optical distortion must be corrected for accurate measurements.

For biomechanical quantification of joint movement, the implicit assumption of optical method is that the measurement of the markers' movements reflects the movement of the underlying bone. However, soft tissue's motion about the bones introduces an experimental artefact which can be an order of magnitude higher than the error from the instrumentation used (Cappozzo et al. 1995). This artefact is acceptable for certain studies requiring low levels of kinematics accuracy.

ISL systems can be very accurate of the order of 0.1 mm and do not suffer from either metallic or atmospheric interference, as do some of the other systems. A disadvantage of the use of a robot-like linkage is the slight awkwardness of its use during complex movements and the limit in the number of segments which can be analysed simultaneously. Another problem with such system is the friction between links which block the system. For the above reasons, ISL system have remained either as tools for obtaining a rough and inexpensive approximation of some joint rotations, or as tools for detailed studies of a single joint in controlled laboratory setting.

1.6 CONCLUSION AND RECOMMENDATION

The selection of measurement system for studying human motion requires carefully matching the nature of the motion, the environment in which the motion is performed and the properties of the measurement system. The high cost of some of the more general systems usually means that a system is purchased for a laboratory with expectation that it could be used in a variety of studies. In order to make optimal use of the measurement system, it is imperative to consider the type of mounting to the human subject, the complexity of the joint movement, and the limited range of rotations and certain other criteria which we have discussed in this chapter.

Errors due to skin movement artefacts can be of the order of 4-26 mm (Ganjikia et al. 2000b, Sati et al. 1996) whereas navigation system errors are of the order of millimetres. This affirms the fact that skin movement is the largest obstacle for a detailed non-invasive analysis of human movement. Consequently, the accuracy specification should not be a predominant factor in the choice of a navigation system technology for an analysis where sensors are mounted on the surface of the skin, since all the sensors mentioned above have error at least one order of magnitude smaller than the error arising from the marker-bone displacement. Considering the magnitude of skin movement artefacts, very accurate, and correspondingly expensive, systems are excessive for many biomechanical analyses.

After a careful study of tracking systems, we have concluded that a magnetic system such as Fastrak would be an appropriate system to be used for knee kinematics analyses. However, we should take into account the problems caused by magnetic perturbation while running an experiment.

The study of different existing measuring instrument demonstrated that none of them to our knowledge are capable of measuring kinematic indices with good accuracy due to their limitations. Most of these instruments propose the use of mechanical linkage. This is one of the largest limitations for knee kinematic measurement. To this day no mechanical linkage is capable of providing the natural movement of knee. For this matter our research group has proposed the use of the 3D knee analyser.

1.7 OBJECTIVES OF THESIS

The aim of this work is to use the 3D knee analyser in clinical setting to overcome the majority of the shortcommings that other existing apparatuses encounter. To this end our research group (Laboratoire de recherche en Imagerie et Orthopédie, LIO) has developed a 3D knee analyser to evaluate knee in 3D and in motion. The 3D Knee Analyser is based on magnetic sensors, an exoskeleton attachment system to fix the sensors on the knee of the subject, a computer and a C program to register the movement numerically, accompanied by a graphical representation of knee. The use of exoskeleton attachment system provides us with a quantitative measure of kinematics indices. The results should be reproducible over different days for intra- and inter-subjects. Our objectives are as follows:

1. The primary objective is to validate the attachment system through a fluoroscopic study. To achieve this, the first step is to study the movement of markers on the skin in fluoroscopy. Then observe the movement of markers on the attachment system when it is placed on the knee. Compare these two results to demonstrate the usefulness of attachment system and to show that the use of exoskeleton attachment system reduces the movement of skin with respect to the underlying bone. Validate the analysis program through two different methods: an experimental and a mathematical method.

2. The second objective is to look at the kinematics indices (abduction, tibial rotation) and their correlation coefficients in three different positions, i.e standing, squatting and sitting, to find out the most reproducible movement.

3. The third objective is to investigate whether having a charge has an effect on the reproducibility of kinematic measurements.

4. Fourth, determine an appropriate reproducible movement between flexion-extension in standing and sitting positions while having a charge over the ankle.

5. Finally demonstrate which method would result in a more uniform and reproducible data over different days between a 3-point and 8-point methods of determining the functional axes.

The fulfilment of these objectives will allow one to use the non-invasive 3D knee analyser in clinical settings. This would initiate the formation of a database for kinematic indices of normal knee movement measurements.

CHAPTER 2

ARTICLE 1: 3-D KNEE ANALYZER VALIDATION BY SIMPLE FLUOROSCOPIC STUDY

2.1 Situation of article in thesis

Looking at literature many researchers have concluded that movement of skin with respect to the underlying bone is large source of error. This movement have to be reduce in order to improve the kinematics measurements of knee in non-invasive fashion. It is essential to have instrument which allows us to measure 6 degrees of freedom (3 translations, 3 rotations). We have selected to use magnetic sensors as we discussed in detail in chapter one. However these sensors cannot be mounted on the skin because of the inaccuracy that skin movement causes in measurements. To this end our research group (LIO) have proposed the use of 3D knee analyzer. 3D knee analyser includes an exoskeleton attachment system, a kinematic tracking system, a computer system, a display screen, and a program with a user interface in C environment for calculating the kinematic indices which, in turn, allows one to follow the 3D movement, both position and orientation, of femur and tibia of healthy subject. In this chapter we will describe the exoskeleton attachment system in detail. I also demonstrate by a fluoroscopy study that this system reduces the movement of skin with respect to the underlying bone. The method of analysis is validated in two different ways throughout a mathematical knee modelling and the experimental method by using of plastic human size knee model.

3-D KNEE ANALYZER VALIDATION BY SIMPLE FLUOROSCOPIC STUDY

Shafagh Ganjikia[1,2], Nicolas Duval[1,2], L'Hocine Yahia[1,2], Jacques de Guise[1,2,3]

[1] Laboratoire de recherche en Imagerie et Orthopédie, Centre de recherche, Centre hospitalier de l' Université de Montréal (CHUM) – Hôpital Notre-Dame, 1560 rue Sherbrooke Est, Montréal, Qc H2L 4M1, Canada

[2] Groupe de recherche en Bioméchanique/Biomatériaux, Ecole Polytechnique, C.P. 6079, Succ. Centre-ville, Montréal, Qc H3C 3A7, Canada

[3] Laboratoire d'Imagerie, de Vision et d'Intelligence Artificielle, Ecole de technologie supérieure, 1100, rue Notre-Dame Ouest, Montréal, Qc H3C 1K3, Canada

Accepted April 2000 for publication in « The Knee »

Key words: 3-D knee analyzer, exoskeleton attachment system, knee fluoroscopy, skin marker, accuracy measurement, 3-D movement estimation

Correspondence to: Shafagh Ganjikia, Biomedical Engineering Department, École Polytechnique, P.O. Box 6079 « Downtown » Station, Montreal, Quebec, Canada H3C-3A7;

Tel : (514)340-4711 Extension 4198; Fax: (514) 340-4611; e-mail: ganjikia@yahoo.com

2.2 Abstract

A fluoroscopic study was performed on 5 healthy subjects to determine the reduction of skin movement with respect to the underlying bone by using a knee exoskeleton attachment system. Root mean square (RMS) errors of marker movements about the abduction-*X* (RMS*Rx*) and tibial rotation-*Z* (RMS*Rz*) axes and displacement in the *XZ* plane (RMS*pxpz*) were calculated, once by placing markers directly on the skin and once on the exoskeleton attachment system. Our results demonstrated that RMS*pxpz*, RMS*Rx* and RMS*Rz* were reduced by a factor of 6 (min 1.8, max 26), 4.3 (min 0.75, max 21) and 6.2 (min 2, max 26.4) on average respectively for 4 subjects out of 5.

2.3 Introduction

The knee is one of the most complicated synovial joints in the musculoskeletal system. Kinematic studies allow the evaluation of surgical operations, such as ligament reconstructions, the inaccurate positioning of condylar prostheses, diagnostic methods for assessing ligament injuries and injury mechanisms in the knee joint. Flexion-extension of the knee leads to a combination of rolling and sliding movements, and consequently forming the components of abduction/adduction and internal/external rotations. Combined motions are well known in biomechanics. It is difficult to quantify them because of their small amplitude, and accurate tools are generally not available. For example, motion-tracking devices classically use markers on the skin, but skin slippage during analysis makes it difficult, or sometimes even impossible, to precisely determine combined motions (Rhyne et al., 1998).

Many researchers such as Murphy *et al.* (1984), Holden *et al.* (1994), Macleod and Morris (1987), Lafortune *et al.* (1992) and Cappozzo *et al.* (1995) were among the first to study movements between the skin and bone during movement analysis. Murphy et al., (1984) have employed invasive bone pins, while Holden *et al.* (1994) used "halo rings", and Macleod and Morris (1987) investigated the relative distance between several skin-mounted markers during walking. Lafortune *et al.* (1992) utilized video X-ray fluoroscopy to obtain qualitative data on skin movement over the lateral condyle of the knee, and the same approach was adoptd by Cappozzo *et al.* (1995). Some of these approaches were invasive or qualitative. In more recent works, Cappello *et al.* (1997), Fuller *et al.* (1997), Chèze *et al.* (1998,1995), and Deluzio *et al.* (1997) all agree that non-invasive methods can be severely corrupted by experimental errors. The largest fraction of such errors is associated with relative movement between externally located markers and the underlying bone, due to the interposition of both passive and active soft tissues.

In 1996, our research group (Sati et al. 1996) proposed an exoskeleton attachment that allowed quasi-solid fixation of magnetic movement sensors with respect to the femur and tibia. This study demonstrated that the system was able to substantially reduce skin movement. However, the original design was modified to improve its ergonomics (practicality, stability and rapidity), comfort and accuracy aspects such as precision of installation.

Our research group developed a knee analyzer, which includes an orthoplastic exoskeleton attachment system a kinematic tracking device (sensors) with a computer a screen for graphical display and a C program with a user interface for calculating kinematic indices. The system allows us to follow 3-D movements (both position and orientation) of the femur and tibia of *in vivo* subject (Figure 2.1).

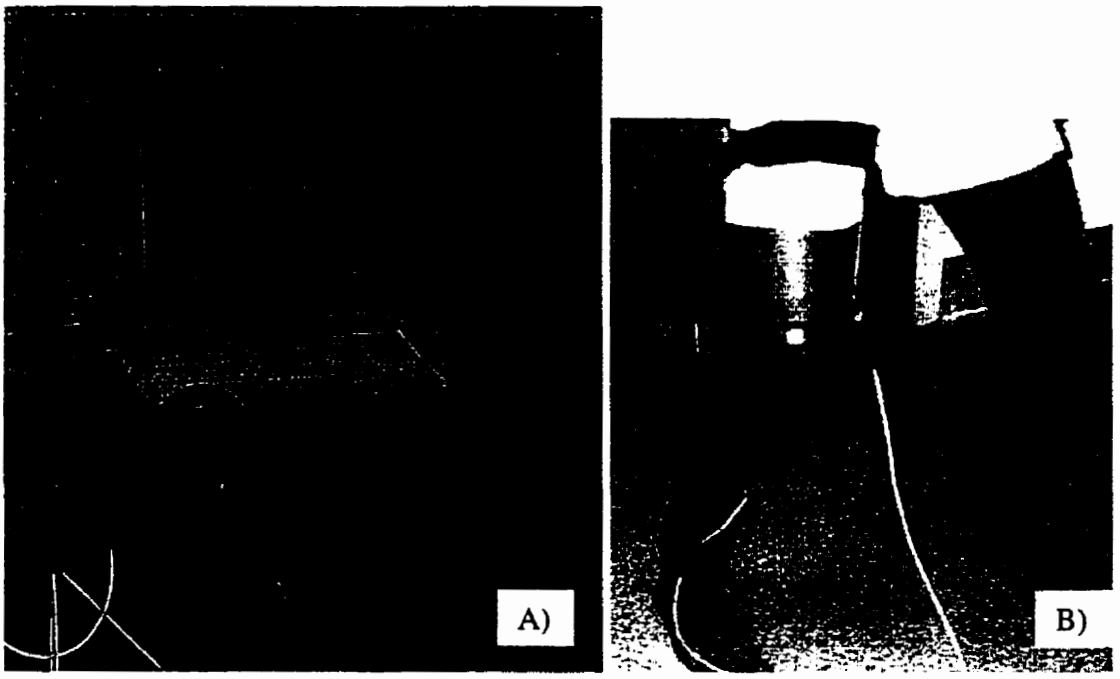

Figure 2.1: A) 3-D knee analyser. B) Exoskeleton attachment system with magnetic sensors.

The goal of the present study is to demonstrate that the improved exoskeleton attachment system effectively reduces skin movement with respect to underlying bone. For this

purpose, we have conducted fluoroscopic experiments to determine the effectiveness of our attachment system by comparing the movement of markers placed on the skin with their movements when they were placed on the exoskeleton attachment system.

2.4 Materials and methods

2.4.1 Exoskeleton knee attachment

Previously, 2 different models had been developed and evaluated. The first version was developed in 1996 (Sati et al. 1996a-1996b), and the second system was designed and fabricated in 1998 (El Maach, 1998). After studying the 2 versions, we took into account all the points that seemed to have been overlooked (Tables 2.1 and 2.2).

Table 2.1: Design criteria of the exoskeleton attachment system (femoral part)

Femoral part	Version 1	Version 2
Ergonomics ➤ Practicality 1. Flat orthoplast 2. Circular orthoplast 3. Medial bar 4. Bridge	1. Both orthoplasts are adjustable. 2. Limited adjustment provided. 3. No place to fix velcro straps. Medial bar is not removable.	1. Only 1 of the orthoplasts is adjustable. 2. Adjustment is made by changing to a fixed position. 3. It has a place for velcro straps. Easily removable.
➤ Stability 1. Flat orthoplast 2. Circular orthoplast 3. Medial bar 4. Bridge	1. Stable (disto-proximal, medio-lateral and antero-posterior). 2. Not stable (antero-posterior). 3. Depends on muscular mass. 4. High tolerance to torsion. High tolerance to flexion-extension.	1. Depends on anatomy. 2. Not stable (antero-posterior). 3. Stable (disto-proximal, medio-lateral and antero-posterior). 4. Low tolerance to torsion. Sufficient tolerance to flexion-extension.
➤ Rapidity of installation	➤ Time-consuming	➤ Rapid
Comfort 1. Flat orthoplast 2. Circular orthoplast 3. Medial bar 4. Bridge	1. The form is not symmetric. 2. It is filled with silicone. The form is conical. 3. Rigid. 4. Limited expansion.	1. The form is symmetric. 2. The form is cylindrical. It is filled with foam. 3. Soft. 4. Rigid.
Degrees of freedom	➤ 6 degrees.	➤ 6 degrees.
Accuracy	➤ Circular orthoplast not adaptable for different anatomies. ➤ Accurate in fluoroscopie study.	● The circular orthoplast installation is not precise. ➤ Not tested because of discomfort.
Safety	100% safe.	100% safe.
Cost	Under $5000.	Under $3000.
Size and weight	➤ 200 g.	➤ 125 g.

Table 2.2: Design criteria of the exoskeleton attachment system (tibial part)

Tibial part	Version 1	Version 2
Ergonomics ▸ Practicality ▸ Stability ▸ Rapidity of installation	▸ No strap for attachment. ▸ No place for magnetic sensor. ▸ Rapid.	▸ Strap for attachment. ▸ No place for magnetic sensor. ▸ Rapid.
Comfort	▸ Comfortable.	▸ Comfortable.
Degrees of freedom	▸ 6 degrees.	▸ 6 degrees.
Accuracy	▸ Accurately placed.	▸ Accurately placed.
Safety	100% safe.	100% safe.
Cost	Under $200.	Under $200.
Size and weight	▸ 50 g.	▸ 50 g.

Below, we give a brief description of the exoskeleton attachment system, which consists of 2 different parts. The femoral part contains 3 orthoplasts, 2 flat and 1 circular, a bridge that holds the orthoplasts together, and a bar on the medial side that is connected to the bridge and can be attached on the thigh. The tibial part is a simple flat bar that can be affixed to the shank by straps.

Connecting the sensors to the skin is complicated because of the large amounts of surrounding soft tissues and anatomical structures that slide between the skin and underlying bone. Therefore, the points selected should have minimal movement. However, this system must have flexible components which do not compromise the accurate 3-D measurement of knee movements.

We will take a closer look at the exoskeleton attachment system to gain a better understanding of how it is positioned on the subject's knee. In Figure 2.2, on the lateral side, the attachment system is placed on the superior part of the posterior condyle. The orthoplast is positioned between the ilio-tibial band and the biceps femoris. On the

medial side, a large circular orthoplast is placed on the femoral epicondyle, and the third orthoplast is positioned on the adductor tubercule behind the adductor magnus.

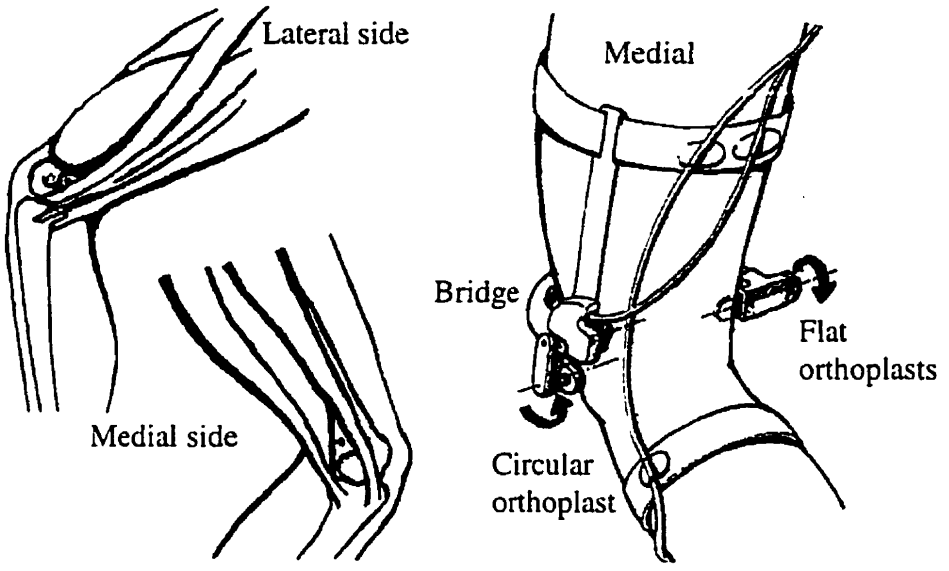

Figure 2.2 : The exoskeleton attachment system. On the lateral side, the femoral part is positioned on the superior part of the posterior condyle. The orthoplast (1) is placed between the ilio-tibial band and biceps femoris. On the medial side, a large circular pad or orthoplast (2) is positioned on the femoral epycondyle and the third orthoplast (3) is positioned on the adductor tubercule behind the adductor magnus. The tibial part is simply positioned on the tibial bone.

The tibial part fixes easily on the tibial bone and is solidified by 2 straps, one close to the tibial plateau and the other lying on the ankle.

We believe that for a person with minimum knowledge of the instrument, installation should be easy and quick. The system is used in a clean environment and should be desinfected with alcohol after each usage.

As a result of comparing of version 1 and 2, a third model was designed and fabricated in 1999. The new design tries to adopt and adjust itself to different anatomical shapes. Analysis of the first 2 versions of the exoskeleton attachment system revealed the need

for many improvements which were incorporated in the new system. For example, the system can now be easily installed in a very short time period. If placed correctly, it should be comfortable. Using a soft medial bar on the femoral part (adjustable with respect to thigh size) is a great advantage to solidify the system, which also contains a box on the medial side of the femoral part for magnetic sensors to eliminate the risk of sensor displacement during the experiment. The medial circular orthoplast has broadened the range of previous models for easy adjustment to different anatomies. The bridge is made rigid to reduce unwanted movements during flexion-extension. Dilatation of muscles and soft tissues is controlled by springs in the orthoplast. In the tibial part, the magnetic sensors are fixed by screws and stay solidly on the tibia by attaching Velcro straps.

2.4.2 General theory

X-rays have been used to produce medical images ever since their discovery by Wilhem Rontgen in 1895. There are 2 procedures of X-ray diagnosis that differ in principle, namely, radiography and fluoroscopy (Andriacchi et al. 1987). In fluoroscopy, the patient's condition is examined by viewing the shadow images directly. This can be done on a fluorescent screen which converts X-rays to visible light. In fluoroscopy, X-rays are emitted from a tube, pass through the knee, and strike a fluorescent screen. The images are then intensified and recorded via video tape.

At this point we recall the method proposed by Sati *et al.* (1996a-1996b) to estimate the 3-D movement of markers relative to the underlying bones from 2-D projections obtained by fluoroscopy. This estimation will permit us to quantitatively verify the behaviour of the exoskeleton attachment system. Because of the point X-ray source, magnification varies by distance from the screen. To evaluate the magnification, 2 opaque rulers are fixed at a distance from each other according to the following linear equation:

$$mag(x) = mag_ruler + slope_{mag} * x \tag{2.1}$$

where mag(x) is the magnification at distance x from the ruler, and $slope_{mag}$ is the slope of magnification which is a constant that only depends on the source.

With this equation, we can find the following simple expression for $slope_{mag}$ by measuring magnification at 2 different points:

$$Slope_{mag} = \frac{mag(x_1) - mag(x_2)}{x_1 - x_2} \tag{2.2}$$

The images that we obtained are measured in pixels, and not in true physical distances. To find the true distances, we have to change the pixel sizes to millimetres by magnification. If we know that magnification at a certain point is, say, 10 pixels/mm, then 2 points that are 25 pixels apart from each other on the image are physically 25/10=2.5 mm apart. In our analysis, we need the true distances of objects located at different depths from the screen, and the above equations are the main tools for this purpose.

We also have to fix a reference system in the femur. This coordinate system is attached to the bone; therefore, in this reference system, coordinates of a point attached to the femur will remain unchanged during any kind of translational or rotational motion of the femur. To construct this coordinate system, we define the axis of the femur as the ***Z*** axis. Then, we consider the mid point of the Blumensaat line and through it, we draw a line perpendicular to the ***Z*** axis. The point of intersection will be the origin of the reference system, and this perpendicular line will be called the ***X*** axis. The ***Y*** axis is then obtained as the cross product of ***Z*** and ***X***. This defines a coordinate system that is attached to the femur and moves along with it. The main idea of our analysis is: to observe the movement of skin markers with respect to the femur in this reference system. Any change in the coordinates of these markers will reflect (qualitatively *and* quantitatively)

skin movement with respect to the underlying bone. The analysis is then reduced to finding the coordinates of a marker in the coordinate system attached to the femur. Using fluoroscopic images, we can determine the coordinates of markers in pixels, in the coordinate system defined by the image. The first step is to identify the reference coordinate axes in each image, followed by finding the coordinates of markers in the reference system, and then changing them to real physical distances with the magnification factor. Another important factor that is very crucial in finding the true coordinates, is the orientation of the femur. In fact, the projection of a 3-D object on a 2-D plane is what we observe in our images. Therefore, we need to know the orientation as well as the magnification factor. To find the orientation of the femur, we use the position of condyles with respect to each other. To understand this point better, consider Figure 2.3A which shows a ML (medio-lateral) view of the 2 condyles. From that figure, it is clear that in order to find rotation Rz about the Z axis and rotation Rx about the X axis, we need to measure Dx and Dz, respectively. Let us concentrate on rotation about the X axis. Even in the absence of any rotation, there might be a non-zero, Dz, since the bottom of the condyles may not necessarily coincide. Therefore, in a real movement with many images, we consider Dz in the first picture as the *reference* value, and in the subsequent images, we subtract the observed Dz in the first frame from the observed Dz in each frame. If f represents an arbitrary frame, then the true quantity that represents a rotation about the X axis for that frame, with respect to the first frame, is $Dz(f) - Dz(1)$, (Figure 2.3B). We then find the rotation angle, using this quantity and dc, the distance between the bottom of the condyles in the antero-posterior (AP) view (figure 2.3C). A similar calculation gives the rotation about the Z axis. From these images, we can easily estimate the 3-D value of the rotational angle. These calculations are depicted in Figure 2.3 and are given by the following expressions:

$$\delta z^{*}(f) = Dz(1) - Dz(f) \tag{2.3}$$

$$\delta z(f) = \frac{\delta z'(f)}{magML_{avge}} \tag{2.4}$$

$$Rx(f) = \arctan\left(\frac{\delta z(f)}{dc}\right) \tag{2.5}$$

$$corrz(f,i) = dYm(i).x\left(\frac{\delta Z(f)}{dc}\right) \tag{2.6}$$

Here, $\delta z'$ is the change in distal condyle projection for frame f, measured in pixels; δz is the true physical distance obtained through related magnification $magMl_{avge}$, dc is the total distance between the distal condyles, and $dYm(i)$ is the distance along the Y axis of the i-th marker in the reference frame (Sati et al., 1996a).

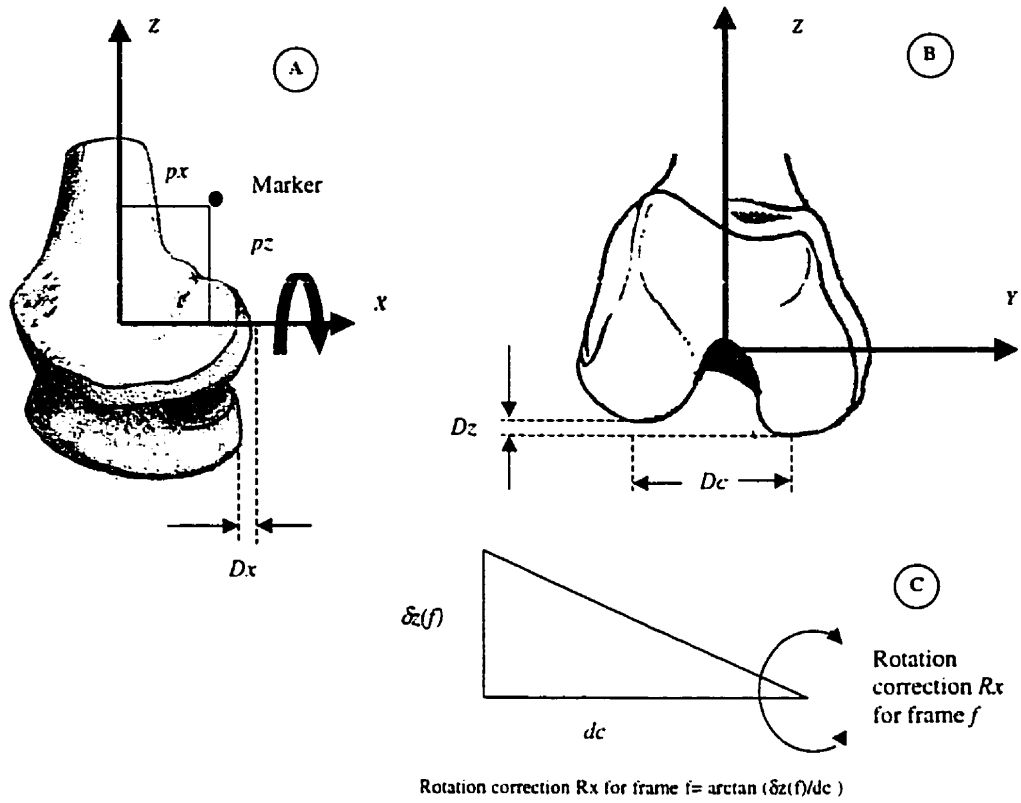

Figure 2.3 : A) and B) *Dx* and *Dz* are the main parameters used for 3-D rotational estimation. Any rotation about the *X* or *Z* axis will change the value of these parameters, and hence allows us to calculate the rotation. This will make it possible to find the true 3-D coordinates from a 2-D image. *Dx* and *Dz* values are scaled to give $\delta z(f)$ and $\delta x(f)$ which are then used to find the rotation angles. C) The rotation angles can be determined by using the right triangle whose sides are $\delta z(f)$ (or $\delta x(f)$) and *dc*, as shown.

The important parameters are:

1) *pmx*, *pmz*: the coordinates of markers in various images before 3-D estimation,
2) *px*, *pz*: the coordinates of markers after 3-D rotational estimation,
3) Root mean square (RMS) *pmxpmz*: the root mean square of *pmx* and *pmz*,
4) RMS*pxpz*: the root mean square of *px* and *pz*,
5) *Rx*, *Rz*: the rotation angles about the *X* and *Z* axis,
6) RMS*Rx* , RMS*Rz* : the angular accuracy of marker measurements,
7) Flexion angles for different images.

2.4.3 Experimental method

Five healthy volunteers with a mean age of 28 years and no history of knee problems were studied. These subjects were further examined by an orthopaedic surgeon to confirm their knee conditions. The duration of the test was approximately 2 hours with total X-ray exposure of 20 minutes. The risk associated with the X-ray dose was about 0.02 Rad/min. This exposure was comparable to a radiography of the dorsal spine. The protocol was approved by the Research Ethics Committee of the CHUM Research Centre.

Two different settings were considered. In the first, markers were placed on the skin, once on the lateral and once on the medial sides (Figure 2.4A) and to further reduce experimental errors during the analysis, we avoided putting markers on both sides at the same time. In the second setting, markers were placed on the attachment system which was then fixed on the knee (Figure 2.4B).

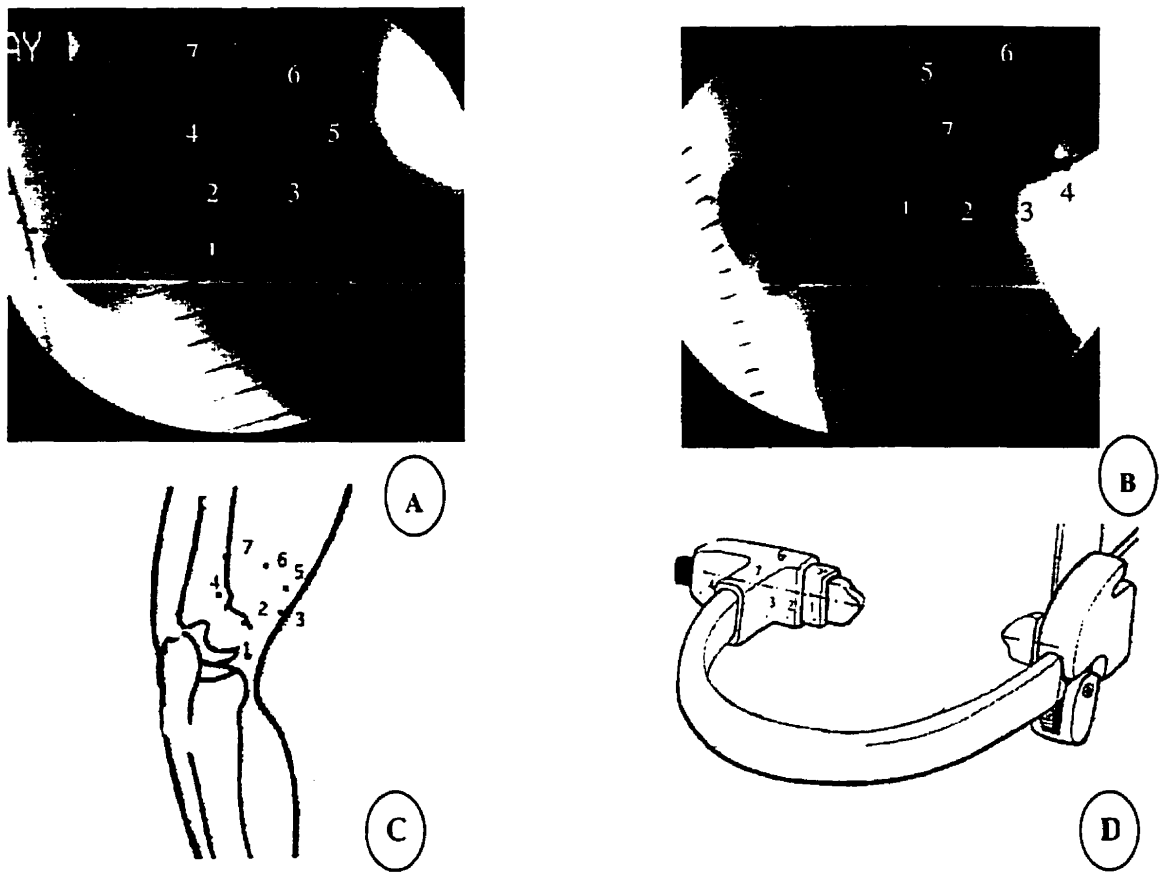

Figure 2.4 : A and C represent markers on the skin. B & D are markers on the exoskeleton attachment.

Each subject went through the same procedure in both settings. In each experiment, the first image involved 2 rulers. We took the fluoroscopic image of 2 spatially-separated rulers to obtain the magnification factors at different distances. For the second and third images, we made the subject face the source and then turn away from it by 90 degrees, keeping his/her body perpendicular to the floor. The gradual 90-degree turn allows us to distinguish between lateral and medial condyles on the images. Two static images (AP and ML) were digitized from this part to obtain the geometric parameters of the experiment (Figure 2.5).

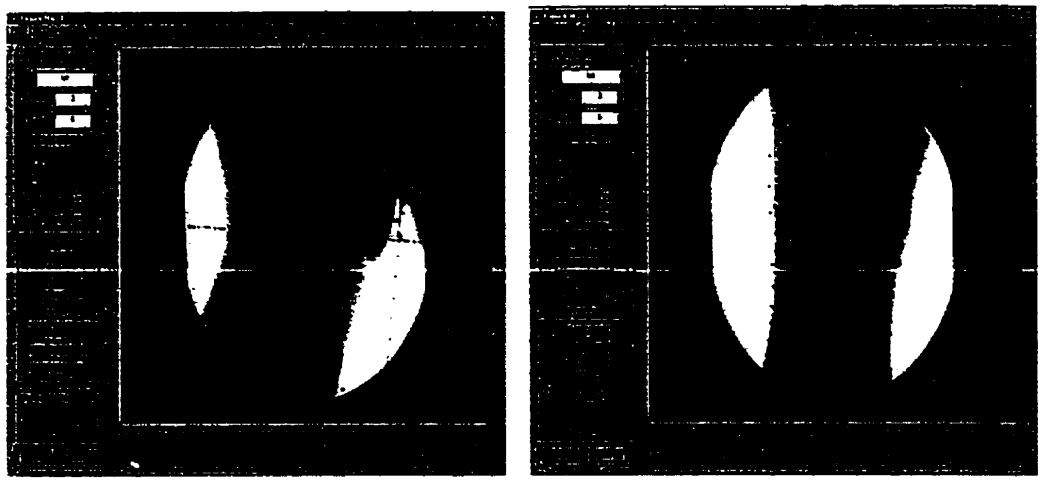

Figure 2.5 : Static images. A) Medio-lateral view. B) Antero-posterior view.

The last part of the experiment focused on the dynamic acquisition of images. The subjects performed active flexion-extension of 3 to 4 cycles within 0 to 100 degrees of flexion angle. All images were recorded on video tape. They were then digitized with 640 x 484 (8-bits) resolution for each 20 degrees of flexion or extension, using a media tool on a Silicon Graphics workstation. The images were analyzed with a Matlab program (fluoroscope) to incorporate the magnification factor and the 3-D estimation of bone orientation.

2.4.4 Analysing tools (fluoroscope)

We have developed a Matlab program to analyze fluoroscopic images using method that was first proposed by Sati et al. (1996a-1996b). The original version lacked an easy-to-use interface; therefore, we equipped our program with an intuitive GUI (graphical user interface). Some improvements were added to make the program more accurate and easier to handle. Virtually all actions are performed by clicking the mouse on appropriate icons and buttons. Several hints and help buttons are provided along the way to guide the user. We believe this is a considerable improvement since the entire procedure is complicated enough that the user can be easily distracted if appropriate tools are not provided (Figure 2.6).

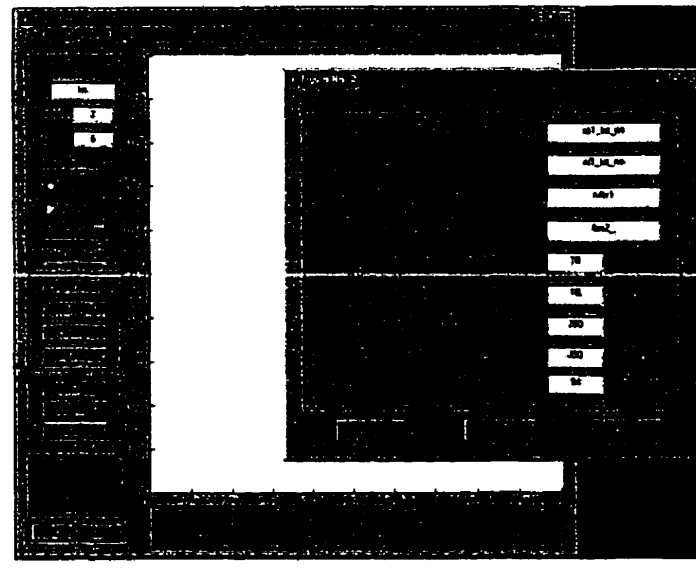

Figure 2.6 : The GUI interface (fluoroscope). The larger window is the main window and the smaller one is the set-up window.

2.4.5 Validation procedures

Program validation can be achieved by observing the coordinates of a marker attached to the femur: if a marker is attached to the bone, its coordinates in the reference system should not change.

Experimental validation

To validate the program, we attached some markers on the medial side of a plastic human size femur and recorded fluoroscopic images for different flexion angles (0, 40, 60 degrees) and then calculated the RMS*pmxpmz*, RMS*pxpz*, RMS*Rx* and RMS*Rz*. Theoretically, this approach is the best since it deals with an almost realistic situation. The practical difficulty with it is user accuracy and precision in marking different points on the images. The poor quality of the images is also a drawback.

Mathematical validation

Using a simple Matlab script, we produced the following images (Figure 2.7): 2 spheres (representing the condyles) are attached to each other at 1 point. With this approach, we

have the advantage of: (a) high quality images, and (b) axes and markers drawn prior to analysis.

The model was controllably rotated around the X and Z axes. Coordinates of the marker in the coordinate systems attached to the image and the bone would give us a means of seeing if our 3-D rotational correction estimation, and hence the main part of our program, works properly. We show 3 images among the 10 that were used in this context (Figure 2.7).

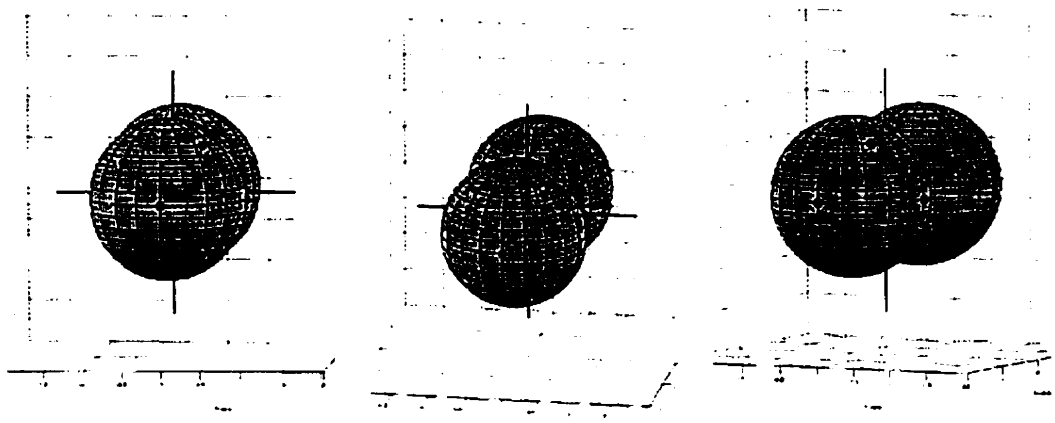

A) Rx= 95° , Rz= 5° B) Rx= 115°, Rz= 5° C) Rx= 100°, Rz= 12°

Figure 2.7 : Mathematical modelization of lateral and medial condyles using 2 spheres connected at 1 point. The dark points correspond to the markers.

2.5 Results and Discussion

2.5.1 Experimental validation

For experimental validation, we used a plastic femur. After attaching 2 markers to it, we produced fluoroscopic images as we would for real subjects. Due to systematic errors, the coordinates of the markers, even when they were attached to the bone, did not remain constant during flexion. It is obvious that a considerable part of this error arises when the

user tries to locate the markers and different reference axes with poor quality images. Table 2.3 demonstrates the RMS errors for 2 markers in experimental validation.

Table 2.3: Accuracy measurements using a plastic knee model for 2 different markers

RMS*pmxpmz*	RMS*pxpz*	RMS*Rx*	RMS*Rz*
3.589963	1.843795	0.888152	0.688507
4.201506	2.0529	0.952872	0.81085

2.5.2 Mathematical validation

Table 2.4 shows the location of a marker in 10 pictures before 3-D estimation (*pmx*; *pmz*) and after (*px*; *pz*).

Table 2.4: Position of a marker before and after 3-D estimation in 10 different images

Image	*Pmx*	*pmz*	*px*	*Pz*
1	-3.4	-3.5	-3.4	-3.5
2	-6.8	-3.5	-3.5	-3.5
3	-10.6	-3.5	-4.2	-3.9
4	-13.6	-3.2	-3.8	-3.1
5	-17.2	-3.7	-4.1	-3.7
6	-3.2	-7.7	-3.4	-3.3
7	-4.2	-11.7	-3.9	-3.7
8	-6.9	-11.7	-3.9	-3.9
9	-10.4	-7.3	-3.8	-3.3
10	-13.7	-11.3	-3.8	-3.6

Since markers were attached to the bone (i.e. the sphere in our simulation), their coordinates should have remained constant (in the reference system attached to the spheres). A quick look at the last 2 columns of the table confirms this fact. It is clear from the first 2 columns, (*pmx* and *pmz)*, that reflect the coordinates of the marker in 2-D images vary by a great factor but after 3-D rotational estimation they remain almost

constant. In Table 2.5, we have calculated RMS error of the marker's position as well as and angular measurements before (first column) and after 3-D rotational estimation (last 3 columns).

Table 2.5: Accuracy measurements using a mathematical model

RMS$pmxpmz$	RMS$pxpz$	RMSRx	RMSRz
6.099439	0.371622	0.149446	0.151664

The data Tables 2..4 and 2.5 demonstrate that when there is no experimental error, the true error, is very small and the position of marker remains constant relative to the bone throughout different images.

After validating the analysing tool (fluoroscope program), we analysed the 5 subjects.

2.5.3 In vivo study

Several researchers (Lafortune et al. 1992, Sati et al. 1996a, Andriacchi et al. 1987 and Angeloni et al. 1992) have shown that relative displacements between external markers fixed on the thigh segment and corresponding landmarks on the femur are about 2 cm. To reduce this error, we proposed use of the exoskeleton attachment system. In our experiment, we placed markers once on the skin and once on the exoskeleton attachment system and these results are reported in Tables 2.6 through 2.10.

Table 2.6: RMS errors for subject 1

Lateral	Marker 1	Marker 2	Marker 3	Marker 4	Marker 5	Marker 6	Marker 7
RMS_*PxPz**	8.8	11.2	9.2	11.8	13.7	15.9	21.5
RMS_*Rx**	2.8	2.2	4.3	0.46	3.2	2.5	4.9
RMS_*Rz**	4.7	6.5	3.7	7.2	7.8	9.3	12.1
RMS_*PxPz*	2.4	1.8	2.2	3.8			
RMS_*Rx*	1.1	0.74	1	0.67			
RMS_*Rz*	0.98	0.88	0.94	2.3			
Medial	Marker 1	Marker 2	Marker 3	Marker 4	Marker 5	Marker 6	Marker 7
RMS_*PxPz**	3.9	4.4	9.7	13.7	14.3	16.3	19.2
RMS_*Rx**	1.6	2.3	1.6	1.9	3.4	2.3	3.8
RMS_*Rz**	1.7	1.4	5.7	8.1	7.9	9.5	10.9
RMS_*PxPz*	0.31	0.42	0.29	0.77			
RMS_*Rx*	0.15	0.11	0.04	0.16			
RMS_*Rz*	0.12	0.23	0.18	0.45			

* Without the attachment system

Table 2.7: RMS errors for subject 2

Lateral	Marker 1	Marker 2	Marker 3	Marker 4	Marker 5	Marker 6	Marker 7
RMS_*PxPz**	23.6	9.6	13.9	6.8	10.5	10.4	11.8
RMS_*Rx**	8.4	2.4	4.8	3.4	4.3	2.9	3.8
RMS_*Rz**	10.2	4.9	6.2	2	4.1	5.2	2.4
RMS_*PxPz*	6.8	5.5	4.8				
RMS_*Rx*	3.1	2.5	2.1				
RMS_*Rz*	2.2	1.9	1.6				
Medial	Marker 1	Marker 2	Marker 3	Marker 4	Marker 5	Marker 6	Marker 7
RMS_*PxPz**	4.4	8.1	6.2	9.2	10.1	12.7	16.6
RMS_*Rx**	1.5	4	0.68	2.8	1.2	1.8	2.03
RMS_*Rz**	1.9	2.2	3.5	4.4	5.6	6.9	9.1
RMS_*PxPz*	5.3	5.4	6.1	5.8	5.7		
RMS_*Rx*	3	3	2	2.2	2.5		
RMS_*Rz*	0.36	0.63	2.8	2.4	2		

* Without the attachment system

Table 2.8: RMS errors for subject 3

Lateral	Marker 1	Marker 2	Marker 3	Marker 4	Marker 5	Marker 6	Marker 7
RMS_*PxPz**	11.9	17.1	17.8	17.1	20.1	20.3	26.2
RMS_*Rx**	3.8	3.8	0.84	2.7	5.2	6.8	6.2
RMS_*Rz**	5.6	8.8	9.9	9.2	10.2	9.3	13.4
RMS_*PxPz*	5.3	3.4	5.8				
RMS_*Rx*	1.6	1.4	1.5				
RMS_*Rz*	2.5	1.3	2.9				
Medial	Marker 1	Marker 2	Marker 3	Marker 4	Marker 5	Marker 6	Marker 7
RMS_*PxPz**	6.7	13.3	11.7	20.1			
RMS_*Rx**	1.5	4.4	2.5	2.3			
RMS_*Rz**	3.4	5.9	6	10.9			
RMS_*PxPz*	6.2	6	5.3				
RMS_*Rx*	2.7	2.7	2.3				
RMS_*Rz*	2.2	2	1.8				

*Without the attachment system

Table 2.9: RMS errors for subject 4

Lateral	Marker 1	Marker 2	Marker 3	Marker 4	Marker 5	Marker 6	Marker 7
RMS_*PxPz**	10.9	7.1	9.1	16.1			
RMS_*Rx**	2.4	2	2.5	2.5			
RMS_*Rz**	5.9	3.6	4.7	9.1			
RMS_*PxPz*	6.5	4.6	5.4				
RMS_*Rx*	1.5	0.91	1.2				
RMS_*Rz*	3.3	2.4	2.7				
Medial	Marker 1	Marker 2	Marker 3	Marker 4	Marker 5	Marker 6	Marker 7
RMS_*PxPz**	6.4	5.9	8.3	10			
RMS_*Rx**	1.9	2.3	1.8	2.9			
RMS_*Rz**	3.2	2.2	4.4	5			
RMS_*PxPz*	4.8	4	4.3				
RMS_*Rx*	1.3	1.5	1.9				
RMS_*Rz*	1.6	1.6	1.4				

* Without the attachment system

Table 2.10: RMS errors for subject 5

Lateral	Marker 1	Marker 2	Marker 3	Marker 4	Marker 5	Marker 6	Marker 7
RMS_*PxPz**	5.4	5.1	6.4	6.2			
RMS_*Rx**	1.9	2.2	2.9	2.8			
RMS_*Rz**	2.3	1.9	2.1	2.3			
RMS_*PxPz*	8.3	7.1	7.7				
RMS_*Rx*	4.3	3.6	4.1				
RMS_*Rz*	2.1	1.9	1.7				
Medial	Marker 1	Marker 2	Marker 3	Marker 4	Marker 5	Marker 6	Marker 7
RMS_*PxPz**	5.6	8.3	6.6	7.4			
RMS_*Rx**	2.8	2.5	2.9	3.7			
RMS_*Rz**	2.4	3.8	2	1.9			
RMS_*PxPz*	7.9	7.7	7.8				
RMS_*Rx*	1.4	1.7	2.4				
RMS_*Rz*	4.4	4	3.9				

* Without the attachment system

In the Tables, we can appreciate that skin movement is smaller in the region of interest, and as we move further up toward the thigh or further down closer to the joint, movement of the markers grows in magnitude (Figure 2.4C and 2.4D). We omitted markers that were difficult to detect due to the poor quality of certain images. More precisely, in Table 2.7, by looking at markers 6 and 7 on the lateral side, which were placed higher on the thigh where more muscular mass or fat was present, we can see that there was a significant skin movement. Similarly, for marker 1 on the lateral side located close to the joint, there was marked movement of skin with respect to the underlying bone. We also observed that if the marker was placed more toward the front (posteriorly) or more toward the back (interiorly) of the thigh, it moved significantly as well (marker 5). These observations were consistent for 4 subjects out of 5 with different muscular masses. Although we have reported the results of the fifth subject, they were not taken into account in the overall average. We believe that in this case the exoskeleton

attachment system was displaced during fluoroscopic acquisition by the X-ray protecting jacket.

We have demonstrated that movement of the markers (Table 2.11) was reduced on the lateral side from 13.7 to 4.6 in the *XZ* plane; and RMS errors of rotation about the *X* axis (*Rx*) were decreased from 3.4 to 1.5 degrees; and RMS errors of rotation about the *Z* axis (*Rz*) were diminished from 6.9 to 2 degrees on average for 4 of the subjects. On the medial side, RMS errors of displacement in the *XZ* plane were reduced from 10.5 to 4.1 mm; RMS errors of rotation about the *X* axis (*Rx*) were decreased from 2.3 to 1.7 degrees; and RMS errors of rotation about the *Z* axis (*Rz*) were diminshed from 5.4 to 1.3 degrees on average for 4 of the subjects.

We have demonstrated that RMS*pxpz*, RMS*Rx* and RMS*Rz* were reduced on the lateral side by a factor of 3.3 (min 2, max 5.2), 2.4 (min 1.7, max 3.3) and 3.7 (min 2, max 5.7), and on the medial side by a factor of 8 (min 1.8, max 26), 6.1 (min 0.75, max 21) and 8.7 (min 2.1, max 26.4), respectively. These results are comparable with what has been reported in the literature (Sati et al. 1996a).

Table 2.11: Mean accuracy measurements for 4 subjects

Lateral	Subject 1	Subject 2	Subject 3	Subject 4	Mean
RMS_*PxPz**	13.2	12.4	18.6	10.8	13.7
RMS_*Rx**	2.9	4.5	4.2	2.4	3.4
RMS_*Rz**	7.3	5	9.5	5.8	6.9
RMS_*PxPz*	2.6	5.7	4.8	5.5	4.6
RMS_*Rx*	0.88	2.6	1.5	1.2	1.5
RMS_*Rz*	1.3	1.9	2.2	2.8	2.0
Medial	Subject 1	Subject 2	Subject 3	Subject 4	Mean
RMS_*PxPz**	11.6	9.6	13	7.7	10.5
RMS_*Rx**	2.4	2.0	2.7	2.2	2.3
RMS_*Rz**	6.5	4.8	6.6	3.7	5.4
RMS_*PxPz*	0.44	5.6	5.8	4.4	4.1
RMS_*Rx*	0.12	2.7	2.6	1.6	1.7
RMS_*Rz*	0.25	1.3	2	1.5	1.3

* Without the attachment system

We have also observed from our results that male subject (Table 2.6) showed a greater reduction factor of movement with the attachment compared to female subjects (Tables 2.7, 2.8 and 2.9).

We have also looked at the movement of markers on the attachment system before and after 3-D estimation in Figure 2.8 A and B in different flexion images. In examining these graphs, we observed that after applying the appropriate 3-D estimation, the coordinates of the markers throughout different flexion images remained constant.

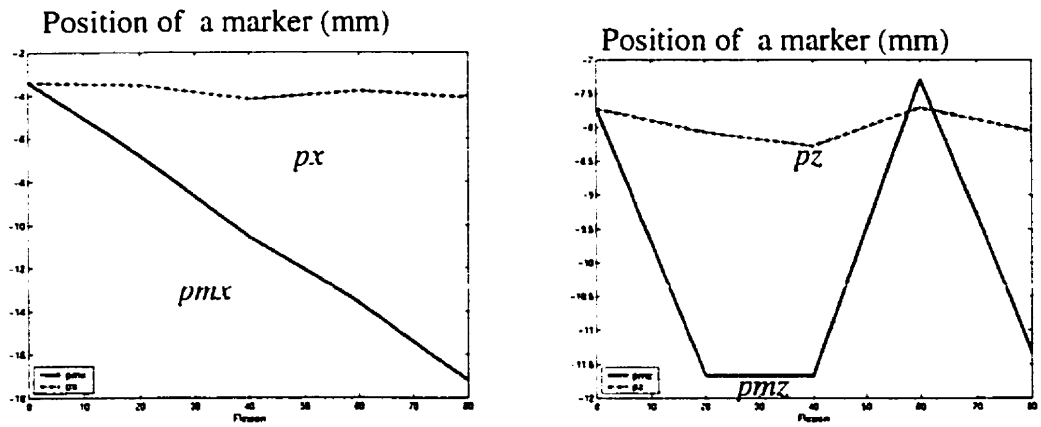

Figure 2.8: Displacement of a marker before (*pmx*, *pmz*) and after (*px*, *pz*) 3-D estimation throughout different flexion angle (0 to 80) degrees.

We believe that we have successfully demonstrated that the exoskeleton attachment system reduced the movement of markers with respect to the underlying bone.

2.6 Conclusion

The relationships between joint pathology and kinematics are well known in orthopaedics (Chèze et al. 1995). To correct the relative movement of markers (or skin) with respect to the underlying bone, some methods try to use a cluster of markers (Deluzio et al. 1997) but they are based on mathematical corrections which are very complicated and sometimes impossible because of variations in individual anatomies. The displacement of the skin markers is mostly associated with skin movement artefacts; therefore the markers are not stationary with respect to the underlying bone, mostly owing to the interposition of both passive and active soft tissues which constitute the major source of experimental errors. Skin movement artefact propagation could thus be reduced by taking into account the relative displacement between skin and the underlying bone, using the attachment system that we have proposed in this paper.

Fluoroscopic study allowed us to measure the displacement of markers as well as kinematic accuracy over 100 degrees of knee flexion-extension. As observed, the

exoskeleton attachment system resulted in reductions of RMS in *XZ*, *Rx* and *Rz* respectively by a factor of 6 (min 1.8, max 26), 4.3 (min 0.75, max 21) and 6.2 (min 2, max 26.4) on average for 4 subjects out of 5. Non-invasive methods can be severely corrupted by experimental errors. The exoskeleton attachment system has demonstrated that the usual errors due to sliding of the skin on bone can be reduced by a large factor, which is a considerable improvement over existent systems.

2.7 Acknowledgements

This work was founded by the NSERC organisations. The authors would like to thank A. Naddaf, S. Mostsharnia, G. parent for their technical assistance and Y. Chevalier for his artistic help.

CHAPTER 3

ARTICLE 2: ÉTUDE BIOCINÉMATIQUE DU GENOU À L'AIDE D'UN ANALYSEUR 3D

3.1 SITUATION OF ARTICLE IN THESIS

In the pervious chapter we have validated the attachment system using fluoroscopy studies. We have demonstrated that the use of attachment system reduced the skin movement. The accuracy measurement were found to be considerably reduced on the skin with respect to the underlying bone on the average by a factor of 8, 6.1 and 8.7 (*XZ*, *Rx*, *Rz*) on the medial side and by a factor of 3.3, 2.4 and 3.7 (*XZ*, *Rx*, Rz) on the lateral side for four subjects when the attachment system was used. It is apparent that a set of reproducible, objective measurements, would be superior both for recording a present condition and for comparison purposes. It is therefore an objective of this chapter to use attachment system for measuring parameters relating to the stability of knee joints (flexion-extension, abduction-adduction and internal-external rotation) which overcomes the disadvantages of other existing apparatus. To this end, this chapter will examine the same 5 healthy subject that were examined in fluoroscopy for evaluating an active flexion-extension in 3 different position (standing, squatting, sitting) to find an appropriate movement which results into a reproducible movement within the same subjects.

ÉTUDE BIOCINÉMATIQUE DU GENOU À L'AIDE D'UN ANALYSEUR 3D

Sh. Ganjikia, BSc (Physics)[1,2], N. Duval, MD[1,2], L.H. Yahia, PhD[1,2], J. A. de Guise, PhD[1,2,3]

1) Laboratoire de recherche en Imagerie et Orthopédie, Centre de recherche du CHUM, 1560 rue Sherbrooke Est, Montréal, Qc. H2L 4M1, Canada

2) Groupe de recherche en Bioméchanique/Biomatériaux, Ecole Polytechnique, C.P. 6079, Succ. Centre-Ville, Montréal, Qc. H3C 3A7, Canada

3) Laboratoire d'Imagerie, de Vision et d'Intelligence Artificielle, Ecole de technologie supérieure, 1100 rue Notre- Dame Ouest, Montréal, Qc. H3C 1K3, Canada

Submitted to « Annales de Chirurgie » December 1999

Mots-clés: biocinématique du genou, abduction-adduction, rotation tibiale, évaluation tridimensionnelle

Correspondence and Reprint Requests :

Shafagh Ganjikia, Biomedical Engineering Department, École Polytechnique, P.O. Box 6079 Station « Downtown », Montréal Québec, Canada H3C3A7;

Tel : (514)340-4711 extension 4198:fax;(514)340-4611; e-mail: ganjikia@yahoo.com

3.2 RÉSUMÉ

But: Le but de cette étude est de valider scientifiquement un analyseur fonctionnel du genou avant son utilisation clinique. L'analyseur est basé sur un système d'attache permettant la fixation externe de capteurs de mouvement et minimisant le mouvement de la peau par rapport aux os sous-jacents. Un des buts spécifiques de l'étude est de déterminer un mouvement du genou assurant une bonne reproductibilité intra sujet. **Matériel et Méthode:** Le système d'attache a été installé dix fois au cours de différentes journées sur 5 sujets. Lors de chaque expérience le sujet a effectué 10 mouvements de flexion-extension active dans 3 positions différentes: debout, assis et squat. Les indices cinématiques abduction/adduction et rotation tibiale ont été analysés et le coefficient de corrélation multiple de Kadaba (Kadaba et al., 1989) de même que la moyenne des coefficients de corrélations pour chaque position ont été calculés. **Résultats et Discussion:** Nos résultats démontrent qu'il n'y a statistiquement pas de différence significative pour les mouvements en flexion/extension obtenus dans les 3 positions. Par contre, la moyenne des coefficients de corrélation montre que les mouvements effectués en position assise présentent la meilleure reproductibilité. La moyenne des coefficients de corrélation multiple pour différentes journées est supérieure à 0.7 pour l'abduction et la rotation tibiale dans les trois positions. **Conclusion:** Ces résultats montrent que l'analyseur peut permettre l'acquisition de la cinématique du genou avec une bonne reproductibilité, de façon non effractive et en 3D.

3.3 SUMMARY

Goal: The goal of this study is to validate scientifically a functional knee analyzer before using it in a clinical setting. The analyzer is based on the use of a femoral and tibial attachment system onto which two magnetic sensors are rigidly placed. The analyzer minimizes the movement of the skin with respect to the underlying bones and it therefore allows a precise measurement of 3D kinematic parameters of the knee. More

precisely, a kinematics study was done to determine an appropriate reproducible movement. **Method and Material:** The analyzer was placed 10 times on 5 different subjects in different days. During each experiment ten cycles of an active flexion-extension in 3 different positions(standing, squatting, and sitting) were recorded. The kinematic indices, abduction-adduction and tibial rotation were analyzed and the multiple coefficient correlation of Kadaba (Kadaba et al. 1989) along with the statistical average of correlation coefficients for each position were calculated. **Results and Discussion:** The results suggest that the flexion-extension movement showed no significant difference statistically for all 3 positions. Nevertheless, the mean average of correlation coefficients for the sitting position were slimly higher than the other two positions. For all 5 subjects, the statistical average of the correlation coefficients for different days was larger than 0.7 for different positions. **Conclusion:** The system allows us to develop a method for evaluating the kinematics of the knee non-invasively in 3-D with reproducible results.

3.4 INTRODUCTION

Essentiel à la locomotion humaine, le genou est une articulation jouissant d'un mécanisme tridimensionnel complexe et fragile dont le dérèglement peut engendrer un handicap fonctionnel majeur. A long terme, un état pathologique mal diagnostiqué ou non décelé peut dégénérer et induire une condition irréversible. Pour mieux comprendre les mouvements du genou, l'analyse d'indices tridimensionnels est nécessaire. Elle est la première étape d'un processus qui permet de poser un diagnostic précis d'une atteinte fonctionnelle du genou et d'en prévoir un traitement adéquat (Hamel, 1997).

Le genou est une articulation à 6 degrés de liberté (3 degrés en rotation et 3 degrés en translation): le principal degré de liberté est la flexion-extension qui permet de rapprocher ou d'éloigner plus ou moins l'extrémité du membre de son origine ou encore de contrôler la distance du corps par rapport au sol.

De plus, l'articulation du genou comporte un deuxième et troisième degré de liberté : la rotation autour l'axe longitudinal de la jambe et la rotation autour l'axe perpendiculaire à l'axe longitudinal. Nous ne considérerons pas dans cet article les 3 degrés de translation.

1. Le premier degré de liberté est conditionné par l'axe transversal X qui traverse horizontalement les condyles fémoraux dans le plan frontal. Les mouvements de flexion-extension s'effectuent autour de cet axe (voir figure 1a).

2. Le deuxième degré de liberté consiste en la rotation autour de l'axe longitudinal Z (rotation interne/externe) de la jambe avec le genou fléchi.

3. Le troisième degré de liberté consiste à la rotation autour de l'axe Y (abduction/adduction) antéro-postérieur, lequel est orthogonal aux deux axes précédents.

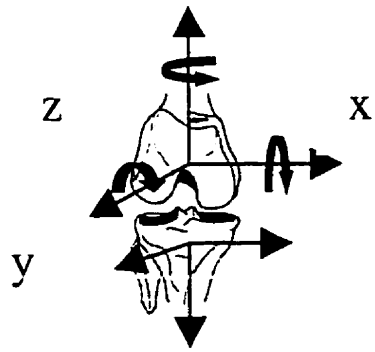

Figure 3.1: Le système d'axes

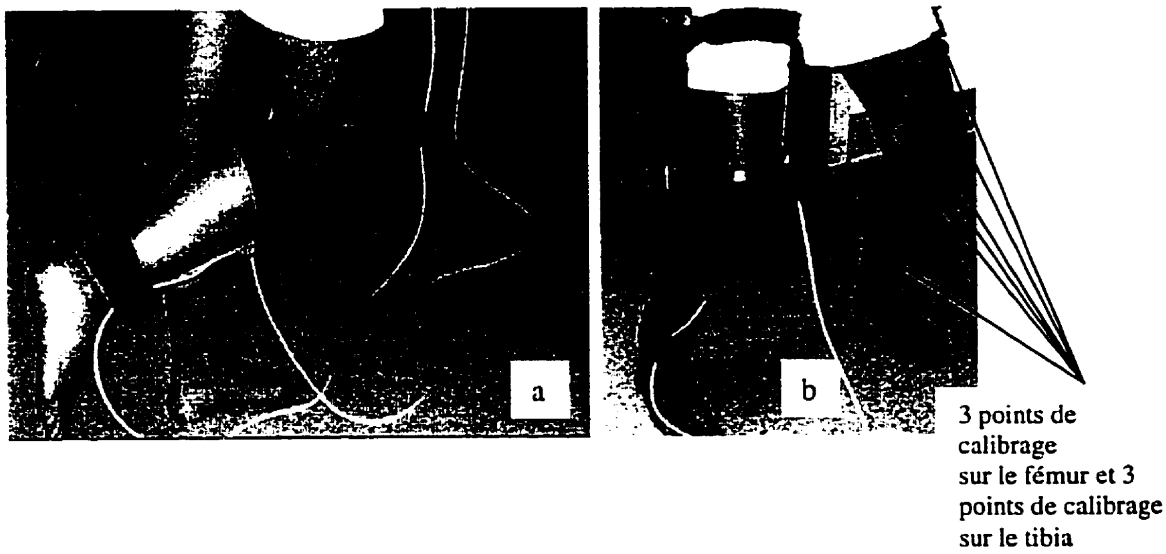

Figure 3.2 : Le système d'attache. Du côté latéral, le système d'attache s'appuie sur la partie supérieure du condyle postérieur. Cet appui se trouve entre la bandelette iliotibiale et le biceps femoris. Du côté médial, le dispositif s'appuie sur le tubercule des adducteur et derrière l'adducteur magnus.

Les plus récents travaux dans le domaine de l'analyse du mouvement du genou, effectués à l'aide de différentes méthodes par A. Cappello et al. (1997), J. Fuller et al.

(1997), L. Chèze et al. (1998), K.J. Deuzio et al. (1997), ont pu avec succès évaluer le mouvement du genou. Malgré leurs méthodes et paramètres diversifiés, ces auteurs semblent d'accord pour dire que le mouvement de la peau par rapport à l'os sous-jacent est une cause majeure d'erreur expérimentale lors de l'évaluation de la cinématique du genou.

Le but de cette étude est de valider scientifiquement un analyseur fonctionnel du genou avant de débuter son utilisation en clinique. Un des objectifs spécifiques est de déterminer un mouvement du genou assurant une bonne reproductibilité intra sujet (Hamel, 1996 and Hagemesiter et al., 1999).

3.5 MÉTHODE ET MATÉRIELS

L'analyseur 3D est composé de senseurs de mouvements, d'un système d'attache permettant de fixer les senseurs sur le genou du sujet et d'un ordinateur permettant l'enregistrement numérique du mouvement, sa représentation graphique et son analyse.

3.5.1 Système de repérage magnétique (Fastrack)

Des capteurs magnétiques sont utilisés afin de suivre dans le temps la position et l'orientation de deux os du genou, soit le fémur et le tibia. Les capteurs magnétiques sont sensibles à un champ magnétique généré par une source émettrice par rapport à laquelle ils donnent leur position et orientation à intervalle régulier (An et al. 1999). La précision statique du système de repérage magnétique est de 0.08 cm, root-mean square (RMS), pour le récepteur de position *X*, *Y* ou *Z*, et 0.15° RMS pour les récepteurs d'orientation (Logan et al., 1988). De plus, il n'existe pas de risques associés à l'utilisation de ce système. Le système n'est pas affecté par des problèmes d'ombrage. Par contre les mesures prises avec le système de repérage magnétique peuvent être affectées par des objets métalliques ou ferromagnétiques qui modifient le champ magnétique émis par la source et reçu par les capteurs magnétiques. Il est donc nécessaire d'effectuer un test d'environnement avant d'y installer la scène expérimentale.

3.5.2 Installation des senseurs de mouvement

Afin de minimiser le mouvement de la peau et des muscles, notre groupe de recherche a mis au point un système d'attache permettant de fixer des capteurs magnétiques de façon quasi solide aux os du fémur et du tibia et d'enregistrer leur mouvement de façon non effractive. La première version fut développée et mise à l'étude par Sati et al. (1996). La présente étude utilise une troisième version du système d'attache, amélioré afin d'optimiser le confort et la facilité d'installation. La partie fémorale du système d'attache comprend 3 othoplasts, une barre de suspension, un boîtier pour placer le capteur magnétique associé au fémur, un pont rigide qui relie les orthoplasts, de même que des vis d'ajustement. La partie tibiale est constituée d'une barre rigide avec bandes velcro pour un positionnement rigide sur le tibia, de même que deux trous et deux vis pour le support du capteur magnétique.

Le placement des senseurs sur les os peut être compliqué par le mouvement des tissus mous et des muscles qui entourent l'os. Pour réduire cette source d'erreur, il importe de choisir des points qui minimisent le mouvement de la peau par rapport à l'os. De même, le positionnement de l'appareil utilisé ne doit pas compromettre la mesure du mouvement 3D du genou. L'étude faite par Sati et al. (1996) nous donne suffisamment d'information pour placer adéquatement notre système d'attache. Afin d'assurer un niveau de précision acceptable tout en limitant le mouvement des masses musculaires et des tissus mous, il est important que le système d'attache soit appuyé le plus directement possible sur les structures osseuses. Du côté latéral, il faut ainsi appuyer le système d'attache sur la partie supérieure du condyle postérieur du fémur. Cet appui se situe entre la bandelette iliotibiale et le biceps femoris. Du côté médial, l'orthoplast s'appuie sur le tubercule des adducteurs et derrière l'adducteur magnus (Figure 3.2). L'étude de Sati et al. (1996) a démontré que le placement du système a été bien choisi, car des résultats satisfaisants ont été obtenus en fluoroscopie (Ganjikia et al., 2000b, Sati et al. 1996). Il est important de porter une grande attention au placement du système au niveau de fémur

et du tibia car les résultats issus du système d'analyse sont en rapport direct avec le placement du système (Figure 1b). Le système est strictement utilisé par notre laboratoire pour des recherches. Une fois que le système aura été validé scientifiquement, il pourra être utilisé en clinique. Il devra être alors suffisamment simple à utiliser et rapide à installer.

Les indices cinématiques peuvent être recueillis et analysés à l'aide d'un logiciel spécial développé en langage C.

3.5.3 Test d'environnement

Cette étape est nécessaire afin de déterminer s'il y a une source d'interférence dans l'environnement, le système de repérage magnétique y étant sensible. À cette fin, une boite en Plexiglas aux dimensions connues avec précision est employée et mesurée à l'aide d'un pointeur muni d'un capteur magnétique identique à ceux utilisés pour les os du genou afin de détecter les sources d'interférence magnétique et de procéder à leur élimination avant les étapes d'acquisition des données expérimentales.

3.5.4 Système d'axes

Nous utilisons le système de référence qui fut employé par Sati et al. (1997). Ce système de coordonnées est basé sur la théorie des axes mécaniques du tibia et du fémur. L'origine du système fémoral est définie comme le point central entre les condyles médial et latéral. L'axe X est l'axe de flexion qui passe par les centres des deux épicondyles. L'axe Z du fémur est défini comme étant l'axe mécanique perpendiculaire à l'axe X et se situe dans le plan formé par l'axe X et l'axe défini par la diaphyse du fémur. Finalement, l'axe Y est simplement le produit vectoriel des axes X et Z. Un deuxième système de référence, placé sur la partie tibiale, est nécessaire pour exprimer les mouvements de rotation du genou. L'axe X du tibia est l'axe qui passe par les centres des plateaux du tibia. L'axe Z est perpendiculaire à l'axe X et se situe dans le plan formé par l'axe X et l'axe défini par la diaphyse du tibia. L'axe Y est le produit vectoriel des axes X

et Z (Figure 3.1). L'orientation relative du tibia par rapport au fémur peut être définie avec une matrice de rotation. Celle-ci peut être décomposée en une série de trois rotations autour d'axes mobiles X, Y', Z''. Ainsi, l'angle de flexion/extension est définie autour de l'axe X du fémur et constitue une rotation Rx. L'angle d'abduction est défini autour de l'axe Y du fémur ayant subi une rotation autour de X et constitue une rotation Ry', d'où $Y'=Rx\ Y$. Finalement, l'angle de rotation tibial externe/interne est définit autour de l'axe Z du fémur ayant subi successivement des rotations autour des axes X et Y' et constitue une rotation Rz'', d'où $Z''=Ry'Rx\ Z$. Cet axe Z'' fémoral coïncide avec l'axe Z tibial (Grood et al., 1983).

3.5.5 Acquisition des indices cinématiques et traitement des données

L'évaluation a eu lieu dans la même salle où nous avons effectué les tests visant à éliminer les sources d'interférence magnétique, préalablement à l'étude cinématique. L'échantillon fut constitué de 5 sujets, tous présentant des genoux non pathologiques tels que déterminés par un examen clinique effectué par un chirurgien orthopédiste. Le système d'attache a été installé dix fois sur le genou droit et les mouvements des senseurs furent associés aux mouvements anatomiques par un calibrage 3 points (Figure 3.2.b) qui assure la correspondance entre l'image 3D du genou générique et les os réels du sujet. Ce processus permet la visualisation simultanée du mouvement du genou virtuel sur un écran d'ordinateur en correspondance instantanée avec celui effectué par le sujet (Sati et al., 1997). Lors de chaque séance, le sujet a effectué 10 mouvements d'extension-flexion active dans 3 positions différentes: debout, assis et squat. Les indices cinématiques d'abduction/adduction et de rotation tibiale en fonction de la flexion ont été analysés et le coefficient de corrélation multiple a été calculé (Kadaba et al., 1989). La fréquence d'acquisition de la cinématique a été fixée à 40 Hz pour un temps d'acquisition de 5 sec. Afin de procéder à des comparaisons quantitatives, les courbes furent parametrisées à l'aide d'une interpolation continue par morceaux, une méthode qui permet de conserver le plus grand nombre de détails possibles sans toutefois nécessiter

un lissage des courbes, ce qui n'est pas requis pour les analyses de la présente étude. Ensuite, pour chaque série de 10 courbes, le coefficient de corrélation multiple a été calculé. Ce coefficient permet d'évaluer la reproductibilité inter et intra sujet des paramètres cinématiques (les calculs sont basés sur les travaux de Kadaba et al. (1989).

$$R_a^2 = 1 - \frac{\sum_{i=1}^{M} \sum_{j=1}^{N} \sum_{t=1}^{T} \frac{(Y_{ijt} - \overline{Y_{it}})^2}{MT(N-1)}}{\sum_{i=1}^{M} \sum_{j=1}^{N} \sum_{t=1}^{T} \frac{(Y_{ijt} - \overline{Y_{i}})^2}{M(NT-1)}}$$

$$\overline{Y_t} = \frac{1}{NT} \sum_{j=1}^{N} \sum_{t=1}^{T} Y_{ijt} \qquad \overline{Y_{it}} = \frac{1}{N} \sum_{j=1}^{N} Y_{ijt}$$

(3.1 – 3.3)

L 'équation 3.1 est le rapport de la moyenne des M moyennes, des T variances le long de chaque série et de N courbes sur la moyenne des M variances, des N*T échantillons de chaque expérimentation. D 'où: M= nombres de cycles, T= moyennes de variances et N= nombre d'essai.

3.6 RÉSULTATS

Nous avons effectué un test d'environnement à l'aide d'une boîte de calibrage et obtenu une erreur (RMS) inférieure à 1 mm pour tous les points numérisés (Figure 3.3). Ces résultats montrent que l'environnement choisi pour l'étude ne présentait pas d'interférence magnétique pouvant affecter les données de façon significative.

Les données expérimentales provenant des 10 essais furent considérées. Nous avons effectué une procédure analytique visant à évaluer la reproductibilité intra sujet des paramètres cinématiques identifiés des mouvements de flexion-extension, d'abduction-adduction et de rotation tibiale.

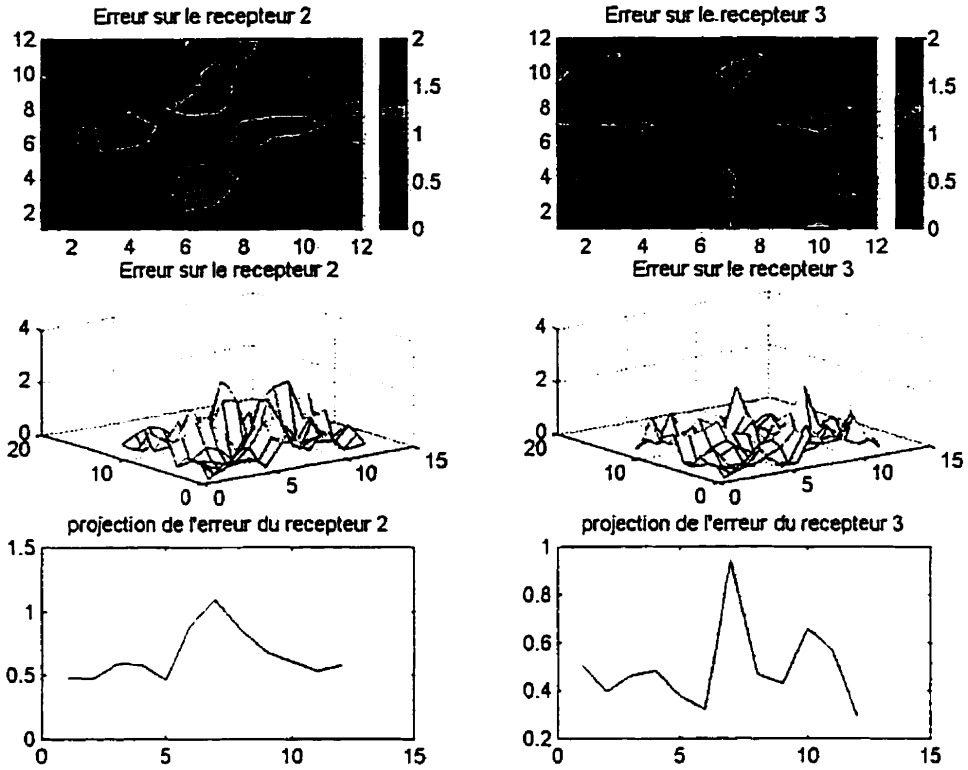

Figure 3.3: Test d'environnement à l'aide d'une boîte de calibrage. L'axe de X représente le nombre de points qui sont numérises et l'axe Y représente l'erreur sur les capteurs (2,3) au niveau de fémur et tibia respectivement.

Des analyses statistiques furent utilisées afin d'évaluer la reproductibilité intra-sujet. À des fins de traitement, des données continues furent générées à partir de données discrètes enregistrées en utilisant un méthode d'interpolation linéaire par morceaux (Figure 3.4).

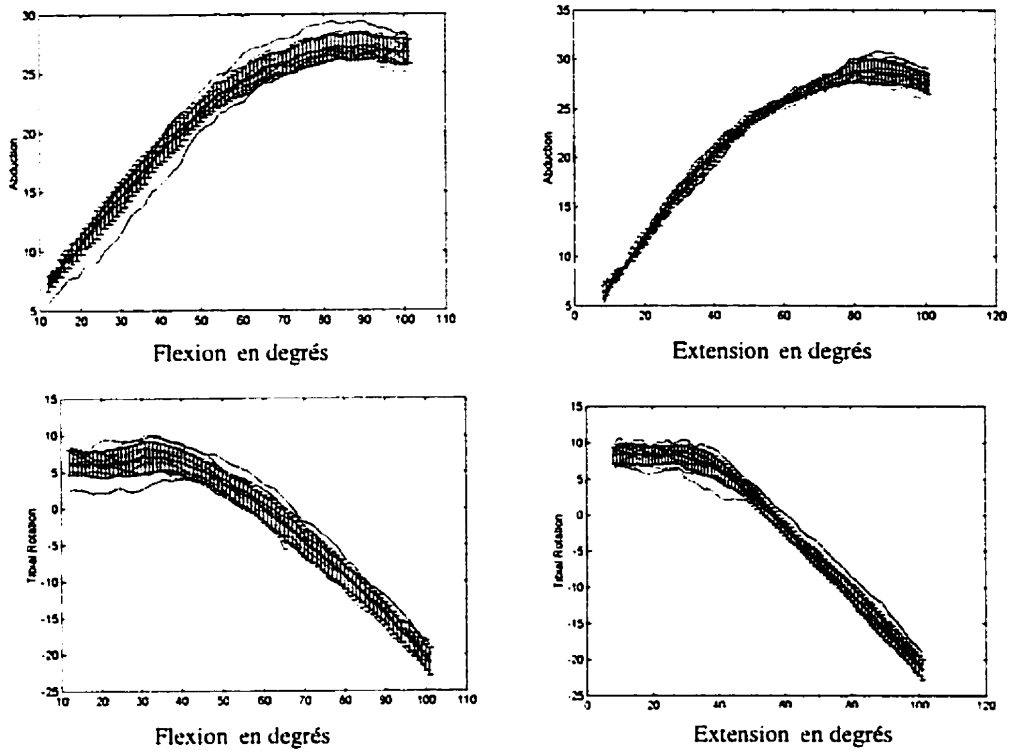

Figure 3.4: L 'abduction et rotation tibiale en fonction de la flexion-extension pour un sujet qui effectue un mouvement en flexion-extension en position assise.

La figure 3.4 représente un résultat typique de 10 cycles pour un sujet avec l'écart type centré autour de la moyenne. Nous avons utilisé un coefficient de corrélation de Kadaba pour permettre d'évaluer la reproductibilité intra-sujet (Kadaba et al., 1989). Pour ce faire, le coefficient de corrélation fut calculé pour 10 essais consécutifs (à différentes journées). L'examen de ces résultats montre une variabilité des courbes selon les jours où les expérimentations ont été réalisées. Les coefficients de corrélation du mouvement dont les valeurs sont plus faibles peuvent être attribuées à une mauvaise installation du système d'attache ou à la fatigue ressentie par les sujets (Figure 3.5.a). Si, par contre, on regarde la moyenne des coefficients de corrélation multiple pour différentes séances, celle-ci est supérieure à 0.7 pour l'abduction et la rotation tibiale pour les 5 sujets dans 3 différentes positions avec un écart type de 0.01 à 0.3 (Figure 3.5.b).

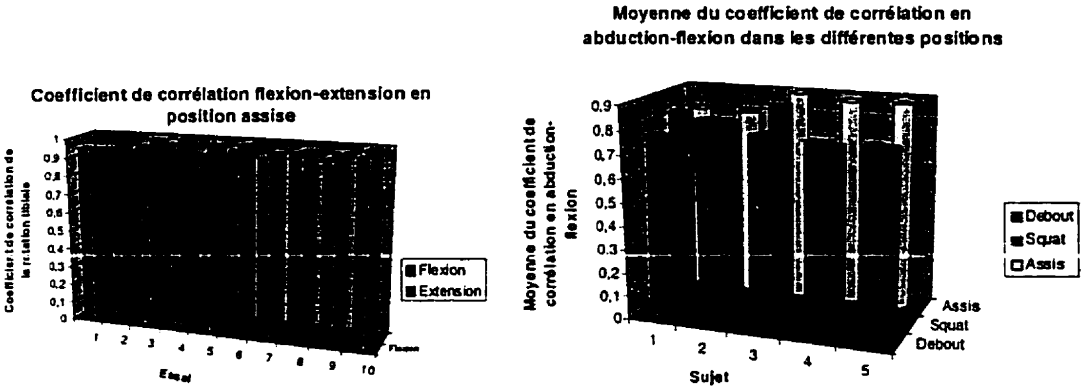

Figure 3.5: a) Le coefficient de corrélation d'abduction en flexion-extension en position assise pour 10 essais consécutifs à différentes journées. b) La moyenne du coefficient de corrélation en abduction dans 3 positions différentes pour 5 différents sujets.

Les tableaux 3.1 à 3.3 indiquent le coefficient de corrélation pour 5 sujets dans des positions différentes.

Tableau 3.1: La moyenne de coefficient de corrélation de 10 essais d'abduction et rotation tibiale en position debout

N=5	Abduction-flexion	Abduction-extension	Rotation Tibiale - flexion	Rotation Tibiale – extension
1	0.77±0.17	0.79±0.13	0.73±0.18	0.76±0.26
2	0.93±0.07	0.89±0.16	0.72±0.20	0.80±0.26
3	0.94±0.04	0.95±0.04	0.79±0.23	0.78±0.21
4	0.79±0.18	0.81±0.16	0.71±0.20	0.76±0.20
5	0.96±0.02	0.97±0.05	0.78±0.28	0.97±0.02

Tableau 3.2: La moyenne de coefficient de corrélation de 10 essais d'abduction et rotation tibiale en position squat.

N=5	Abduction-flexion	Abduction-extension	Rotation Tibiale - flexion	Rotation Tibiale – extension
1	0.72±0.05	0.83±0.01	0.74±0.26	0.71±0.09
2	0.97±0.03	0.95±0.05	0.96±0.02	0.96±0.03
3	0.71±0.20	0.95±0.02	0.84±0.13	0.85±0.10
4	0.74±0.20	0.95±0.03	0.70±0.20	0.78±0.13
5	0.87±0.16	0.94±0.09	0.75±0.12	0.70±0.17

Tableau 3.3: La moyenne de coefficient de corrélation de 10 essais d'abduction et rotation tibiale en position assise.

N=5	Abduction-flexion	Abduction-extension	Rotation Tibiale - flexion	Rotation Tibiale-extension
1	0.82±0.10	0.81±0.18	0.87±0.01	0.76±0.03
2	0.98±0.02	0.99±0.02	0.88±0.10	0.89±0.15
3	0.91±0.02	0.89±0.10	0.91±0.02	0.86±0.17
4	0.88±0.08	0.95±0.05	0.71±0.3	0.79±0.20
5	0.90±0.24	0.76±0.05	0.71±0.22	0.74±0.2

Un test ANOVA non-paramétrique démontre qu'il n'y a aucune différence statistiquement significative pour la reproductibilité des mouvements effectués en différentes positions. Par ailleurs, si l'ANOVA non-paramétrique n'est pas utiliser, il faut donc appliquer la correction en Z de Fischer avant de calculer l'ANOVA car le coefficient de corrélation multiple n'est pas distribué normalement (Fisz, 1980). On observe par contre que la moyenne des coefficients de corrélation pour les mouvements en position assise était plus élevée que pour les deux autres positions, ce qui indique que le mouvement en position assise a une meilleure reproductibilité (Tableau 3.4) .

Tableau 3.4: Test d'ANOVA comparant les positions debout , squat et assise.

Test d'ANOVA	P-level	Debout	Squat	Assis
Abduction-flexion –debout – squat-assis	0.06	0.88±.09	0.80±0.09	0.90±0.06
Abduction-extension-debout-squat-assis	0.56	0.88±0.07	0.92±0.05	0.88±0.09
Rotation tibiale-flexion-debout-squat-assis	0.32	0.75±0.03	0.79±0.09	0.81±0.09
Rotation tibiale-extension-debout-squat-assis	0.96	0.80±07	0.79±0.08	0.81±0.07

3.7 DISCUSSION ET CONCLUSIONS

La reproductibilité des paramètres cinématiques est une caractéristique importante pour toute évaluation d'ordre clinique. Il est donc essentiel de déterminer si l'enregistrement d'une série de mouvements actifs est suffisamment représentatif de la cinématique du genou d'un sujet et s'il existe des paramètres cinématiques de référence auxquels on peut identifier un sujet dont le genou est normal. L'objectif de ce travail était de déterminer un mouvement du genou assurant une bonne reproductibilité intra-sujet. Cette étude nous permet également d'évaluer la reproductibilité des paramètres cinématiques associés à une série de mouvements effectués par une même personne puisque tous les mouvements sont interprétés en fonction des mêmes conditions expérimentales. Nous avons évalué les indices cinématiques (abduction, rotation tibiale) pour 5 sujets et ces résultats montrent que le système d'attache permet l'acquisition de la cinématique du genou avec une bonne reproductibilité.

Cette étude mènera vers le développement d'une méthode permettant l'évaluation fonctionnelle objective et non invasive de la cinématique 3D du genou. Les étapes futures comprennent une étude avec un échantillon composé d'un nombre accru de sujets, ainsi qu'une étude inter observateurs. Dans un temps ultérieur il faudra vérifier si

l'addition d'une charge au niveau de la cheville pourrait influencer la reproductibilité intra-sujets. Finalement, des recherches additionnelles seront nécessaires pour identifier des mouvements reproductibles correspondants à des situations spécifiques, tels que la marche, le saut et la montée d'escalier.

3.8 REMERCIEMENTS

Les auteurs tiennent à remercier Dr. A. Naddaf, F. Ganjikia, le CRSNG, le centre de recherche du CHUM et son personnel, dont plus particulièrement : V. Roy, Y. Chevalier, et G. Parent.

CHAPTER 4

ARTICLE 3: KINEMATIC STUDY OF THE KNEE WITH A THREE-DIMENSIONAL KNEE ANALYZER

4.1 Situation of article in thesis

In the pervious chapter, we have examined an appropriate movement which results into a reproducible movement within the same subjects for 3 different positions (standing, squatting, sitting). The results showed that the knee analyzer allows us to collect kinematics indices with good reproducibility. Our results suggested that the mean average of the multiple correlation coefficient for different days was larger than 0.7 for different positions for all 5 subjects in 3 positions. There were no significant statistical difference among 3 different positions. However, the multiple correlation coefficient of flexion-extension movement while the subject is sitting yields slimly higher than standing and squatting position. In this chapter we will test the reproduciblity of kinematic indices by putting a 3 kg charge on the ankle and we tested two different sets of experiment with 2 different methods of calibration (3-point and 8-point) that we will elaborate in details.

KINEMATIC STUDY OF THE KNEE WITH A THREE-DIMENSIONAL ANALYZER

Shafagh Ganjikia[1,2], Nicolas Duval[2], L'Hocine Yahia[1,2], Jacques de Guise[1,3]

[1] Laboratoire de recherche en Imagerie et Orthopédie, Centre de recherche, Centre hospitalier de l' Université de Montréal (CHUM) – Hôpital Notre-Dame, 1560 rue Sherbrooke Est, Montréal, Qc H2L 4M1, Canada

[2] Groupe de recherche en Biomécanique/Biomatériaux, Ecole Polytechnique, C.P. 6079, Succ. Centre-ville, Montréal, Qc H3C 3A7, Canada

[3] Laboratoire d'Imagerie, de Vision et d'Intelligence Artificielle, Ecole de technologie supérieure, 1100, rue Notre-Dame Ouest, Montréal, Qc H3C 1K3, Canada

Submitted to Clinical Biomechanics journal March 2000

Key words: 3D knee analyzer, knee kinematic indices, correlation coefficient, active flexion-extension.

Correspondence to : Shafagh Ganjikia,

Biomedical Engineering Department, École Polytechnique, P.O. Box 6079
Station « Downtown », Montréal, Québec, Canada H3C3A7;

tel (514)3404711 extension 4198; fax (514) 340-4611; e-mail: ganjikia@yahoo.com

4.2 ABSTRACT

The three-dimensional (3D) analyzer developed by our group was used to 1) investigate if a 3-kg charge has an effect on the reproducibility of kinematic measurements, 2) determine an appropriate reproducible movement between flexion-extension in the standing and sitting positions, and 3) demonstrate whether a 3-point or 8-point method of establishing functional axes would result in uniform and reproducible data on different days. We measured flexion-extension, abduction-adduction, internal-external rotation in 5 healthy subjects employing correlation coefficients to observe reproducibility of the data. The results show that the 3-kg charge had no significant effect on the reproducibility of these kinematic indices and no statistical difference in kinematic indices between the standing and sitting position. The 8-point method produced uniform data over different days but there was no statistical difference between the 2 methods. The system allowed us to develop a non-invasive method of evaluating the kinematics of the knee with reproducible results in 3D.

4.3 INTRODUCTION

The human knee is a very complicated joint. Its motion is not limited to a hinge-type action around a single transverse axis. In addition to flexion-extension, the knee can also bend towards and away from the centerline of the body in what is known as abduction-adduction or *varus-valgus* motion. Besides these 2 types of rotation, the knee can turn around its long axis in internal-external rotation (Netter, 1991). There are also three translational displacements: medial-lateral shift along an axis in the mediolateral direction; anterior-posterior drawer along an axis in the anterior-posterior direction; and compression-distraction along the superior-inferior direction of the tibia. In this paper, we will concentrate on rotation movements (flexion-extension, abduction-adduction and internal-external rotaion). The incidence of knee lesions is increasing as a result of intensive sports activities. According to Gottlob (Gottlob, 1998), 165, 000 ligament reconstructions were performed in 1997 in the U.S. and an estimated 175, 000 surgical procedures will be done in 2000 with a cost of up to $ 2 million per year.

Physicians examine knee motions subjectively, and compare their observations at different times on the basis of their memory and the accuracy of their descriptions. In the past, abnormal motions between the tibia and femur would be detected through manipulation of the knee by hand (Hewett et al.1997, Eihab et al. 1994). Often, the motion of a knee with torn ligaments is subtle and difficult to quantify or even to compare with the patient's uninjured knee. Since the normal knee is capable of substantial motion, it is desireable to measure its precise angular rotation quantitatively to allow comparison and determine the extent of injury (Wroble et al. 1990).

The inadequacy of existing instruments for knee evaluation prevents the diagnosis of injury and/or the evaluation of different treatment methods. Clinical test instruments such as the KT1000 (Torzilliet al., 1991) and the Crucialmeter (Beacon et al., 1999)

have been proposed, but their applications are controversial in terms of the reliability and repeatability of inter-subject studies on different days. Furthermore, these instruments evaluate the knee in only 2 dimensions (2D). The measurement or the estimation of knee laxity under a load using commercial devices such as KT1000 (Torzilliet al., 1991) or Telos Stress Devices (Stäubli, 1990) gives clinicians an understanding of the efficacy of surgical treatment or help to diagnose ligament ruptures. Given the three-dimensional (3D) nature of knee movement, it is important to complete measurements of knee laxity by global assessment (in 3D). Reproducible, objective measurements would therefore be useful for recording kinematic indices under a charge. Characterization of joint performance by kinematic analysis is a technique which may complement traditional evaluation protocols and offer the advantage of quick accurate assessment. To this end, a study to determine an appropriate reproducible movement is necessary as well.

The literature on knee joint kinematics has been difficult to compare due to the use of different anatomical landmarks, axis nomenclature, and analytical methods. For example, finding the functional axes from video-based images is usually a difficult task. It is commonly believed that the finite helical axis (FHA) can be identified through video-based motion analysis by studying incremental images. Through simulation, Chèze *et al.* (Chèze et al., 1998) confirmed that accurate calculation of the FHA is only possible if the magnitude of rotational parameters is large enough. They, however, proposed identification of the functional axes by studying the FHA via large rotational parameters. One of the problems that arises from this type of method is that it does not consider the other rotational movements created by flexion-extension, namely, abduction and internal-external rotations of small amplitude. To this end, we propose the use of 3-point and 8-point of determining functional axes in parallel in this study.

The specific objectives of this study were to: 1) investigate if a 3-kg charge has an effect on the reproducibility of kinematic measurements using a 3D knee analyzer, 2) determine an appropriate reproducible movement between flexion-extension in standing

and sitting positions, and 3) demonstrate whether a 3-point and 8-point methods of determining functional axes would result in uniform and reproducible data on different days.

4.4 MATERIALS AND METHODS

4.4.1 3D knee analyzer

Our research group has developed a functional 3D knee analyzer that allows 3D evaluation of the knee in motion. The analyzer is composed of magnetic sensors, an attachment system fixing the sensors quasi solid on the knee (femur and tibia), a computer and a program to register movement numerically and which allows graphic representation. Kinematic indices of femoral and tibial position and orientation are measured by 2 magnetic sensors placed solidly on the bone via the attachment system that minimizes sensor movement (Figure 4.1.a).

The femoral part contains 3 orthoplasts, a bridge that holds the orthoplasts together, and a bar on the medial side that is connected to the bridge and can be attached on the thigh. The tibial part is a simple bar that can be attached to the shank by straps. On the lateral side, the attachment system is placed on the superior part of the posterior condyle. The first orthoplast is positioned between the ilio-tibial band and the biceps femoris. On the medial side, the second (large circular) orthoplast is located on the femoral epicondyle, and the third orthoplast is attached on the adductor tubercule, behind the adductor magnus (Figure 4.1.b).

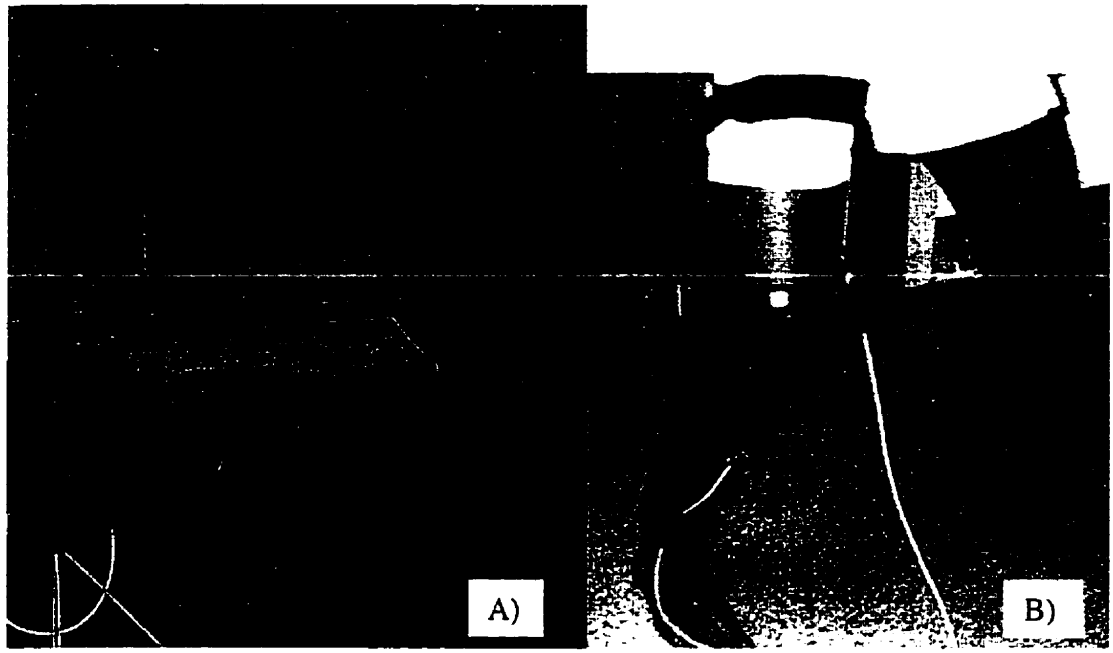

Figure 4.1: A) 3D knee analyzer. B) The attachment system on the lateral side is placed on the superior part of the posterior condyle. The orthoplast is positioned between the ilio-tibial band and the biceps femoris. On the medial side, large circular pads or othoplasts are placed on the femoral epicondyle, and the third orthoplast is positioned on the adductor tubercule behind the adductor magnus.

The tibial part is easily placed on the tibial bone and is fixed by 2 straps, one close to the tibial plateau, and the other, on the ankle.

Calibration relates movement of the sensors to flexion/extension, abduction/adduction and tibial rotation.

4.4.2 The coordinate system

To overcome the axes problem, we employed 2 different methods in parallel to define a axes system. In the first method, we used 3 points on the femur and 3 points on the tibia and a generic 3D image of the knee that allowed us to visualize real knee movement in the laboratory frame. For our purpose, we adopted the referential axes system based on the theory of mechanical axes of the femur and tibia (Sati et al., 1997). The origin for

this coordinate system is defined by a point that passes through the center of the medial and lateral epicondyles. The X axis is the flexion axis that passes through the center of the medial and lateral epicondyles. The Z or mechanical axis of the femur is perpendicular to the X axis and is placed on the plane formed by the X axis and the diaphys of the femur. Finally, the Y axis is the cross product of the Z and X axes. A second reference axis on the tibia is necessary to measure rotational knee movement. The X axis of the tibia goes through the center of the tibial plateau while the Z axis is perpendicular to the X axis and is placed on the plane of the X axis and diaphys of the tibia. The Y axis is then defined as the cross product of the Z and X axes.

The second method uses 8 points to define a coordinate system attached to the femur and 8 other points for the tibia. We digitize 3 arbitrary non-colinear points on the lab floor. The "normal" of this plane is Z_{abs_femur}. The projection on the floor of the vector, formed by connecting a point on the heel to a point on a toe perpendicular to the Z_{abs_femur}, forms the Y_{femur}. The next step is to construct the vector U_{femur} that passes through a point on the patella and the midpoint of the line connecting a point on the pubic tubercle and the greater trochanter. This vector, U_{femur}, is brought back until it is perpendicular to the Y_{femur} axis. The result forms the Z axis of the femur. X_{femur} is then formed as the cross product of Z_{femur} and Y_{femur} ($Y_{femur} \times Z_{femur} = X_{femur}$). The X_{femur}, Y_{femur} and Z_{femur} axes described above, constitute the coordinate system of the femur. A coordinate system for the tibia is constructed in the same way. Once again, we use 3 points on the floor to create a plane and a "normal" of this plane Z_{abs_tibia}. The Y_{tibia} axis is the projection, on the floor, of the vector that passes through a point on the heel and a point on a toe. This vector is perpendicular to Z_{abs_tibia} and Z_{tibia} is defined by a vector going through the midpoint of the 2 points on each side of the ankle and a point on the patella. The vector is taken back until it is perpendicular to Y_{tibia}. Finally, X_{tibia} is constructed as the cross product of Z_{tibia} and Y_{tibia} ($Z_{tibia} \times Y_{tibia} = X_{tibia}$). Figure 4.2 illustrates these points.

The orientation of the femur relative to the tibia in both 3- and 8-point methods can be found with a rotation matrix. This matrix can be decomposed into a series of 3 rotations around the moving axes X, Y' and Z''. The flexion-extension angle is defined around the X axis of the femur and defines rotation R_x. The abduction angle is the rotation around the Y axis of the femur that has undergone rotation around X and defines rotation $R_{y'}$, where $Y' = R_x Y$. Finally, internal-external rotation is defined by rotation around the Z axis of the femur that has undergone 2 successive rotations around X and Y' and defines rotation $R_{z''}$ where $Z'' = R_{y'}$ Rx Z. Z'' of the femur coincides with the Z axis of the tibia. These 2 methods are used in parallel for experimental recording (Grood et al. 1983).

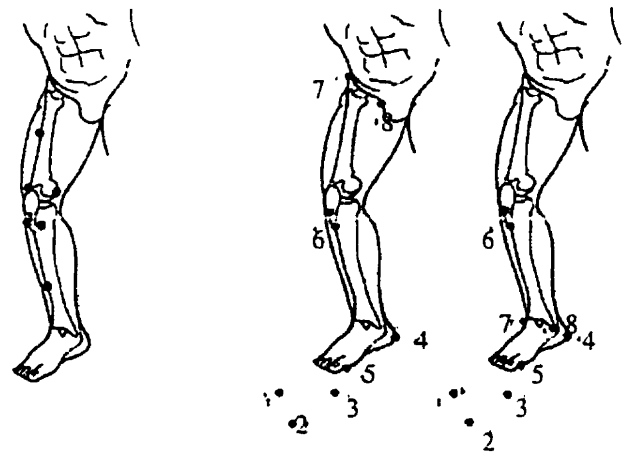

Figure 4.2: Two different methods used to define coordinate systems for the femur and tibia. A) The coordinate system using 3 points on the femur and 3 points on the tibia. B) The coordinate system using 8 points on the femur. Points 1, 2 and 3 represent the plane on the floor with Z_{abs_femur} normal to this plane. The Y axis is the projection of the vector passing through points 4 and 5 on the plane formed by points 1, 2 and 3. The Z axis is tilted vector ⊥ to Y formed from the line which goes through point 6 on the patella and the mid point of points 7 and 8 (the pubic tubercle and the great trochanter). X is the cross product of Y and Z.

C) The coordinate system using 8 points on the tibia. Points 1, 2 and 3 represent the plane on the floor with Z_{abs_tibia} perpendicular to it. The Y axis is the projection on the floor of the vector joining points 4 and 5 and is ⊥ to Z_{abs_tibia} . The Z axis is the tilted vector ⊥ to Y formed by a line which goes through point 6 on the patella and is connected to the mid point of 7 and 8 (on the medial and lateral ankle). X is the cross product of Y and Z.

4.4.3 Experimental acquisition

Our experiment was divided into 2 different settings. Five healthy volunteers with a mean age of 28 and no history of knee problems were studied. All subjects were further examined by an orthopedic surgeon to confirm their knee condition. In the first set of experiments, the exoskeleton attachment system was installed once and was not replaced throughout the complete procedure. We then recorded 10 cycles of active flexion-extension movement in the standing position by alternatively placing and removing a 3-kg charge 10 times over the ankle (5 times with and 5 times without the charge).

The second set of experiments was performed on different days by placing and removing the attachment system on the knee with the 3-Kg charge over the ankle at all times. We recorded 10 cycles of active flexion-extension, 10 times in the standing and sitting positions with the 3-point and 8-point systems in parallel.

In each set of experiments, kinematic indices for flexion-extension, abduction-adduction, and tibial rotations were obtained by a program in C++ environment developed in our laboratory. Simple statistical methods are inadequate to compare kinematic and dynamic data obtained on different days in different subjects. Hence, in our study, we used the multiple correlation coefficien (Neter et al. 1985 and Winer, 1971), R^2_a , to evaluate the similarity between various data recorded within a test day. In equation 1, the numerator of the ratio represents variation of the mean at time point t for a particular day, and the denominator represents total variability of the grand mean for that day. In equation 4, the numerator represents variance of the mean at time point t over all test days, and the denominator represents total variability the grand mean of all test days. The multiple correlation coefficient is bound to be between 0 and 1, with larger values indicating a higher similarity among the data (Kadaba et al., 1989).

$$R_a^2 = 1 - \frac{\sum_{i=1}^{M} \sum_{j=1}^{N} \sum_{t=1}^{T} \frac{(Y_{ijt} - \overline{Y_{it}})^2}{MT(N-1)}}{\sum_{i=1}^{M} \sum_{j=1}^{N} \sum_{t=1}^{T} \frac{(Y_{ijt} - \overline{Y_i})^2}{M(NT-1)}} \tag{4.1}$$

where Y_{ijt} is the tth point in time of the jth run on the ith test day. $\overline{Y_{it}}$ is the average at the tth point in time on the ith test day.

$$\overline{Y_{it}} = \frac{1}{N} \sum_{j=1}^{N} Y_{ijt} \tag{4.2}$$

whereas $\overline{Y_i}$, the grand mean on the ith day, is given by the following equation:

$$\overline{Y_i} = \frac{1}{NT} \sum_{j=1}^{N} \sum_{t=1}^{T} Y_{ijt} \tag{4.3}$$

If all experiments for 1 subject are done on the same day, one should put i=1.

The coefficient of multiple correlation evaluating the similarity or repeatability of data within different test days is given by:

$$R_a^2 = 1 - \frac{\sum_{i=1}^{M} \sum_{j=1}^{N} \sum_{t=1}^{T} \frac{(Y_{ijt} - \overline{Y_t})^2}{T\,(MN - 1)}}{\sum_{i=1}^{M} \sum_{j=1}^{N} \sum_{t=1}^{T} \frac{(Y_{ijt} - \overline{Y})^2}{(MNT - 1)}} \tag{4.4}$$

where $\overline{Y_t}$ is the average at tth point in time over NM flexion-extension cycles,

$$\overline{Y_t} = \frac{1}{MN} \sum_{i=1}^{M} \sum_{j=1}^{N} Y_{ijt} \tag{4.5}$$

and $\overline{Y}$, the grand mean over time, is given by

$$\overline{Y} = \frac{1}{MNT} \sum_{i=1}^{M} \sum_{j}^{N} \sum_{t=1}^{T} Y_{ijt} \tag{4.6}$$

4.5 RESULTS AND DISCUSSION

The uncertainty that prevails in kinematic measurement poses difficulties in knee surgery evaluation. It is therefore necessary to quantify kinematic measurements to compare knee motion with statistical norms or past records to monitor the progress of treatment (Cappello et al., 1997). To this end, we used a 3D knee analyzer to measure kinematic indices of flexion-extension, abduction-adduction and internal-external rotation.

The first set of experiments is reported in tables 4.1 through 4.4 which present the mean of multiple correlation coefficients with and without charge on the ankle, using the 3-

point and 8-point methods of defining the system of axes. The mean of multiple correlation coefficients was found to be larger than 0.7. One-way none-parametric ANOVA showed that the 3-Kg charge had no significant effect on the kinematic indices (abduction and tibial rotation) in 5 out of 8 cases (Table 4.5). Note that the correlation coefficient is not a normal distribution. If none-parametric ANOVA are not to be used, one should use the Z Fisher transformation before caculating ANOVA to normalize the correlation coefficient. More over, we observed that fatigue in 1 of our subjects caused a gradual decrease in multiple correlation coefficients throughout consecutive tests on the same day (Fisz, 1980).

Figure 4.3 is a histogram presentation of the correlation coefficients with and without the charge. In our analysis, we separated flexion from extension to increase the specificity of our study.

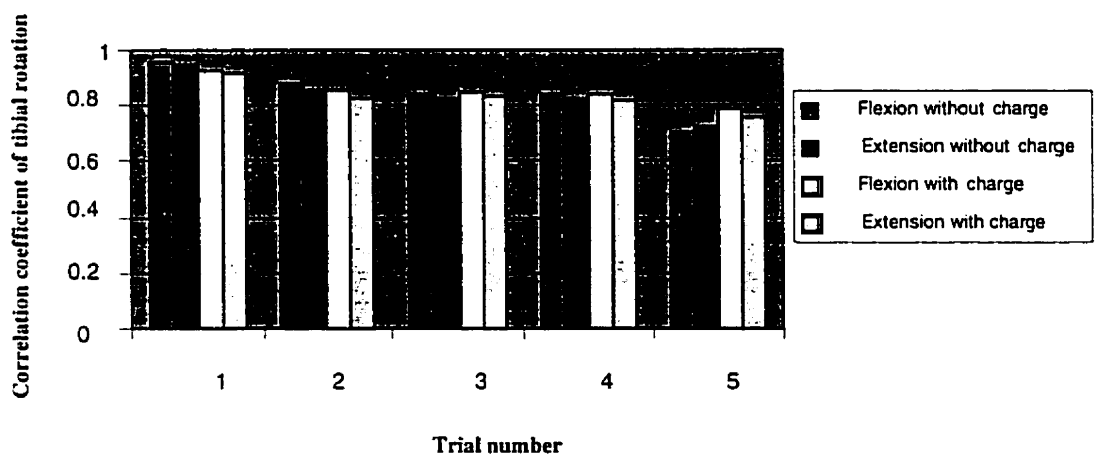

Figure 4.3: Multiple correlation coefficient of tibial rotation in the standing position for a typical subject. The X axes represents the trial number and the Y axis is the correlation coefficient. Note the gradual decrease in the correlation coefficient from the 1st to the 5th trial due to fatigue of the subject.

Table 4.1: Multiple correlation coefficient of abduction and tibial rotations in the standing position without a charge, using the 3-point method of calibration

N=5	Abduction-flexion	Abduction-extension	Tibial rotation-flexion	Tibial rotation-extension
1	0.98	0.98	0.93	0.90
2	0.71	0.70	0.75	0.75
3	0.98	0.96	0.93	0.93
4	0.95	0.94	0.73	0.77
5	0.95	0.95	0.85	0.81

Table 4.2: Multiple correlation coefficient of abduction and tibial rotations in the standing position with a charge 3-kg, using the 3-point method of calibration

N=5	Abduction-flexion	Abduction-extension	Tibial rotation-flexion	Tibial rotation-extension
1	0.99	0.99	0.89	0.90
2	0.76	0.82	0.70	0.72
3	0.97	0.96	0.89	0.85
4	0.96	0.96	0.70	0.70
5	0.97	0.97	0.84	0.71

Table 4.3: Multiple correlation coefficient of abduction and tibial rotation in the standing position without a charge, using the 8-point method of calibration

N=5	Abduction-flexion	Abduction-extension	Tibial rotation-flexion	Tibial rotation-extension
1	0.99	0.98	0.94	0.93
2	0.84	0.90	0.73	0.73
3	0.98	0.96	0.93	0.93
4	0.95	0.94	0.70	0.77
5	0.92	0.94	0.70	0.73

Table 4.4: Multiple correlation coefficient of abduction and tibial rotation in the standing position with a 3-kg charge using the 8-point method of calibration

N=5	Abduction-flexion	Abduction-extension	Tibial rotation-flexion	Tibial rotation-extension
1	0.99	0.99	0.94	0.92
2	0.91	0.91	0.72	0.83
3	0.97	0.96	0.89	0.85
4	0.96	0.96	0.70	0.71
5	0.96	0.96	0.71	0.71

Table 4.5: ANOVA 1-way testing the effect of charge on kinematic indices using the 2 different methods for determining the coordinate system of axes (3- and 8-point methods)

3 points			8 points		
P-Level	No charge	Charge	P-Level	No charge	Charge
0.18	0.91±0.1	0.93±0.09	0.21	0.93±0.06	0.96±0.03
0.19	0.91±0.1	0.94±0.07	0.03	0.94±0.03	0.96±0.03
0.007	0.83±0.1	0.80±0.1	0.41	0.80±0.1	0.79±0.1
0.04	0.83±0.08	0.78±0.09	0.68	0.81±0.1	0.80±0.09

In the second set of experiments, we placed the attachment system over the knee on different days with the 3-kg charge over the ankle at all times. We employed both the 3- and 8-point methods during recording of the kinematic indices. Tables 4.6 and 4.7 present the mean of intra subjects correlation coefficients in the standing and sitting positions, using the 3-point method to determine the system of axes. Tables 4.8 and 4.9 present the mean of intra subjects multiple correlation coefficients in the standing and sitting positions, obtained by the 8-point method to determine the system of axes. Tables 4.6 to 4.9 demonstrate that the kinematics indices were reproducible and found to be between 0.7 and 0.99 for all cases. Static 1-way ANOVA revealed that there was no significant difference between multiple correlation coefficients of the standing and sitting positions in the majority of cases with the 3-point and 8-point methods. In just 2

cases, this test showed a significant difference in p-levels between the standing and sitting positions (Table 4.10).

Figure 4.4 depicts the multiple correlation coefficients for a typical subject, using the 3-point and 8-point methods. This graph illustrates the mean with error bars for 10 cycles of experiments on 10 different days. We studied the collected data for all 5 subjects in 2 different positions. The results in most cases using the 8-point method showed uniform data. The other method produced no particular pattern for inter-subject analyses.

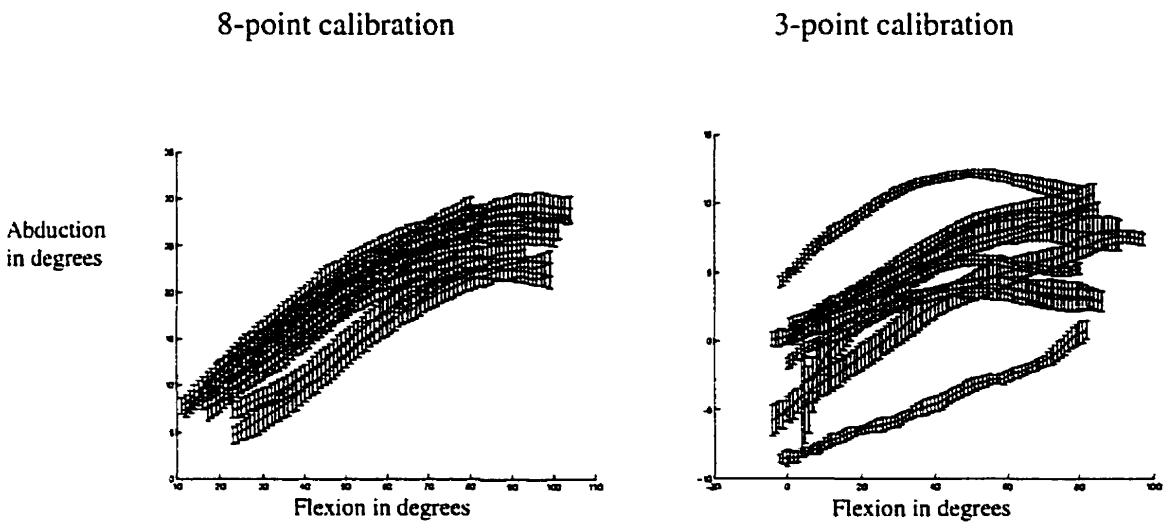

Figure 4.4: A and B represent the intra-subject mean and error bar for 10 cycles during 10 different trials (on different days). The data in A seems to follow the pattern, and were obtained using the 8-point method for the coordinate system. B is the 3-point method with the data showing a random shape in this particular case.

Table 4.6: Multiple correlation coefficient of abduction and tibial rotation in the standing position with a 3-kg charge, using 3-point calibration.

N=5	Abduction-flexion	Abduction-extension	Tibial rotation-flexion	Tibial rotation-extension
1	0.95	0.96	0.72	0.83
2	0.88	0.79	0.75	0.70
3	0.97	0.96	0.76	0.73
4	0.82	0.76	0.76	0.77
5	0.98	0.98	0.81	0.81

Table 4.7: Multiple correlation coefficient of abduction and tibial rotation in the sitting position with a 3-kg charge, using 3-point calibration.

N=5	Abduction-flexion	Abduction-extension	Tibial rotation-flexion	Tibial rotation-extension
1	0.94	0.96	0.85	0.88
2	0.77	0.87	0.75	0.74
3	0.91	0.89	0.72	0.78
4	0.76	0.93	0.75	0.75
5	0.94	0.96	0.79	0.77

Table 4.8: Multiple correlation coefficient of abduction and tibial rotation in standing position with a 3-kg charge, using 8-point calibration.

N=5	Abduction-flexion	Abduction-extension	Tibial rotation-flexion	Tibial rotation-extension
1	0.79	0.78	0.73	0.71
2	0.87	0.89	0.84	0.84
3	0.88	0.83	0.82	0.81
4	0.93	0.93	0.77	0.78
5	0.99	0.99	0.76	0.81

Table 4.9: Multiple correlation coefficient of abduction and tibial rotation in the sitting position with a 3-kg charge, using 8-point calibration.

N=5	Abduction-flexion	Abduction-extension	Tibial rotation-flexion	Tibial rotation-extension
1	0.76	0.81	0.80	0.81
2	0.88	0.92	0.85	0.86
3	0.83	0.89	0.78	0.83
4	0.94	0.98	0.78	0.76
5	0.97	0.98	0.84	0.92

Tables 4.11 and 4.12 show the average intra-subject correlation coefficients for different days. Even though the multiple correlation coefficients are very low in most cases, these results are still very interesting since sensitivity analysis (Kadaba et al., 1989) confirms that rotation axes could have different patterns for kinematic parameter measurements, and we observed a more uniform pattern in the data obtained with the 8-point method of determining the system of axes (Figure 4.4). ANOVA showed no significant statistical difference between the 2 methods (Table 4.13).

Table 4.10: ANOVA 1-way comparing the standing position to the sitting position with a 3-kg charge, using 3-point of calibration.

3-point			8-point		
P-Level	Standing	Sitting	P-Level	Standing	Sitting
0.03	0.92±0.06	0.87±0.09	0.24	0.89±0.07	0.88±0.08
0.49	0.89±0.1	0.92±0.04	0.06	0.88±0.08	0.92±0.07
0.71	0.76±0.03	0.77±0.05	0.3	0.78±0.04	0.81±0.03
0.45	0.77±0.05	0.78±0.06	0.14	0.79±0.05	0.83±0.06

Table 4.11: Intra-subject multiple correlation coefficients on different days with a charge over the ankle (using 8-point calibration)

N=5	Abduction-flexion		Abduction-extension		Rotation-flexion		Rotation-extension	
	Standing	Sitting	Standing	Sitting	Standing	Sitting	Standing	Sitting
1	0.003	0.003	0.01	0.01	0.12	0.15	0.13	0.13
2	0.08	0.24	0.1	0.23	0.07	0.13	0.12	0.16
3	0.03	0.007	0.03	0.01	0.35	0.14	0.33	0.21
4	0.3	0.21	0.37	0.63	0.08	0.21	0.01	0.31
5	0.83	0.69	0.86	0.72	0.05	0.31	0.28	0.46

Table 4.12: Intra-subject multiple correlation coefficients on different days with a charge over the ankle (using 3-point calibration)

N=5	Abduction-flexion		Abduction-extension		Rotation-flexion		Rotation-extension	
	Standing	Sitting	Standing	Sitting	Standing	Sitting	Standing	Sitting
1	0.06	0.04	0.05	0.07	0.07	0.07	0.07	0.11
2	0.03	0.04	0.04	0.06	0.03	0.17	0.13	0.17
3	0.13	0.1	0.14	0.12	0.28	0.03	0.46	0.03
4	0.05	0.04	0.06	0.22	0.05	0.12	0.03	0.12
5	0.2	0.29	0.3	0.32	0.18	0.03	0.26	0.05

Table 4.13: Anova 1-way testing intra subject correlation coefficients using 2 different methods of calibration (3-point and 8-point)

	P-Level	8-point	3-point
Abduction-flexion in the standing position	0.31	0.24±0.34	0.09±0.07
Abduction-flexion in the sitting position	0.22	0.23±0.28	0.1±0.1
Abduction-extension in the standing position	0.28	0.27±0.36	0.12±0.1
Abduction-extension in the sitting position	0.21	0.32±0.34	0.16±0.1
Tibial rotation-flexion in the standing position	0.75	0.13±0.12	0.12±0.1
Tibial roatation-flexion in the sitting position	0.11	0.14±0.07	0.09±0.06
Tibial rotation-extension in the standing position	0.64	0.17±0.13	0.19±0.2
Tibial rotation-extension in the sitting position	0.1	0.25±0.13	0.1±0.06

Due to the errors inherited by the uncertainty of defining the axes, one cannot consider the amplitudes of abduction-adduction and internal-external rotations as reliable measures at this point (Cappello et al. 1997). We believe that the focus should be on finding more reliable means to define the axes, and consequently enable researchers to perform more accurate inter-subject experiments. This will certainly help clinicians to overcome the poor accuracy and lack of a complete measurement, with related deficiencies, over a normal range of motions (Fuller et al., 1997). Reliable and complete measurement of joint movement needs accuracy in the order of 1 mm and 1 degree (Deluzio et al., 1997).

4.6 CONCLUSION

The only remedy for symptomatic chronic ligament rupture is surgery. In juxtaposition with surgery, surgeons need a reliable instrument, that will allow them to evaluate the results of their work (Hafzy et al., 1988). These measurements have to be reproducible and quantitative. Many studies have demonstrated that in the long run, the accuracy of implantation plays a very important role in successful outcomes (Hafzy et al., 1996). Surgeons emphasize the importance of evaluation before and after treatment (surgery).

This evaluation calls for an instrument that would allow the kinematics of the knee articulations to be measured and assessed in a non-invasive fashion. Most existing instruments are capable of evaluating the knee statically. Given the complicated 3D nature of the knee, it is more appropriate to study its 3D behavior globally. In this work we used the 3D knee analyzer developed in our laboratory and showed a 3-Kg charge on the ankle had no effect on the reproducibility of flexion-extension. The results also demonstrated that flexion-extension movements presented no significant statistical difference for the standing and sitting positions in the majority of the cases. However, it would be interesting to test different charges and determine the tolerable range. 8-point method, for determining a system of axes generated more uniform data for different days for most subjects. The mean of the intra subject correlation coefficients was found to be between 0.7 to 0.99. 3D knee analyzer has potential to be used in clinical settings after investigating other specific movements such as walking, jumping and climbing.

4.7 ACKNOWLEDGEMENTS

This work was founded by the NSERC organisations. The authors would like to thank A. Naddaf, S. Mostsharnia, G. parent for their technical assistance and Y. Chevalier for his artistic help.

CHAPTER 5

DISCUSSION

5.1 GENERAL DISCUSSION

The human muscloskeletal system is composed of a series of jointed links. Six independent parameters, or degrees of freedom, are needed to describe the location and orientation of each link in space. For the knee joint, due to the limitations posed by the movement of skin and soft tissues, measurements of more subtle movements such as internal-external and abduction-adduction rotations are undermined. Consequently there still stands the basic question as to what constitutes a *'normal'* motion for a knee.

Early measurements with exoskeletal linkages were limited to the sagittal plane (Liberson, 1965). More recently, triaxial and spatial exoskeletal linkage have been used to measure the three-dimensional kinematics of the knee joint (Lamoreux, 1971).

There are two problems with this type of linkages: one is the nonrigid fixation of the transducer to the lower limb segments such as foot-ground contacts and muscular actions can cause the linkage to shift relative to femur and tibia and secondlly, the position of the linkage with respect to the internal bony structure of the knee joint must be accurately defined to allow for accurate functional and clinical interpretation of the transducer output. A few researchers (Murphy, 1990; Lafortune & Lake, 1991; Karlsson & Lundberg 1994) have suggested the invasive methods such as insertion of Steinmann traction pins into the femur and tibia of human subjects but this method represents a highly invasive and stressful technique to measure the three-dimensional motion of tibio-femoral articulation, especially compared to the non-invasive character of skin markers and exoskeletal linkages.

For example, Chèze et al. put markers (at least three) on each bone. Then, they measure the movements of marker by a video-based motion analyzer. The authors are concerned with the accuracy of obtaining the finite helical axis of motion (FHA) from a video-based motion analysis. To obtain kinematics of the relative movement of one bone with respect to the other one. They use the location of corresponding markers from a frame i to frame i+1, they calculate the FHA and hence find the relative displacement of the two bones between these two frames. The problem in this method is the following: markers do not represent the accurate location of bones, so there is an error (up to 2 cm) in the accurate measurement of the location of bones. If we allow such an error in our measurement when we calculate FHA from frame i to i+1, the error in finding FHA is too large. In fact it is shown that the error is inversely proportional to the magnitude of the rotational magnitude. This means, for frame i to i+1, the rotational magnitude is usually very small, and therefore the error is pretty large. His main objective in this study is to show this error quantitatively. To this end, he simulates a knee joint movement (thigh and shank) by obtaining some data and refining and filtering them to obtain an accurate FHA from these accurate data. Then some random errors added to the location of the markers throughout a simulation. These random errors represent the possible error that one encounters while calculating the location of markers based on video techniques. Then he calculates the new FHA for this perturbed data and observes that if the rotational magnitude is anything less than 20 degrees. Therefore he concludes that if one wants to use FHA which is calculated based on the observation of markers in a video-based motion anaylzer, then the rotational magnitude should be large otherwise the result is in accurate. Since, the angular motions other than flexion-extension are of relativly small amplitudes, therefore, the skin markers will not provide a satisfactory answer.

5.1.1 3D kinematic measuring devices and 3D tracking system

We have described the currently existing 3D kinematic measurement devices in Chapter 1. These exoskeletal linkage devices assume that they are perfectly rigid between the

linkage and the bones. We have already demonstrated that contrary to their believes, these type of devices would not be considered sufficiently good mainly due to their limitation.

We also looked at motion tracking system devices in terms of their mechanism of operation and their advantages and limitations. We concluded that currently, the magnetic sensors are best suited for our experiments. Accuracy of magnetic systems is of order of 2.5 mm (rms) in position and 0.5 degree in rotation. However these systems can be calibrated to increase their position accuracy to 1 mm (rms). They are easy to use and portable but they also have limitations such as unwanted sensitivity to metallic objects, low sampling rates (60 Hz) and small number of sensors. These limitations, however, did not interfere with our experimental purposes. Prior to each experiment, we had tested the experiment's environment to assure the accuracy of our measurements. We used a digitized Plexiglas box to calculate the error of measurement to assure the absence of magnetic interference and then proceeded with our experiment only if the error were found to be less than 2 mm.

The sampling rate was sufficient for our experimental purposes. We only needed 2 sensors, one on the tibia and one on the femur. Motion-tracking devices classically use markers which are set on the subject's skin, but the slip of skin during the analysis makes it difficult, or sometimes even impossible, to determining the combined motions. For this reason, we cannot simply attach the magnetic sensor on the skin.

As was discussed in Chapter 2, our research group has developed a 3D knee analyser to address these difficulties. This device consists of an exoskeleton attachment system, a kinematic tracking system (or sensors), a computer system, a screen for display, and a C program with a user interface for calculating the kinematic indices which, in turn, allows us to follow the 3D movement of femur and tibia of *in vivo* subject. The first version was introduced by Sati et al. (1996). Even thought the results were satisfactory, the system encountered certain difficulties in experimental settings. For example, adjustment

of the exoskeleton attachment system was somewhat complicated and lengthy and the system was not comfortable.

A second version was then fabricated and went under study but this version also failed to answer all the needs. Some of the short comings of the first version were addressed in this newer version but some new problems were also born. As we saw in Chapter 2, the second version had problems such as poor resistance of the bridge, very uncomfortable orthoplasts due to their symmetric form which did not follow the anatomical structure, and the possible and undesirable movement of orthoplasts.

As a results, a third model was designed and fabricated in 1999. The new design tries to adopt and adjust itself to different anatomical shapes. This new system is a major improvement over the other previous two models. All the drawbacks of the other two models were ameliorated in this version.

5.1.2 Fluoroscopic validation

Through a fluoroscopic study, we have compared the movement of markers over the skin and over the exoskeleton attachment system in order to determine if the use of attachment system would reduces the movement of skin with respect to the underlying bone. This study showed that the skin movement was reduced by a fair amount on average. More precisely, We have shown that the RMS error of displacement in *XZ* plane on the lateral side was reduced from 13.7 to 4.6 mm and RMS error of rotation about *X* axis (Rx) from 3.4 to 1.5 degrees, RMS error of rotation about *Z* axe (Rz) from 6.9 to 2 degrees on the average for 4 subjects. On the medial side, RMS error of displacement in *XZ* plane was reduced and 10.5 to 4.1 mm and RMS error of rotation about X axis (Rx) from 2.3 to 1.7 degrees, RMS error of rotation about *Z* axis (Rz) from 5.4 to 1.3 degree on the average for 4 subjects. The last subject showed no significant improvement when using the exoskeleton attachment system due to its displacement.

For analysis, I have modified an existing program which was developed in 1996 by Sati et al. The main motivation in these modifications was to make an easy- to-use program which was more accurate and modular. I validated this program through both experimental and mathematical methods. Using experimental validation, the accuracy of measurement was found to be 1.9 mm on average in *XZ* plane, and of order of 0.91 degree about *X* axis (*Rx*) and 0.75 degree about *Z* axis (*Rz*).

The mathematical validation demonstrated an accuracy of 0.37 mm in *XZ* plane and 0.14 degree about X axis (*Rx*) and 0.15 degree about *Z* axis (*Rz*).

The results are adequately accurate for our main objective in this study, which is the validation of our attachment system in clinical settings.

5.1.3 Kinematic Studies

In Chapter 3, we considered different settings to perform our kinematics study. To find the most reproducible movement, we studied kinematic indices of abduction and tibial rotation in 3 different positions: standing, squat, sitting. We observed that there was no statistical significant difference among the 3 positions. However, the mean correlation coefficient of sitting position was slightly higher. The mean average of correlation coefficient was found to be higher than 0.7 with standard deviation in the range of 0.03 to 0.3 for all 5 subjects in 3 different positions. We have demonstrated that using 3D knee analyser allows us to measure the kinematics indices throughout intra-subject study with high reproducibility. The findings of the present study have indicated that angular motions other than flexion-extension are of relatively small amplitudes for abduction-adduction and internal-external rotation. The Finite Helical Axis (FHA) method is unreliable for kinematic measurements because it has been demonstrated by Chèze *et al.* 1998 that an accurate calculation of FHA is only possible if the magnitude of rotational parameters is large enough.

5.1.4 Kinematic studies under a 3 kg charge

In chapter 4, we tested if adding a charge on the ankle would change the reproducibility of kinematic indices. The results, however, have shown no significant statistical difference. Nevertheless It has been observed that in one subject among 5, the fatigue had caused a gradual decrease in correlation coefficient of abduction and tibial rotation.

The mean of correlation coefficients was found to be larger than 0.7 with standard deviation in the range 0.01 to 0.3.

Another point of focus and experiment was to place and replace the exoskeleton attachment system with charge to identify the most reproducible movement between standing and sitting positions in 10 different trials. The results of intra-subject study for all 5 subjects showed no significant statistical difference in the majority of cases.

In this set of experiments we had used 2 different methods for defining the system of axes, i.e. the 3-point and 8-point methods and statistical analysis showed no difference between the two methods. However we observed that the 8-point method resulted in more uniform patterns for an inter subject study in some cases.

The observation from 3-point and 8-point methods is an interesting result. To our knowledge, there is no other group that has done repeted intra-subjects study of kinematic measurements. Nonetheless, these results are still preliminary and further investigations are needed to provide a solid ground for our observations. Moreover, we were not able to perform an inter-subject study due to inaccuracy in defining the reference axes system at this point. We believe that the focus should be pointed at finding more reliable means to define the axes and reliable calibration method.

I was able to accomplish and demonstrate some interesting results through this study by providing a 3D knee analyser. The exoskeleton attachment system was validated using scientific methods and mathematical tools.

It is obvious that the invasive method are more accurate but the apparent superiority is achieved at the expense of discomfort and contamination of patient body. The present study has provided data which allow a unique perspective on the so-called repeated kinematic measurements mechanism of the tibio-femoral joint. We are confident that in the near future, we will be able to provide a system to evaluate the knee non-invasivly and minimise the risk of contamination and discomfort for the patient due to invasive methods.

CHAPTER 6

CONCLUSIONS AND RECOMMENDATIONS

6.1 GENERAL CONCLUSION AND RECOMMENDATION

Fluoroscopic study has demonstrated that the attachment system considerably reduces the movement of skin with respect to the underlying bone. We have calculated the accuracy measurement on the lateral and medial sides separately. For example, the results showed the movement on the lateral side is grater than the medial side as was expected due to the anatomy knee.

The method and the developed Matlab program, which were discussed in Chapter 2, were found to be accurate up to 0.5 mm and 0.2 degree (Ganjikia et al., 2000b)in displacement and in angular rotations, respectively. The main difficulty in the analysis was due to the poor quality of images and hence the inaccuracy in defining the reference axes on the bone. One would expect much more accurate results if one could use more recent and advanced imaging techniques of contour detection to define the reference axes more accurately. Furthermore, more precise results would be expected if one were able to take simultaneous static ML and AP images and 3D reconstruction of the knee.

Using the 3D knee analyzer, we have measured kinematic indices related to flexion-extension, abduction-adduction, internal-external rotaions. We investigated the most reproducible movement among standing, squatting and sitting positions. Throughout an intra-subject study, the results showed reproducible kinematic indices (Ganjikia et al., 1998, 1999a –1999b-1999c, 2000a).

However we were not able to perform an inter-subject study due to inaccuracy in defining the reference axes system at this point. We believe that the focus should be pointed at finding more reliable means to define the axes and reliable calibration method , since the errors that are inherited by the uncertainty in defining the axes prevents researchers from performing more accurate inter-subject experiments. This will certainly help clinicians to overcome the poor accuracy and lack of a complete measurement, and related deficiencies, over a normal range of motions.

We tested the 8-point method of defining axes in our study and the preliminary study has shown that the results from the 8-point method offers a more uniform pattern compared to the 3-point method. To draw a more solid conclusion, however, we believe that more subjects should be tested with both methods.

We have observed that having charge over the ankle has not influenced the reproducibility of kinematic indices. Nevertheless, it seems reasonable to assume that the presence of charge, to some extend, should influence the reproducibility due to the additional muscular forces. It would also be useful to test different charges (i.e. 2 kg, 3 kg, 6 kg and 10 kg) to determine a tolerable range (Ganjikia et al., 1999d-1999e and Ganjikia et al. 2000a).

If the attachment system is to be used in an environment in which metallic objects are present, one should consider using other tracking systems such as optical ones (Optotrack). This will be best suited for evaluating knee prostheses since some of the available prostheses contain aluminium or other metallic composites.

The 3D knee analyser has shown a great potential to be used in clinical settings. It still requires further investigation of other particular movements such as walking, jumping and climbing.

REFERENCES

AN K.-N., JACOBSEN M.C., BERGLUND L.J. and E.Y.S. CHAO. (1988). Application of a Magnetic Tracking Devie to Kinesiologic Studies. *Journal of Biomechanics*, 21, 7, 613-620.

ANDREWS J.G. and YOUM Y. (1979). A Biomechanical Envestigation of Wrist Kinematics._*Journal of Biomechanics* , 12, 83-89.

ANDRIACCHI T.P. (1987). Clinical application of the SELSPOT system. Biomechanics symposium ASME 84, 339-342.

ANGELONI C., CAPPOZZO A., CATANI F. and LEARDINI A. (1992). Quantification of relative displacement between bones and skin and plated_mounted markers. Proceedings of the Eight Meeting of the European society of biomechanics Rome. Italy, 238-239.

BEACON J.P. (1999). Orthopaedic mesurment and display system.United states Patent, patent number: 5935086.

BRESINA STEPHEN J., VANNIER MICHAEL W., LOGAN SAMUEL E. and WEEKS PAUL M. (1986).Three Dimentional wrist Imaging: Evaluation of Functional and pathologic Anatomy by computer. *Clinics in plastic surgery*, 13, 3, 389-405.

CAPPOZZO A., CATANI F., DELLA CROCE U. and LEARDINI A. (1994). "Position and Orientation in Space of Bones During Movement: Anatomical Frame Definition and Determination," *Clinical Biomechanics*, 3, 171-178.

CAPPOZOA. CATANI F. and LEARDINI. (1995). Skin movement artifacts in human movement photogrammetry. Proceeding of the 14th congress of the international society of biomechanics. Paris, France, 13.

CAPPOZZO A., CATANI F., DELLA CROCE U. and LEARDINI. (1995).Position and orientation in space of bones during movement: Anatomical frame definition and determination. *Clinical Biomechanics*, 10, 4, 171-178.

CAPPELLO A., CAPPOZZO A., LA PALOMBARA PF., LUCCHETTI L. and LEARDINI. (1997). A. Multiple anatomical landmark calibration for optimal bone pose estimation. *Human Movement Science*, 16, 259-274.

CHÈZE L., FREGLY B.J. and DIMNET J. (1998). Error analysis of such skin-based methods. *Journal of Biomechanics*, 131:149.

CHÈZE L., FREGLY B.J. and DIMNET J. (1998). Determination of joint functional axe from noisy marker data using the finite helical axis. *Human Movement Science*, 17, 1-15.

CHÈZE L., FREGLY B.J. and DIMNET J. (1995). A solidification procedure to facilitate kinematic analyses based on video system data. *Journal of biomehanics*, 28, 879-884.

DELUZIO KJ., WYSS UP., ZEE B., COSTIGAN PA. and SORBIE C. (1997). Principal component models of knee kinematics and kinetics : normal vs. pathological gait patterns. *Human Movement Science*, 16, 201-217.

DANCE D.R. (1988). Diagnostic Radiology with X-Rays, The Physics of Medical Imaging, Webb, S. Edition Adam Hilger, 2, 21-73.

EL MAACH I. (1998). *Développement d'un nouveau système pour analyser la biocinématique du genou. Application: évaluation de l'orthèse plantaire*. Department of Biomedical Engineering, Master Thesis. L'École Polytechnique de Montréal, Canada.

EIHAB M. A., HEFZY M. S. and AFJEH A. (1994). Determination of the three-dimensional Dynamic Response of the Tibio-Femoral Joint Using a Dae Solver. *Advances in Bioengineering*. ACME, 421-422.

FRASER G.A. (1987). Joint laxity measurement. United States Patent, patent number 4649934.

FINE E. J. (1987). Goniometric feedback device and method for monitoring angles of body joints. United states Patent, patent number 4667685.

FULLER J., LIU LJ., MURPHY MC. and MANN RW. (1997). A comparison of lower-extremity skeletal kinematics measured using skin-and pin-mounted. *Human Movement Science*, 16, 219-242.

FISZ MAREK. (1980). Probability theory and mathematical statistics. 3d ed. *Mathematical statistics* Huntington, N.Y. Krieger Pub. Co. 257-350.

GROOD ES. and SUNTAY WJ. (1983). A joint coordinate system for the clinical description of three-dimensional motions : application of the knee. *J Biomech Eng*, 105, 136-144.

GOTTLOB CA. (1998). American Academy of Orthopedic Surgeons, New Orleans Conference.

GOLLEHON DL., TORZILLI PA. and WARREN RF. (1985). The role of posterolateral and crucaite ligaments in human knee stability (a biomechanical study). Trans Othrop Res Soc, 10, 270.

GANJIKIA SH., DUVAL N., YAHIA L.H. and DE GUISE J.A. (1998). Validation d'un analyseur fonctionnelle du genou. Journée scientifique des étudiants du C.H.U.M. Montreal, Canada.

GANJIKIA SH., DUVAL N., YAHIA L.H. and DE GUISE J.A. (1999). Analyzer Validation, 6th International PCL study group symposium. Cape town, South Africa, 20.

GANJIKIA SH., DUVAL N., YAHIA L.H. and DE GUISE J.A. (1999). Knee analyzer validation. In Archives of physiology and Biochemistry. Beaune, France, 77.

GANJIKIA SH., DUVAL N., YAHIA L.H. and DE GUISE J.A. (1999). Validation d'un analyseur fonctionnelle du genou. In proceedings of Journée de la recherche du POES (Programme d'orthopédie Édouard-Samson. Montreal, Canada.

GANJIKIA SH., DUVAL N., YAHIA L.H. and DE GUISE J.A. (1999). Validation d'un analyseur fonctionnelle du genou. In proceedings of Journée scientifique, département de chirurgie de l'université de Montréal, Canada.

GANJIKIA SH., DUVAL N., YAHIA L.H. and DE GUISE J.A. (2000). The kinematic study of the knee under a 3-kg charge using the 3D knee analyzer. In proceedings of the 19th Southern Biomedical Engineering conference. Virginia, USA.

GANJIKIA SH., DUVAL N., YAHIA L.H. and DE GUISE J.A. (2000). 3-D Knee analyzer validation by simple fluoroscopic study. The Knee (in press).

HOLDEN J. P., ORSINI J.A. and HOLDEN S.J. (1994). Estimates of skeletal motion: movement of surface –mounted targets relative to bone during gait. In proceedings of the thirteenth Southern Biomedical Engieering Conference, Memphis, USA.

HEWETT T. E., NOYES F. and LEE M. (1997). Diagnosis of complete and partial posterior cruciate ligament Ruptures. *The American Orthopaedic Socity for Sports medicine*, 648-654.

HAMEL G. (1997). *Définition de paramètres cliniques représentatifs de la cinématique tridimensionnelle de genou normaux*. Mémoire de maîtrise. Département de génie Biomédical, L'École Polytechnique de Montréal, Canada.

HAGEMEISTER N., DUVAL N., YAHIA L.H. and DE GUISE J.A. (1999). In vivo reproducibility of a new non-invasive diagnostic tool for three-dimensional knee evaluation. *The Knee*, 6, 175-181.

HEFZY M. S. and GROOD E. (1988). Review of knee Models. *Appl. Mech*, 41, 1, 1-13.

HEFZY M. S. and V-COOKE T. D. (1996). Review of Knee models update. *Appl. Mech. Rev*, 49, 187-193.

KINZEL G.L., HALL A.S. and HILLBERRY B.M. (1972). Measurement of total motion between two segments 1-Analytical development, 2-Description of application. *Journal of Biomechanics*, 5, 93-105, 283-295.

KADABA M.P., RAMAKRISHNAN HK., WOOTTEN ME., GAINEY J., GORTON G. and COCHRAN GVB. (1989). Repeatability of kinematic, kinetic and electromyographic Data in Normal Adult Gait. *J Othrop Res*, 7, 849-860.

KARLSSON D. and LUNDBERG A. (1994). Accuracy estimation of kinematic dara derived from bone anchored external markers. In proceedings of the international symposium on 3-D analysis of human movement, 27.

LAMB S. (1990). Dynamic sagittal knee test apparatus. United States Patent, patent number 4911177.

LAMOREAUX L. (1971). Kinematic Measurements in Walking. *Bulletin of Prosthetic Research*. BPR, 10, 15:3-84.

LEWIS J.L. (1988). Description and error evaluation of an *in vitro* Knee joint testing system. *Journal of Biomechanical Engineering*, 110, 238-248.

LOGAN S.E. GROSZEWSKI P., KRIEG J.C. and VANNIER M. (1988). Upper extremity kinematics assessment using four coupled six degree of freedom sensors. *Biomedical sciences Instrumentation*, 24, 1- 6.

LOGAN S. E., VANNIER M.W., BRESINA S. J. and WEEKS P. M. (1985). Wrist kinematic analysis using a 6 degree of freedom digitizer. Proceeddings of the Seventh Annual Conference of the IEEE Engierring in medicine and biology Society chicago Illinois, 13-17.

LAFORTUNE M.P., CAVANAGH P.R., SOMMER H.J. and KALENAK A. (1992). Three-dimensional kinematics of the human knee during walking. *J. Biomechanics*, 25, 347-357.

LAFORTUNE M.A. and LAKE M.J. (1991). Errors in 3D analysis of human movement. In international conference on 3-D analysis of human movement, 55-56.

MCLEOD P.C. (1989). Dynamic joint motion analysis technique. United States Patent, patent number 4804001.

MILLS O.S. and HULL M.L. (1991). Apparatus to Obtain Rotational Flexibility of the Human Knee Under Moment Loads In Vivo. *Journal of Biomechanics*, 24, 6, 351-369.

MORRIS J.R. W. (1973). Accelerometry- a technique for the Measurement of Human Body Movements. *Journal of Biomechanics*, 6, 6, 729-736.

MURPHY M.C. (1990). Geometry and kinematics of the normal human knee. Ph.D. Thesis. M.I.T, Boston, USA.

MACLEOD A. and MORRIS J.R.W. (1987). Investigation of inherent experimental noise in kinematic experiments using superficial markers In Biomechanics X-B (Johnson B., editor) Human Kinetics Publishers, Champaign IL. 1035-1039.

MORNEBURG T and PRÖSCHEL PA. (1998). Differences Between Traces of

Adjacent Condylar Points and Their Impact on Clinical Evaluation of Condyle Motion. *The international Journal of Prosthodontics* 11, 4, 317-324.

NETTER F. H. (1991). The CIBA Collection of Medical Illustrations, 8, 94-98.

NETER J, WASSERMAN and KUTHER M. (1985). Applied linear statistical models, 2nd Edition. Homewood, IL, Irwin, 241-242, 643-654.

QUINN T.P. and MOTE C.D. JR. (1990). A Six-Degree-of-Freedom Acoustic Transducer for Rotation and Translation Measurement Across the knee. *Journal of* biomechanical *Engineering*, 112, 371-378.

RHYNE T. M. and TREINISH L. (1998). Visualisation of combined motions in human joints, *Computer Graphics and Applications*, 10-14.

SOMMER H. J. (1981). A Technique for the calibration of Instrumented Spatial Linkages used for Biomechanical Kinematic measurements. *Journal of Biomechanics*, 14, 91-98.

SATI M. (1995). Computer Assisted Knee Surgery System: Planning of Prosthetic Ligament Insertion. Thesis of doctrine. L'École Polytechnic de Montreal, Canada.

SATI M., DE GUISE J.A., LAROUCHE S. and DROUIN G. (1996). Quantitative assessment of skin-bone movement at the knee. *The Knee*, 3, 3, 121-138.

SATI M. DE GUISE J.A., LAROUCHE S. and DROUIN G. (1996). Improving in vivo knee kinematic measurements: application to prosthetic ligament analysis. *The Knee*, 3, 4, 179-190.

SIEGLER S. (1988). The 3 Dimensional Kinematics and flexibility characteristics of the human ankle and Subtalar joint-part i: Kinematics. *Journal of Biomechanics*, 110, 364-373.

STÄUBLI HU. (1990). Stressradiography. In: Knee ligaments: structure, function, injury and repair. New York: Raven Press, 449-459.

TOWNSEND M.A. (1997). Total Motion Knee goniometry. *Journal of Biomechanics*, 10, 183-193.

TORZILLI PA. (1991). Measurement reproducibility of two commercial knee test devices *Journal of Orthopaedic Research*, 730-737.

VOGT L, BERNHARDT M. and BANZER W. (1998). Three-dimensional kinematic data of the trunk and pelvis in incline treadmill walking. 3rd Int. World Congress on Low Back and Pelvic Pain, Vienna.

VOGT L, MOSHREF Y, BERNHARD M. and BANZER W. (1999). Lumbar corsets: Their effect on threedimensional kinematics of the pelvis. ACSM, Seattle.

WROBLE RANDALL R. and VAN GINKEL LAURA A. (1990). Repeatability of the Kt-1000 arthrometer in a normal population. *The American Journal of Sports medicine*, 18, 4, 396-399.

WINER BJ. (1971). Statistical principales in experimental design. *Mathematical statistics* 2nd Edition. New York, McGraw-Hill. 261-288.

ZVI L. (1989). A quantitative Comparison of Position Measurement System and Accelerometry. *Journal of Biomechanics*, 22, 4, 295-308.

ZVI L. (1991). Combining Position and Acceleration Measurements for Joint Force Estimation. *Journal of Biomechanics*, 24, 12, 1173-1187.

ANNEX I : ANNEXES FOR CHAPTER 1

Annex I-A: DEFINITION OF CRITERIA

Accuracy: Kinematic accuracy must be of the order of 1 degree for rotation and 1 mm for displacement to ensure that the system's kinematic error remains small compared to other systematic errors associated with the attachment of the system to patient. The system must maintain a high accuracy throughout the entire range of motion.

Size: The size of system should be reasonable to occupy a small space in the testing room, and should be preferably portable.

Safety: The system must not pose any risk to the individual and must be completely non-invasive.

Cost: The system should not cost more than $ 20.000.00 in order to keep the analysis cost effective.

Degrees of freedom: Only systems which provide the full 6 degrees of freedom are suitable for the visualisation of knee kinematics, hence we only consider such systems here.

Availability: The system should be available within a reasonable time limit (e.g. 1 month).

Limits: Technical obstacles such as calibration, shadowing, friction, noise interference, etc., should be minimised to ensure the ease of use. There should be some technical references on the evaluation of the system on an absolute or relative basis with other systems.

ANNEX II : ANNEXES FOR CHAPTER 2

Annex II-A: Fluoroscopic Protocol

In this annex, we will outline the procedure which should be followed during a fluoroscopic data acquisition.

Objectives: To characterise and compare the movement of skin with respect to the underlying bone, i.e. femur, with and without the attachment system.

List of materials:

- A Super VHS tape
- A number of 3 mm diameter metallic ball-bearings
- Some duct tape
- Two radio opaque rulers
- A human size plastic femur

Things to remember

- Have the subject sign the consent form before performing any experiment
- Make sure that the subject has not been exposed to X-ray recently
- Before starting the recording process, make sure that everything is visible on the fluoroscopic screen

- The direction is important (i.e. facing source) thus make sure the same convention is followed for all the subjects.
- Perform low acceleration movements .
- Make sure that the right knee is used!

How to proceed for the knee model or the subjects

A. Preparation

- Markers have to be fixed by pieces of duct tape, small enough so that they do not interfere with the movement of the skin.
- Do not put all of the makers along one straight line, otherwise distinguishing them on the image will be difficult.
- Spread out the markers evenly on one side at a time (Lateral or Medial).

B. Grating factor

- Place the table in vertical position
- Place one of the rulers on the table and the second one with some distance from the table.
- Measure the distance between the two rulers.
- Measure the distance between the table and the camera.
- Start recording.

C. AP (Antro-posterior) Static view

- Take both rulers out.

- Place one ruler on the patella and the second ruler on the lateral side (make sure they are perpendicular to each other).
- Place all markers on one side (lateral or medial).
- Place the subject facing the source and start recording.

D. ML (Medio-lateral) Static view

- Withouth moving the rulers, rotate the model or the subject by 90 degrees and take another image.
- Start recording.

E. Dynamic measurement

- Keep the model or the subject in sagittal plane and perform a flexion-extension 3 to 4 times from 0 to 100 degrees.
- Proceed with the recording

F. Markers on attachment

- Place markers on the attachment system.
- Place the attachment system on the right knee.
- Repeat the same procedures from A to D.

Data recording during experiment

Subject's name:

Date:

Time:

Technician's name:

Right or Left knee:

Number of markers:

Lateral or medial:

Distance between the rulers in mm:

Distance between the table and the camera in mm:

Orientation (draw diagram):

Width of knee in mm:

Annex II-B: Matlab program

We have developed a Matlab program to analyse the fluoroscopic images using the method which was first employed by Sati et al. (1996). This newly developed program reflects many new aspects by addressing the following issues: automating the use of program , robustness, expandability and providing an easy to use interface.

The new version of this program that we have developed has a complete Graphical User Interface (GUI) which by giving useful hints, walks the user through all the steps of the program. It also gives the user the ability to go back and make corrections before proceeding to next step. Each complete cycle of calculation is divided up into 4 parts: (1) Instrument Set-up, (2) Collecting static information, (3) Collecting dynamic information and (4) Computations.

1. Instrument Set-up

In a window which pops up for this purpose, user enters all the parameters of the experiment such as the name of image files, the various distances between different elements and the actual gratings of rulers. At the end, user can save this information for future references (Figure 2.6).

2. Static Information

By clicking on appropriate points, user measures the gratings of different rulers in both ML and AP views, the locations of markers in both views and similar information of this type. At the end, the program saves these data for internal use of the program. Up to this point, no calculation has been performed and these data are just the raw data that are gathered through the interactive clicking by user.

3. Dynamic Information

This parts is concerned with collecting dynamic data from different flexion-extension images. By clicking on appropriate points, user enters the location of different markers, identifying posterior condyles and distal ones and measures the required quantities which will be used to reflect the 3-D nature of the 2-D images.

4. Calculations

Once all the required raw data have been collected, the program can compile them to obtain various useful information. At this point, it is important that user specifies which knee (right or left) was tested and where the markers were located (lateral or medial). All the raw data from the last three steps are read into the program and at the end, the following information will be reported:

1. pm x ; pm z : the coordinates of markers in various images, before making the rotational estimation,
2. p x ; p z : the coordinates of markers after making the rotational corrections,
3. RMS pm x pm z : the root mean square of pm x and pm z ,
4. RMS p x p z : the root mean square of p x and p z ,
5. R x ; R z : Rotation angels about the X and Z axes,
6. RMS Rx , RMSRz : angular accuracy of markers
7. Flexion angles for different images.

Improvements Over the earlier program

The original version lacked an easy-to-use interface. In the old version, starting the program would result in many windows popping up simultaneously and it was the

responsibility of the user to keep the track of these windows. Now there is only one window, with only one image at a time and this reduces any possible confusion which could arise otherwise. These are some improvements that are made to make this program easier to use and more accurate. Almost all of the actions are performed by clicking mouse on appropriate points and buttons and several hints and help buttons are provided to guide the user. We believe this is a big achievement since the whole program is complicated enough that the user can be easily distracted if appropriate tools are not provided. Another improvement was to break the whole process into the above mentioned four logical steps (i.e. instrument set-up, collecting static information, collecting dynamic information and calculations).

- The user can organize his/her actions accordingly, and is allowed stop at the end of each step, to continue possibly at a later time without the need to restart from the beginning. For example once the static information has been entered, the results are saved in some files, so the user can come back later and start from where he/she had left off, namely can start with dynamic information.

- User has the ability to go back and correct a mistake or redo the very last part. This reduces the time spent and the burden on the user since these types of programs which require a great deal of attention from the user side are bound to confuse the user, and simple mistakes are very common to happen. This feature reduces the load on user by a great factor.

- Some calculations which used to be the responsibility of the user are now done by program. For example, once a line is marked, drawing the perpendicular line is more accurate if done by the program rather than user, so we have taken advantage of these facts. Our program has reduced the steps that were not necessary for the user to take and has carried them over to the machine. At various points, program needs to find the distance between a point and a line. In the old version, this was done by drawing a line from that point, perpendicular to the original line and then marking the

intersection point and then finding the length of the segment in between. This method would result in an approximate value since at each step that user has to click on a point, an error is bound to enter to the calculations since the judgement is based on the precision of the user. Besides, it requires an extra step for the user to take and by drawing unnecessary lines, images get more crowded with various lines and points. To overcome this, we let the program do this; once the coordinates of a point and the equation of a line are known, the program calculates the distance mathematically which is more accurate and results in less work for the user, more accurate results, and cleaner images.

- There are two distinguished sets of coordinate systems. One is attached to the image window, which does not move, nor rotates, and the second one which is attached to the femur and moves along with the femur. At various points, one has to move back and forth between these two coordinate systems. This is now done through the general associated rotation matrix and results in a more accurate calculations.

- One can add more features to the program, as needed, with the least effort since different steps are separated and changing one part does not affect the rest of the program. This, in turn, makes it an expandable program.

Prior to application, we tested the program's validity with two different methods: experimental method and mathematical which has been demonstrated in this chapter.

Annex II-C: Position markers before and after 3D estimation

In this annex we present position of markers before and after making the 3D corrections for all 5 subjects, as well as its average over 4 of them. It should be noted that based on the relative movement of skin with respect to the bone, the RMS of markers' positions may reduce or increase when the 3D corrections are applied.

RMS error of position markers before and after 3D estimation for subject 1

Lateral	Marker 1	Marker 2	Marker 3	Marker 4	Marker 5	Marker 6	Marker 7
RMS_*PmxPmz* *	10	10.4	10.4	12.9	14.5	15.5	18.2
RMS_*PxPz**	8.8	11.2	9.2	11.8	13.7	15.9	21.5
RMS_*PmxPmz*	3.8	3.1	3.1	5.1			
RMS_*PxPz*	2.4	1.8	2.2	3.8			
Medial	Marker 1	Marker 2	Marker 3	Marker 4	Marker 5	Marker 6	Marker 7
RMS_*PmxPmz* *	3.5	5.2	3.3	6.2	11.2	16.9	20.1
RMS_*PxPz**	3.9	4.4	9.7	13.7	14.3	16.3	19.2
RMS_*PmxPmz*	0.27	0.48	0.37	0.57			
RMS_*PxPz*	0.31	0.42	0.29	0.77			

* Without the attachment system

RMS error of position markers before and after 3D estimation for subject 2

Lateral	Marker1	Marker2	Marker 3	Marker 4	Marker5	Marker 6	Marker 7
RMS_*PmxPmz* *	21.9	8.5	12.3	5.4	12.3	12.1	14.2
RMS_*PxPz**	23.6	9.6	13.9	6.8	10.5	10.4	11.8
RMS_*PmxPmz*	2.7	3.1	3.6				
RMS_*PxPz*	6.8	5.5	4.8				
Medial	Marker1	Marker2	Marker 3	Marker 4	Marker5	Marker 6	Marker 7
RMS_*PmxPmz* *	5.4	7.3	8.3	8.9	11.8	12.9	16.8
RMS_*PxPz**	4.4	8.1	6.2	9.2	10.1	12.7	16.6
RMS_*PmxPmz*	4.6	5	5	4.3	3.7		
RMS_*PxPz*	5.3	5.4	6.1	5.8	5.7		

* Without the attachment system

RMS error of position markers before and after 3D estimation for subject 3

Lateral	Marker1	Marker2	Marker 3	Marker 4	Marker5	Marker 6	Marker 7
RMS_*PmxPmz* *	11.5	15.9	16.7	19.8	21.9	21.9	26.6
RMS_*PxPz**	11.9	17.1	17.8	17.1	20.1	20.3	26.2
RMS_*PmxPmz*	3.9	3.3	5.1				
RMS_*PxPz*	5.3	3.4	5.8				
Medial	Marker1	Marker2	Marker 3	Marker 4	Marker5	Marker 6	Marker 7
RMS_*PmxPmz* *	3.9	9.1	10.5	17.9			
RMS_*PxPz**	6.7	13.3	11.7	20.1			
RMS_*PmxPmz*	4.3	5.2	4.8				
RMS_*PxPz*	6.2	6	5.3				

*Without the attachment system

RMS error of position markers before and after 3D estimation for subject 4

Lateral	Marker 1	Marker 2	Marker 3	Marker 4	Marker 5	Marker 6	Marker 7
RMS_*PmxPmz* *	10.9	6.9	9	16.1			
RMS_*PxPz**	10.9	7.1	9.1	16.1			
RMS_*PmxPmz*	4.6	4.2	4.9				
RMS_*PxPz*	6.5	4.6	5.4				
Medial	Marker 1	Marker 2	Marker 3	Marker 4	Marker 5	Marker 6	Marker 7
RMS_*PmxPmz* *	6.7	5.9	8.7	10.5			
RMS_*PxPz**	6.4	5.9	8.3	10			
RMS_*PmxPmz*	5.8	4.8	5.5				
RMS_*PxPz*	4.8	4	4.3				

* Without the attachment system

RMS error of position markers before and after 3D estimation for subject 5

Lateral	Marker1	Marker2	Marker 3	Marker 4	Marker5	Marker 6	Marker 7
RMS_*PmxPmz* *	6.6	5.6	7.6	6.8			
RMS_*PxPz**	5.4	5.1	6.4	6.2			
RMS_*PmxPmz*	8.1	6.9	7.7				
RMS_*PxPz*	8.3	7.1	7.7				
Medial	Marker1	Marker2	Marker 3	Marker 4	Marker5	Marker 6	Marker 7
RMS_*PmxPmz* *	5	7.8	5.8	6.9			
RMS_*PxPz**	5.6	8.3	6.6	7.4			
RMS_*PmxPmz*	7.3	6.9	7.3				
RMS_*PxPz*	7.9	7.7	7.8				

* Without the attachment system

Mean accuracy measurement for the 4 subjects

Lateral	Subject 1	Subject 2	Subject 3	Subject 4	Mean
RMS_*PmxPmz* *	13.1	12.4	19.2	10.7	13.9
RMS_*PxPz**	13.2	12.4	18.6	10.8	13.7
RMS_*PmxPmz*	3.8	3.1	4.1	4.6	3.9
RMS_*PxPz*	2.6	5.7	4.8	5.5	4.6
Medial	Subject 1	Subject 2	Subject 3	Subject 4	Mean
RMS_*PmxPmz* *	9.5	10.2	10.4	8.0	9.5
RMS_*PxPz**	11.6	9.6	13	7.7	10.5
RMS_*PmxPmz*	0.42	4.9	4.8	5.4	3.8
RMS_*PxPz*	0.44	5.6	5.8	4.4	4.1

* Without the attachment system

Reduction factors for the 4 subjects with and without exoskeleton attachment

Lateral	Subject 1	Subject 2	Subject 3	Subject 4	Average
RMS_*PmxPmz*	3.5	4	4.7	2.3	3.6
RMS_*PxPz*	5.2	2.2	3.9	2	3.3
RMS *Rx*	3.3	1.7	2.8	2	2.4
RMS *Rz*	5.7	2.6	4.2	2.0	3.7
Medial	Subject 1	Subject 2	Subject 3	Subject 4	average
RMS_*PmxPmz*	22.5	2.1	2.2	1.5	7.0
RMS *PxPz*	26.	2	2.2	1.8	8
RMS *Rx*	21	0.75	1.0	1.4	6.1
RMS *Rz*	26.4	3.8	2.1	2.4	8.7

ANNEX III: ANNEXES FOR CHAPTER 3

Annex III-A: Kinematic experiemetal protocol

In this annex we are including a experimental protocol for kinematic measurements.

Kinematic experiemental protocol

Name:

Age:

Knee history:

Date:

1) Make sure that everything is connected and the Fastrack is turned on.
2) Environment test:
   - Put the sensors over the calibration box.
   - Digitize points 2 to 14 on the box.
   - Check the accuracy of measurement using a matlab program (Boîte-test) and confirm that it is less than 2mm.
3) Put the sensors on the attachment system (tibial and femoral part).
4) Install the attachment system.
5) Geometric calibration (3-point)
   - Femur: interne, extern, center of femoral diaphyse
   - Tibia: interne, extern, center of tibial diaphyse
6) Calibration of axes (3-point)

- Femur: interne, extern, center of femoral diaphyse
- Tibia: interne, extern, center of tibial diaphyse

7) Digitization by probe
   - Femur: interne, extern, center of femoral diaphyse
   - Tibia: interne, extern, center of tibial diaphyse
8) Test procedures
   - 10 cycles of flexion-extension in standing position
   - 10 cycles of flexion-extension in squatting position
   - 10 cycles of flexion-extension in sitting position
9) If the test are in same day replace the attachment system and repeat 4 to 8 procedures 10 times.
10) If the test are not in same day repeat 1 to 8 procedures as is necessary.

Annex III-B: Mean multiple correlation coefficient

This annex includes 4 bargraphs which represent mean multiple correlation coefficient of abduction during flexion, abduction during extension, tibial rotation during flexion and tibial rotation during extension for 3 different positions (standing, squatting and sitting) for all 5 subjects.

Average of correlation coefficient of tibial rotation during flexion

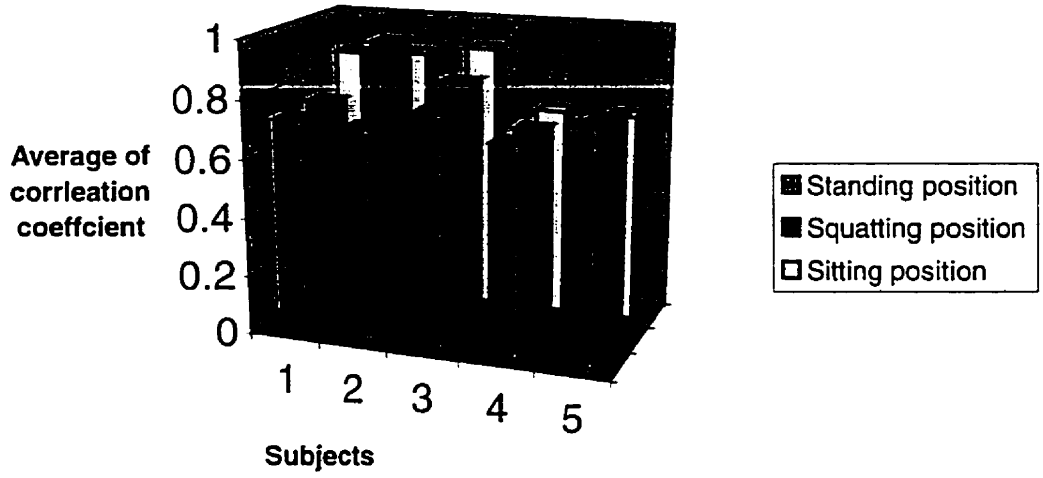

Average of correlation coefficient of tibial rotation during extension

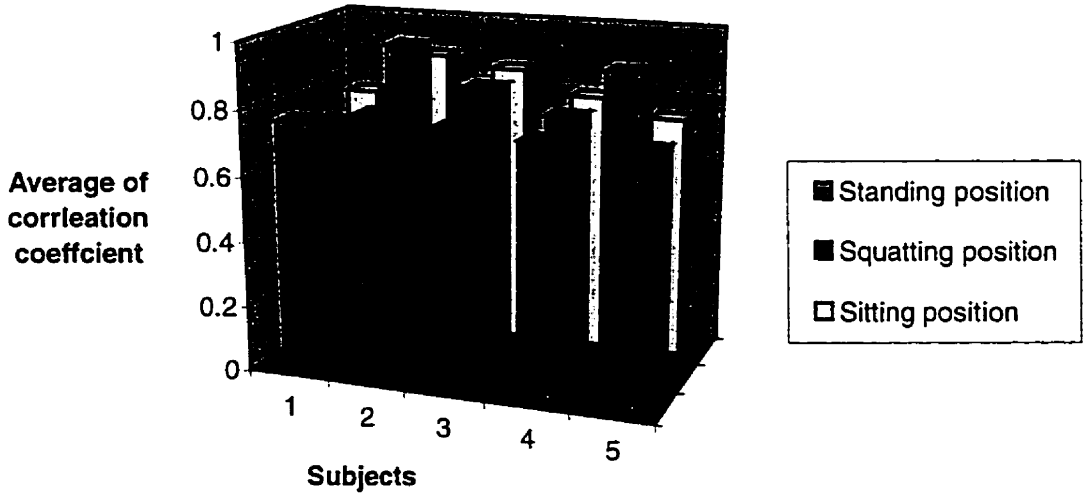

Average of correlation coefficient of abduction during extension

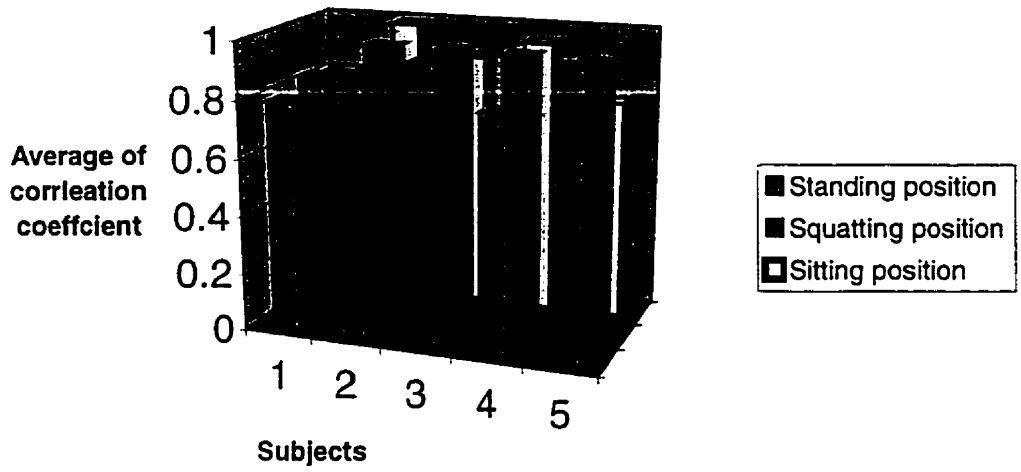

Average of correlation coefficient of abduction during flexion

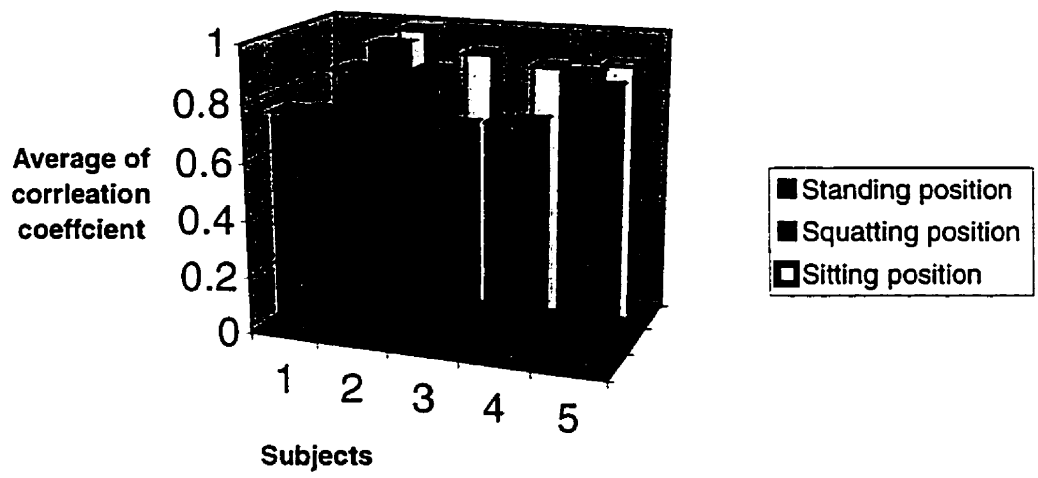

ANNEX IV: ANNEXES FOR CHAPTER 4

Annex IV-A: Kinematic experiment protocol

In this annex we shall list various protocols for different sets of experiments.

Kinematic experiment protocol

First set of experiment

Name:

Age:

Knee history:

Date:

1. Make sure that everything is connected and the Fastrack is turned on.

2. Environment test:

- Put the sensors over the calibration box.
- Digitize points 2 to 14 on the box.
- Check the accuracy of measurement using a matlab program (Boîte-test) and confirm that it is less than 2mm.

3. Put the sensors on the attachment system (tibial and femoral part).

4. Install the attachment system.

5. Geometric calibration (3-point)

- Femur: interne, extern, center of femoral diaphyse
- Tibia: interne, extern, center of tibial diaphyse

6. Calibration of axes (3-point)

- Femur: interne, extern, center of femoral diaphyse
- Tibia: interne, extern, center of tibial diaphyse

7. Digitization by probe

- Femur: interne, extern, center of femoral diaphyse
- Tibia: interne, extern, center of tibial diaphyse

8. Perform the 8-point calibration in parallel with the 3-point calibration method.

- Place a T wooden bar between feet on the floor.
- Make sure that the subject's heels are against the head of the T and his/her feet are touching the bar as shown below:

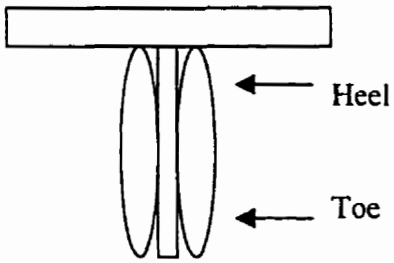

- Make sure that the subject's body is straight.
- Digitize the following points in given order

Femur

- Points 1, 2 and 3, representing the floor plane
- points 4, 5 (heel and toe)
- point 6 on the patella
- points 7 and 8 (the pubis tubercle and the great trochantaire).

Tibia

- Points 1, 2 and 3, representing the floor plane
- Points 4 and 5 (heel and toe)
- point 6 on the patella
- Points 7 and 8 (on the medial and lateral sides of ankle)

9. Testing procedure

- Place a charge over the ankle and record 10 cycles of flexion-extension in standing position
- Remove the charge and record the same motion
- Repeat the above process 5 times with charge and 5 times without it.

Second set of experiments

1. Repeat the above steps 1 through 8.

2. Testing procedure

- Charge should remain in place for throughout the entire experiment

- Perform 10 cycles of flexion-extension in standing and sitting positions
- Remove the attachment system and replace it again and repeat the above step 3 to 8 if it is within the same test day. If it is on different test days repeat steps 1 to 8.
- Repeat the above procedure 10 times while keeping the charge.

Annex IV-B: Bargrahs of correlation coefficient

In this annex we will be looking at different bargraphs to gain a better feeling for the data which were previously presented in various tables.

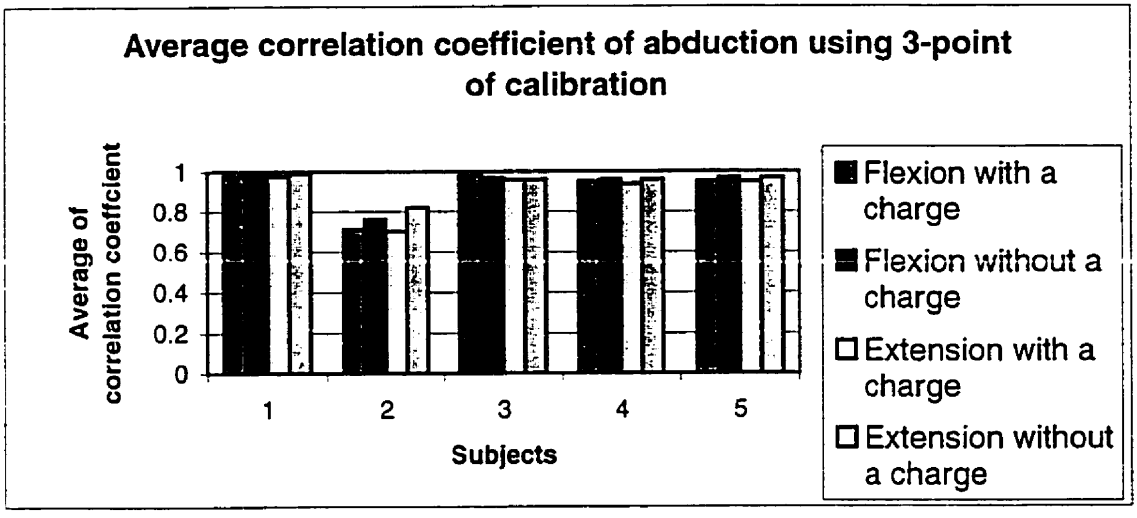
Average correlation coefficient of abduction using 3-point of calibration
Average of correlation coefficient
1
0.8
0.6
0.4
0.2
0
1
2
3
4
5
Subjects
Flexion with a charge
Flexion without a charge
Extension with a charge
Extension without a charge

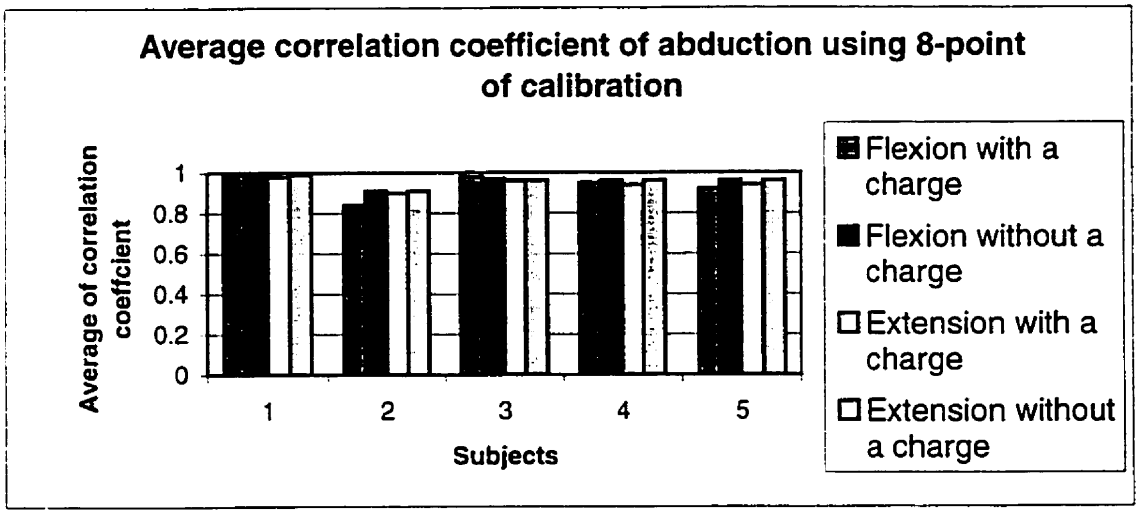
Average correlation coefficient of abduction using 8-point of calibration
Average of correlation coefficient
1
0.8
0.6
0.4
0.2
0
1
2
3
4
5
Subjects
Flexion with a charge
Flexion without a charge
Extension with a charge
Extension without a charge

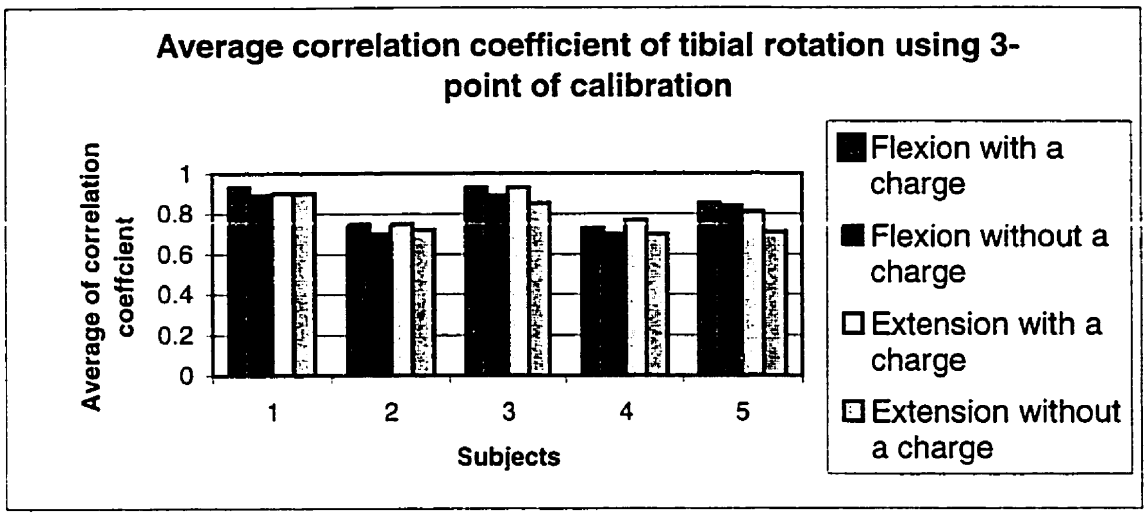
Average correlation coefficient of tibial rotation using 3-point of calibration
Average of correlation coefficient
1
0.8
0.6
0.4
0.2
0
1
2
3
4
5
Subjects
Flexion with a charge
Flexion without a charge
Extension with a charge
Extension without a charge

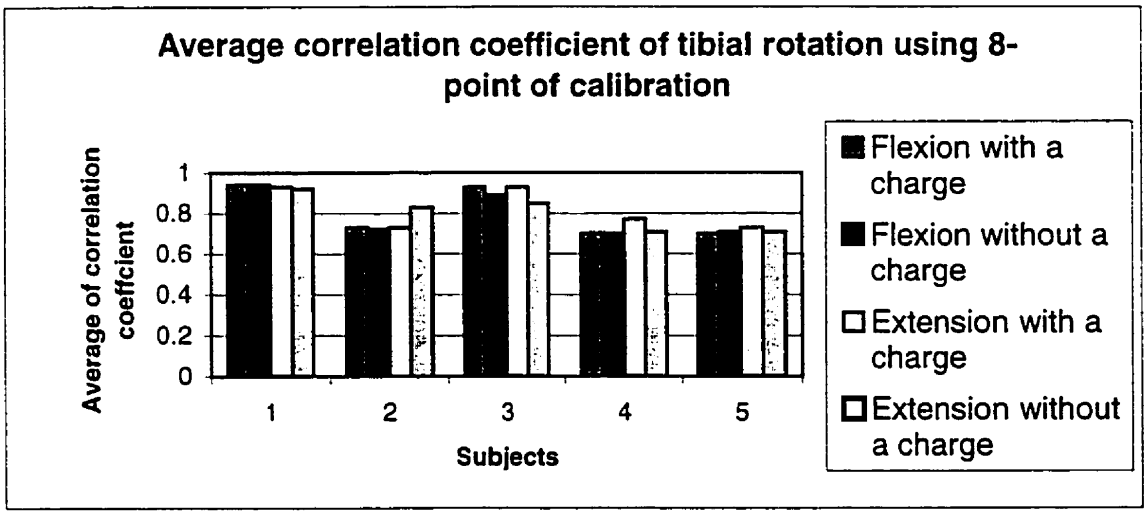
Average correlation coefficient of tibial rotation using 8-point of calibration
Average of correlation coefficient
1
0.8
0.6
0.4
0.2
0
1
2
3
4
5
Subjects
Flexion with a charge
Flexion without a charge
Extension with a charge
Extension without a charge

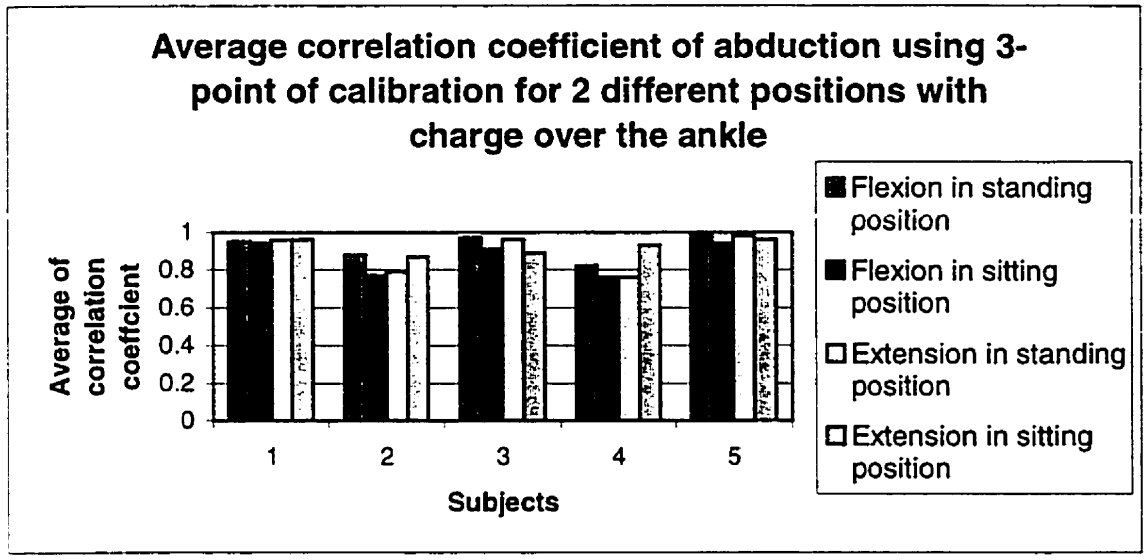
Average correlation coefficient of abduction using 3-point of calibration for 2 different positions with charge over the ankle
Average of correlation coefficient
1
0.8
0.6
0.4
0.2
0
1
2
3
4
5
Subjects
Flexion in standing position
Flexion in sitting position
Extension in standing position
Extension in sitting position

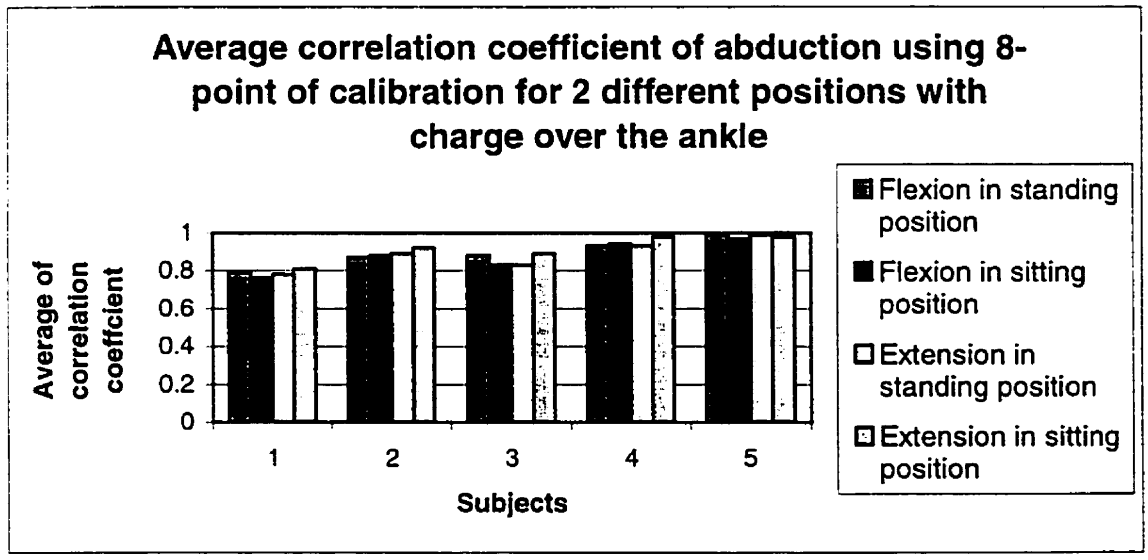
Average correlation coefficient of abduction using 8-point of calibration for 2 different positions with charge over the ankle
Average of correlation coefficient
1
0.8
0.6
0.4
0.2
0
1
2
3
4
5
Subjects
Flexion in standing position
Flexion in sitting position
Extension in standing position
Extension in sitting position

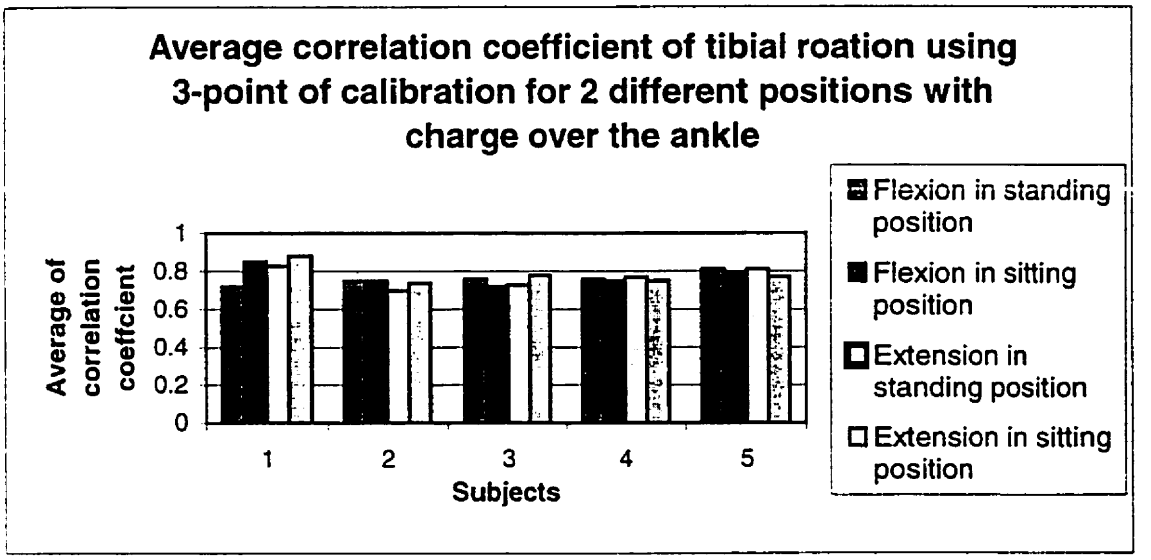
Average correlation coefficient of tibial roation using 3-point of calibration for 2 different positions with charge over the ankle
Average of correlation coeffcient
1
0.8
0.6
0.4
0.2
0
1
2
3
4
5
Subjects
Flexion in standing position
Flexion in sitting position
Extension in standing position
Extension in sitting position

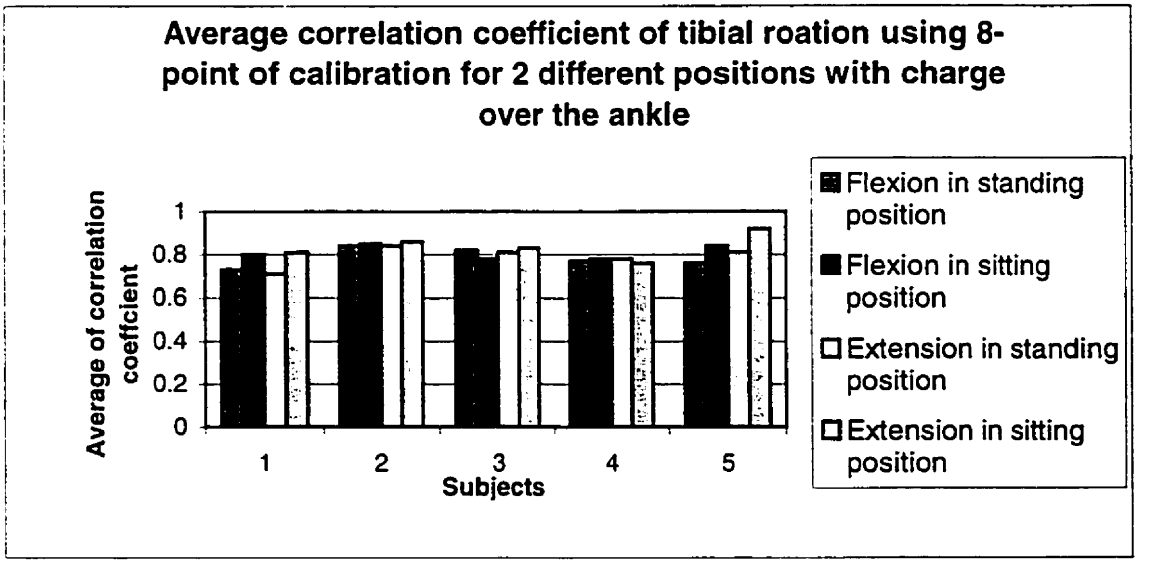
Average correlation coefficient of tibial roation using 8-point of calibration for 2 different positions with charge over the ankle
Average of correlation coeffcient
1
0.8
0.6
0.4
0.2
0
1
2
3
4
5
Subjects
Flexion in standing position
Flexion in sitting position
Extension in standing position
Extension in sitting position

Annex IV-C: Two different methods of calibration

In this annex, we have collected various graphs which show the averages and the error bars of various measurements. They represent intra-subjects studies using 2 different methods of calibration (3-point & 8-point).

Flexion in standing position using 3-point calibration subject 1

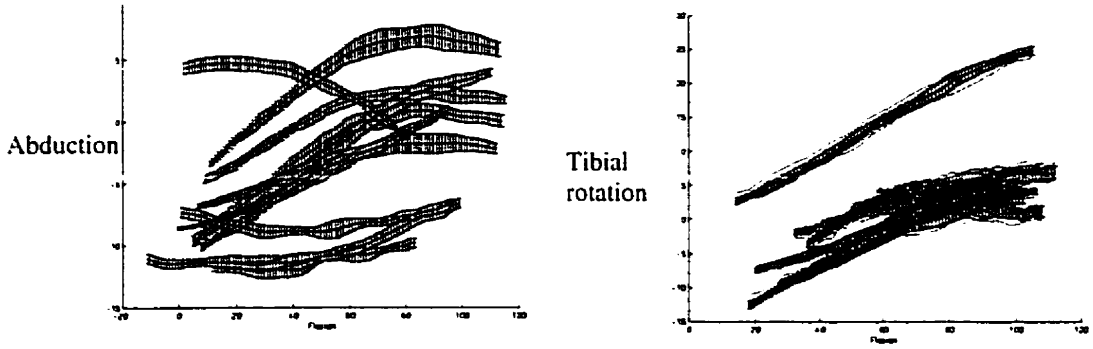

Flexion in standing position using 3-point calibration subject 2

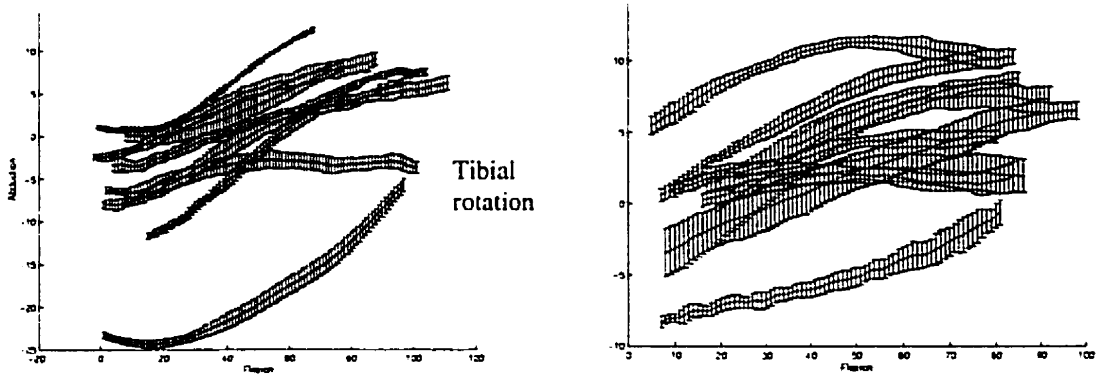

Flexion in standing position using 3-point calibration subject 3

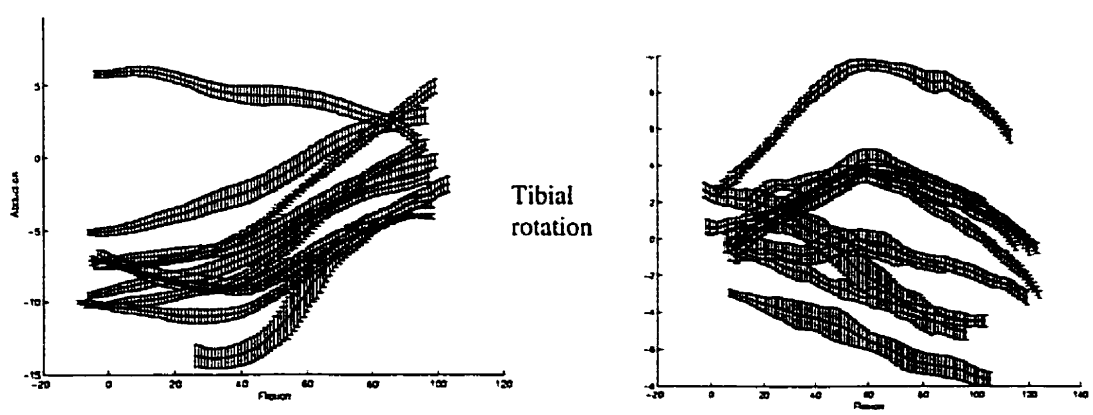

Flexion in standing position using 3-point calibration subject 4

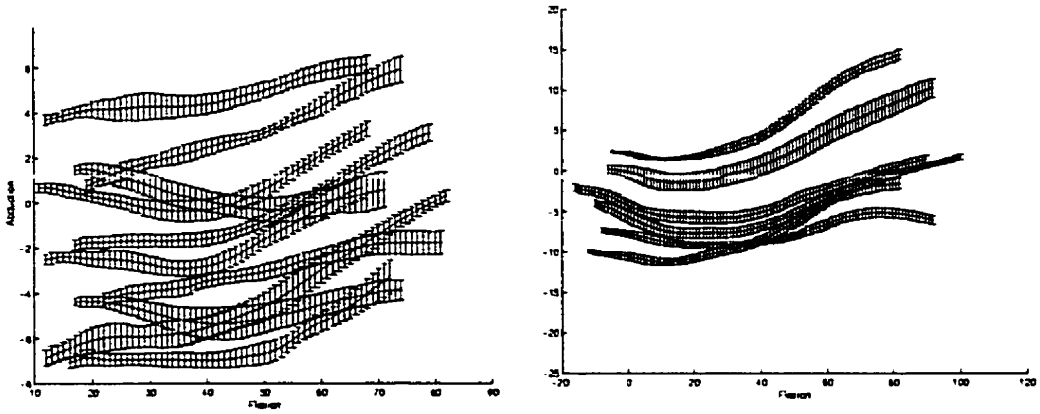

Flexion in standing position using 3-point calibration subject 5

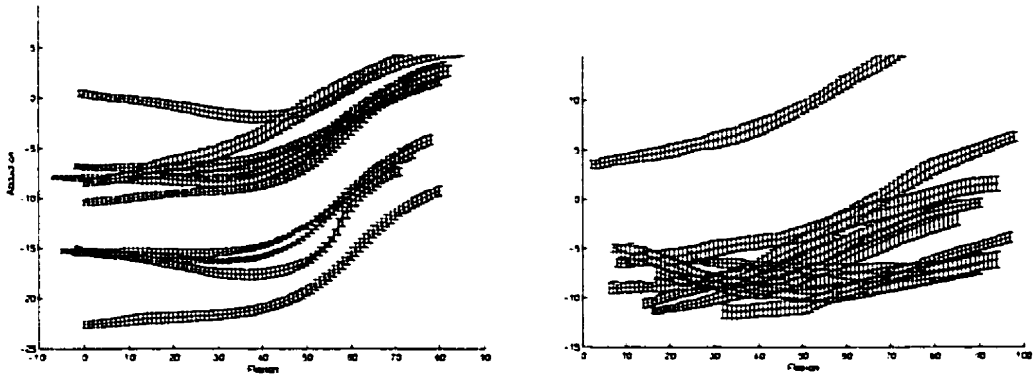

Flexion in standing position using 8-point calibration subject 1

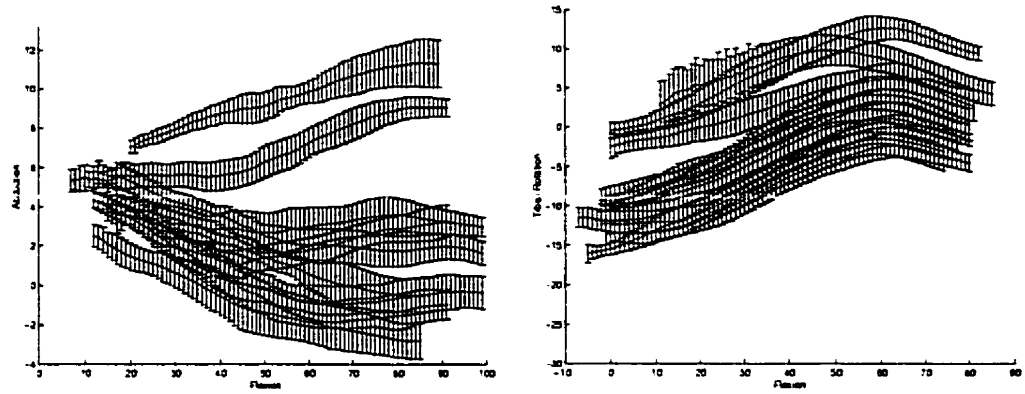

Flexion in standing position using 8-point calibration subject 2

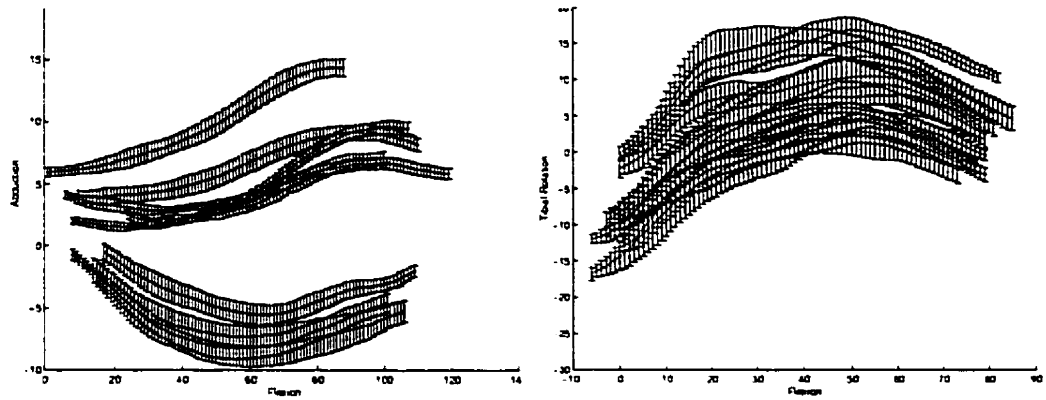

Flexion in standing position using 8-point calibration subject 3

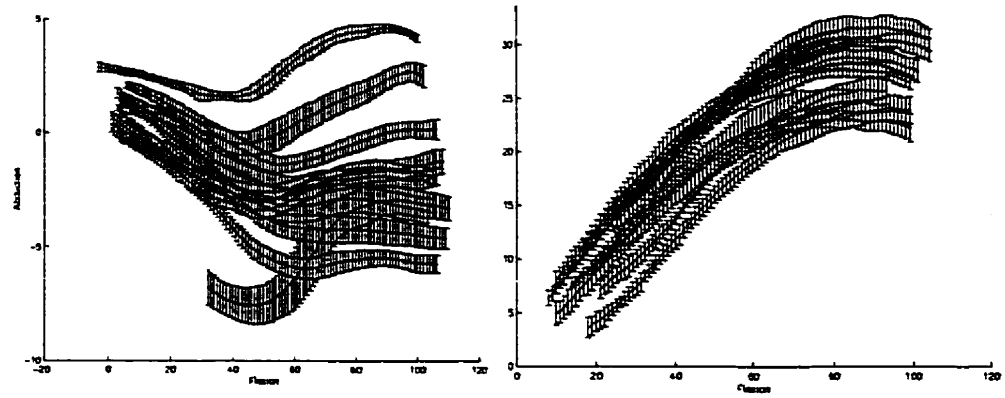

Flexion in standing position using 8-point calibration subject 4

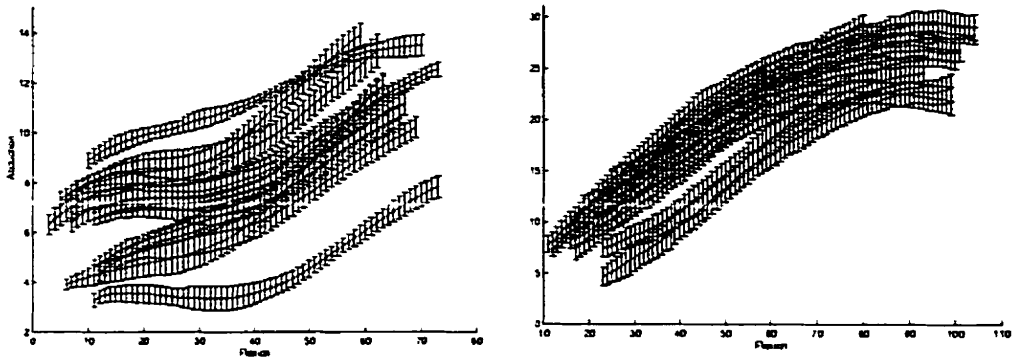
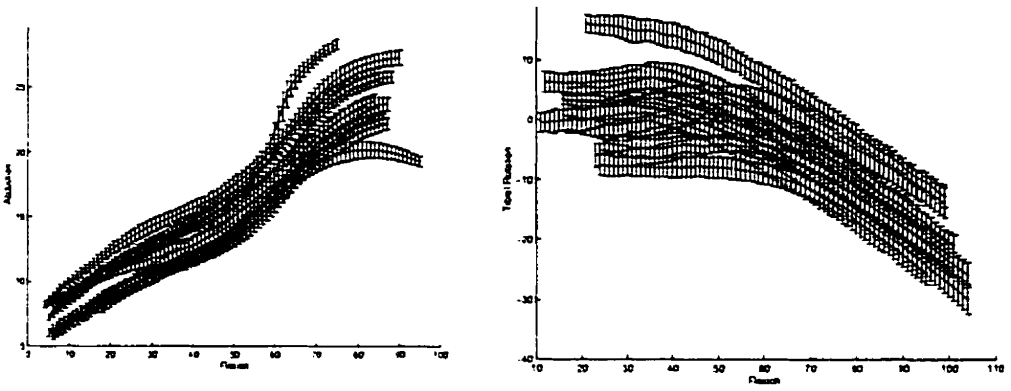
Flexion in standing position using 8-point calibration subject 5